



Appendix A

Geologic Summary Smith Ranch-Highland Uranium Project Mine Unit 1 ACL Application

**Cameco Resources
PO Box 1210
Glenrock, Wyoming 82637**

June, 2017

TABLE OF CONTENTS

1.0	INTRODUCTION	3
2.0	REGIONAL GEOLOGY	3
3.0	SITE GEOLOGY	4
4.0	MINE UNIT 1 CORING & OBSERVATION WELL PROGRAM	7

FIGURES

Figure A-1	Project Location Map
Figure A-2	Geologic Map
Figure A-3	Stratigraphic Column and Generalized Stratigraphic Section
Figure A-4	Regional Structure Map
Figure A-5	Cross Section Index Map, Area within 2 km of Mine Unit 1
Figure A-6	Cross Section A-A'
Figure A-7	Cross Section A'-A''
Figure A-8	Cross Section B-B'
Figure A-9	Cross Section B'-B''
Figure A-10	Q Sand Isopach Map, Area within 2 km of Mine Unit 1
Figure A-11	Q Sand Structure Map, Area within 2 km of Mine Unit 1
Figure A-12	Mine Unit 1 Cross Section Index Map
Figure A-13	Cross Section C-C'
Figure A-14	Cross Section D-D'
Figure A-15	Cross Section E-E'
Figure A-16	Roll Front Schematic and Q Sand Roll Front System
Figure A-17	Mine Unit 1 Roll Front Map
Figure A-18	Core Hole and Observation Well Location Map
Figure A-19	Core Holes UG-1, ST-1 and DG-1 Geophysical Logs and Cored Intervals
Figure A-20	Core Hole ST-2 Geophysical Log, Cored Interval and Core Photographs
Figure A-21	Core Hole ST-3 Geophysical Log, Cored Interval and Core Photographs
Figure A-22	Core Hole ST-4 Geophysical Log, Cored Interval and Core Photographs
Figure A-23	Core Hole ST-5 Geophysical log, Cored Interval and Core Photographs
Figure A-24	Core Hole DG-2 Geophysical Log, Cored Interval, Core Photographs and Observation Well 1OW-001 Completion Interval
Figure A-25	Core Hole DG-3 Geophysical Log, Cored Interval, Core Photographs and Observation Well 1OW-002 Screened Interval
Figure A-26	Core Hole DG-4 Geophysical log, Cored Interval, Core Photographs and Observation Well 1OW-003 Screened Interval

Figure A-27 Core Hole DG-5 Geophysical Log, Cored Interval, Core Photographs and Observation Well 1OW-004 Screened Interval

Figure A-28 Observation Well 1OW-005 Geophysical Log and Screened Interval

Figure A-29 Mine Unit 1 Roll Front and Flow Path Map

TABLES

Table A-1 Mine Unit 1 Core Hole Information Summary

Table A-2 Mine Unit 1 Observation Well Summary

ATTACHMENTS

Attachment A-1 MU1 Core Description and Analysis Including MU1-DG, MU1-ST, & MU1-UG.

1.0 INTRODUCTION

An Alternative Concentration Limits (ACL) application is being prepared by Cameco Resources for Mine Unit 1 located at its Smith Ranch-Highland Uranium Project (SRH) facility in Converse County in east-central Wyoming (Figure A-1). An evaluation and summary of the regional and site geology, ore deposit geology and Mine Unit 1 coring and observation well programs has been completed in support of the ACL application, as part of the mine unit closure plan.

2.0 REGIONAL GEOLOGY

The SRH Permit area is located in the southwestern portion of the Powder River Basin which is a topographic and structural basin extending over almost 24,000 square miles of northeastern Wyoming and southeastern Montana. Figure A-2 illustrates the extent of the Powder River Basin in Wyoming. The basin incorporates a sedimentary rock sequence that has a maximum thickness of approximately 15,000 feet along the synclinal axis. The sediments range in age from Recent (Holocene) to early Paleozoic (Cambrian) and overlie a basement complex of Precambrian-age igneous and metamorphic rocks. A discussion of the geologic history of the Powder River Basin is found in Appendix D-5 of the SRH Permit (PRI, 2014).

2.1 Stratigraphy

A stratigraphic column of the Powder River Basin (Figure A-3) shows the relationship of geologic formations of interest including the Tertiary-age Wasatch (Eocene) and Fort Union (Paleocene) Formations. The uranium-bearing sandstones in the southern Powder River Basin lie within the upper Fort Union and lower Wasatch Formations.

Aside from Quaternary-aged alluvial, stream valley sediments and windblown deposits and the remnants of the White River Formation at Pumpkin Buttes, the Wasatch Formation is the youngest geologic bedrock unit in the southern Powder River Basin and within the SRH Permit area (Figure A-2). The Wasatch consists of interbedded claystones, silty sandstones, thin lignites and cross-bedded arkosic sandstones deposited in a non-marine floodplain- tributary system.

The Fort Union Formation unconformably underlies the Wasatch Formation and includes geologic members from oldest to youngest, the Tulluck, the Lebo Shale and the Tongue River Members. The Tongue River Member of the upper Fort Union Formation is lithologically similar to the Wasatch, consisting of interbedded lenticular claystones and silty claystones, fissile shale, sandy siltstones, coal beds and arkosic sandstones deposited in a fluvial environment. The total thickness of the Fort Union Formation in the southern Powder River Basin is approximately 3,000 feet.

2.2 Structure

The Powder River Basin is a late Cretaceous to early Tertiary structural asymmetrical syncline with its axis oriented in a general northwest-southeast direction along the western margin of the basin (Figure A-4). Within the central portion of the SRH Permit area, The Wasatch and Fort Union Formations dip gently northwestward, reflecting the general axial plunge in that direction. At the eastern and western boundaries of the permit area, the strata dip generally toward the axis some 2 degrees to 5 degrees to the west and east, respectively. Near the outcrop of the Wasatch-Fort Union contact the strata dip as much as 20 degrees.

No major faults or folds in the bedrock have been detected by exploration or development programs conducted in the SRH Permit area. A series of subparallel anticlines and synclines having a relief ranging from 10 to 20 feet were found in the northeast portion of the permit area (PRI, 2014). The closest mapped faulting in the region occurs near the margins of the Powder River Basin, located more than 10 miles southwest of the SRH Permit boundary (Figure A-4).

3.0 SITE GEOLOGY

As previously described, the geologic formations of interest in the SRH Permit area are the lower Wasatch and Upper Fort Union Formations. The sandstone and claystone units within the upper Fort Union and lower Wasatch Formations can be correlated across the permit area. As many as 15 separate potential host sandstone units have been identified at SRH depending on the specific location. Individual sandstone units may be discontinuous in some areas or merge with underlying or overlying sandstone units.

3.1 Stratigraphy

Site specific stratigraphic nomenclature has been established for the correlation, mapping and development of the wellfields of the various SRH mine units. In the western portion of the permit area (Smith Ranch), the upper Fort Union sandstone units are identified alphabetically, in descending order the W Sand, U Sand, S Sand through the I Sand. The W Sand unit is the shallowest unit and the I Sand the deepest. The shale units are identified from the shallowest X Shale unit, V Shale, in descending order through the J Shale (Figure A-3). Not all the identified sand and shale units are present within all mine units, as many of the stratigraphic units coalesce or “pinch-out”.

At Mine Unit 1, the Q Sand is the host production stratigraphic unit and consists of fine- to very coarse-grained, poorly to moderately sorted arkosic sandstone. The Q Sand is continuous across Mine Unit 1 wellfield and varies in thickness from 10 to 75 feet, with an average thickness of 37 feet. The R Shale overlies the Q Sand and the P Shale underlies the Q; both shale units are composed of bentonitic claystone, fissile shale and siltstone with some discontinuous sand lenses and minor lignitic stringers. The R Shale and P Shale vary in thickness across the mine unit but are present throughout Mine Unit 1. The R Shale separates and hydrologically confines the Q

Sand from the overlying S Sand while the P Shale separates and confines the Q Sand from the underlying O Sand (Figure A-3). A characterization and discussion of the hydrologic properties of the Q Sand and its confining units is found in the Pre-operational Wellfield Data Submittal for Mine Unit 1 (PRI, 1997), and in the Mine Unit 1 Hydrologic Assessment and Groundwater Modelling report located in Appendix B of this ACL application.

Although the Q Sand is continuous across the Mine Unit 1 wellfield, it thins or “pinches out” in areas outside of the mine unit, and the P and R Shales subsequently coalesce in nearby mining areas. Figure A-5 shows the mining areas in the general vicinity of Mine Unit 1 including Mine Units 2, 3, 4 & 4A, K and K North along with an index to cross section transects. The Q Sand is discontinuous in several of the nearby mine units. Regional structural cross sections A-A’ and A’-A” (looking north) and B-B’, B’-B” (looking east), (Figures A-6 through A-9) show the heterogeneous, discontinuous nature of the production sand in the area surrounding Mine Unit 1. The overlying and underlying aquifers (S Sand and O Sand, respectively) are also highlighted on the cross sections. The north-south oriented cross sections (Figures A-8, A-9) also reveal the generally low angle northerly dip of the strata.

The heterogeneity of the production sand in the general region around Mine Unit 1 can also be observed in the Q Sand isopach map (Figure A-10). The isopach was constructed using thickness data interpreted from geophysical logs of production, injection and monitor wells, and from exploration and delineation drill holes. Several hundred logs in an area approximately 2 kilometers from Mine Unit 1 were analyzed. Drilling data from the area southeast of Mine Unit 1 is fairly sparse but the does reveal the paucity of the Q Sand in that area.

Three cross sections constructed specifically for Mine Unit 1 C-C’, D-D’ and E-E’ (Figures A-13 through A-15) show the varying thickness of the Q Sand and the continuous presence of the overlying R Shale and the underlying P Shale. Occasional sand stringers are noted in the P Shale and the R Shale, however the lateral extent of these discontinuous sands is very limited. The cross sections include geophysical logs from some of the core holes and observation wells that were completed as part of the Mine Unit 1 closure plan (see Section 4.0 below). Cored intervals of the core holes and screened intervals in the observation wells are noted on the cross sections. Isopach maps of the Q Sand, the overlying R Shale and the underlying P Shale in Mine Unit 1 are found in Appendix B of this ACL application.

3.2 Structure

The subsurface strata at Mine Unit 1 dip at a low angle toward the north (basin-ward) as shown in the Q Sand structural contour map (Figure A-11), which depicts the elevation of the top of the Q Sand. Structural cross sections of Mine Unit 1 (Figures A-13 through A-15) do not indicate significant folding or the presence of bedding displacement by faulting. Evidence of faulting was not noted in the correlation of hundreds of geophysical logs during the resource evaluation and wellfield planning stages of Mine Unit 1.

Faulting or a fault related fracture system was not detected during pre-mining pumping tests performed at Mine Unit 1. The aquifer testing demonstrated a lack of hydrologic communication between the production sand aquifer and the underlying aquifer (O Sand) and the overlying aquifer (S Sand), (PRI, 1997). The lack of hydrologic communication between aquifers indicates the absence of vertical preferential flow paths through the P Shale and R Shale confining units. Additionally, natural fracturing was not observed in tightly cemented sandstone or well-indurated shale core samples recovered during the recent coring program at Mine Unit 1 (Section 4.0 below). Petrographic work conducted on core from Mine Unit 1 (Swapp, 2016) did not indicate the presence of micro-fracturing in the samples analyzed.

3.3 Ore Deposit Geology

The uranium ore deposits in the SRH permit area are of the roll-front type where mineralization is present within stratigraphically separate sandstone units, each with its own frontal system. The deposits are found at the interface of a naturally occurring chemical boundary between reduced and oxidized sandstone facies. Alteration fronts generally are oxidized updip and unoxidized downdip. The oxidized or altered side of the roll can be indicated by tan, yellow, orange or red colors in the sandstones. The sandstones of the unoxidized side of the front are typically gray.

Due to the nature of fluvial sandstone composition, an individual sand member may have several vertically superimposed subsidiary roll-fronts or sub-rolls. This is caused by small permeability differences in the sandstone resulting in development of multiple roll-fronts that overlie each other (stacked) in complex patterns (Figure A-16). The fronts are anisotropic, with the bulk of the high-grade ore being contained within a few feet of the oxidation-reduction contact, and the balance of the ore grading into reduced ground. Individual sub-roll fronts can commonly be traced for thousands of feet, and in plan view are typically sinuous. The ore grades along these roll-fronts can vary considerably, and portions of the front may not contain economic mineral concentrations.

Seven sub-rolls were identified in the Q Sand roll-front system of Mine Unit 1 and are designated, from shallowest to deepest, the Orange, Green, Red, Blue, Pink and Purple horizons. Figure A-16 illustrates the sub-rolls in the Q Sand depicted in a geophysical log with the color-coded horizons representing the different mineralized zones.

The lateral distribution of the mineralized zones in Mine Unit 1 is shown in Figure A-17. During the wellfield planning stages of Mine Unit 1, mapping of the Q Sand roll-front system was performed utilizing the geophysical logs from exploration and delineation drilling. The geophysical log signature and mineralization intercept data were then used to determine the extent of the ore-grade mineralization along the sub-rolls within the Q Sand front system at Mine Unit 1. The number of mineralized zones increases towards the eastern side of the mine unit which can be attributed to the general increase in Q Sand thickness. The general orientation of

the fronts indicate that groundwater flow at the time of the formation of the roll-fronts was south-southwest to north-northwest.

4.0 MINE UNIT 1 CORING & OBSERVATION WELL PROGRAM

Eleven holes were cored and five observation wells were installed in the Q Sand in support of the geochemical and groundwater transport model, as part of the ACL application for the Mine Unit 1 closure plan. Given the long term groundwater flow across Mine Unit 1 is from south-southwest to north-northwest, which is comparable to the flow direction at the time of the formation of the roll-front deposits, the planned core hole locations were spotted upgradient of Mine Unit 1, in the production zone / crossgradient and downgradient of the production zone. Core hole and observation well locations are shown in Figure A-18. Information summaries of the core holes and observation wells are presented in Tables A-1 and A-2.

4.1 2014 Program

Three drill holes were cored in the Q Sand during 2014 including UG-1 (upgradient), ST-1 (production zone/ cross-gradient) and DG-1 (downgradient). Each hole was initially drilled with a 6 1/4" bit to a pre-determined core point depth then cored with a 10' length x 3" inside diameter split inner barrel coring assembly. The cores were recovered at the surface, described and preserved in storage bags by vacuum sealing; samples were later selected and shipped for analysis. The holes were then drilled to TD, geophysically logged for resistivity, gamma and spontaneous potential (SP) and then plugged and abandoned. Geophysical logs of the cored intervals of DG-1, ST-1 and UG-1 are shown in Figure A-19.

Fifteen preserved core samples (five from each core hole) were selected and delivered to the University of Wyoming Department of Geology and Geophysics for analysis including mineralogy, petrography, petrofabrics and whole rock chemistry. The Q Sand samples were characterized as texturally immature arkosic sandstones deposited and buried extremely rapidly and with minimal sediment transport from a granitic source terrain (Swapp, 2016). The primary minerals are quartz, plagioclase feldspar, potassium feldspar, clay minerals (smectite, kaolinite, illite and chlorite), various ferromagnesian minerals and trace amounts of white mica. Accessory minerals include pyrite (occurring as framboids), ilmenite, sphene, apatite, garnet, epidote, calcite, zircon, and monazite. Some of the feldspar is altered to clay; this alteration is post-deposition (authigenic). Grain sizes range from fine- to very coarse- and sorting is poor. Individual grains are highly angular in most samples. The complete results of the mineralogic/petrographic study are found in Attachment A-1.

4.2 2016 Program

Supplemental cores were taken at Mine Unit 1 during 2016 including production zone/cross-gradient holes ST-2 through ST-5 and downgradient holes DG-2 through DG-5. The 3" diameter cores were recovered on site, photographed, described and preserved by vacuum sealing. The

holes were then drilled to TD and geophysically logged. Core samples from generally transmissive zones of each hole were subsequently selected and sent for mineralogical, chemical and physical property analyses. The results of the core analysis were utilized for the Geochemical and Groundwater Transport Model; details of the analysis can be found in the report located in Appendix C. A brief, general description (from field notes) of the selected core samples is listed below; diagrams of core hole geophysical logs of the cored intervals and core photos of sampled intervals are shown in Figures A-20 through A-27.

Core hole ST-2, 463'-464' sandstone, light gray to gray, reduced, fine- to medium-grained, occasional coarse-grained, occasional thin carbonaceous laminations; 472'-473' sandstone, oxidized, medium- to coarse-grained, poorly sorted, with lignitic clasts (Figure A-20).

Core hole ST-3, 463'-464' sandstone, gray to dull orange, coarse-grained interval is oxidized, some lignite present; 474'-475' sandstone, light brown to medium brown, gray, oxidized, fine- to very coarse-grained with occasional pebbles, carbon trash fragments; 477'-478' sandstone, light brown, oxidized, coarse-grained (Figure A-21).

Core hole ST-4, 479'-480' sandstone, light brown, oxidized, coarse-grained, moderately sorted, with gray clay lamination; 488'-489' sandstone, tan to light brown, oxidized, coarse-grained, moderately sorted, gray, fine-grained at base; 496'-497' sandstone light gray to gray, reduced, fine- to medium-grained, moderately sorted; 497'-498' sandstone, gray to light gray, reduced, fine-grained, with 5% clay content (Figure A-22).

Core hole ST-5, 494'-495' sandstone, dull orange, fine- to coarse-grained, oxidized; 499'-500' sandstone, dull orange, coarse-grained, oxidized; 501'-502' sandstone, dull orange, coarse-grained, oxidized; 503'-504' sandstone, light gray, fine-grained, well cemented with calcite, thin carbonaceous lamination (Figure A-23). Note in the photograph that the well cemented interval lacks the presence of natural fracturing.

Core hole DG-2, 477'-478' sandstone, medium- to very coarse-grained, some clay clasts; 482'-483' sandstone, medium- to coarse-grained, reduced, poorly sorted; 487.5'-488.5' sandstone, very fine-grained reduced, silty with occasional gravel lenses; 504'-505' sandstone, light gray, reduced, fine- to very coarse-grained (Figure A-24).

Core hole DG-3, 524'-525' sandstone, fine- to medium-grained, reduced; 543'-544' sandstone, gray, reduced, fine- to very coarse-grained with gravel, poorly sorted; 551'-552' sandstone, gray, reduced, fine- to very coarse-grained with gravel (Figure A-25).

Core hole DG-4, 516'-517' sandstone, gray, reduced, fine- to very coarse-grained, carbonaceous stringer towards top (Figure A-26).

Core hole DG-5, 528'-529' sandstone, dull orange, gray, oxidized, medium- to very coarse-grained with gravel clasts; 541'-542' sandstone, gray, reduced, medium- to coarse-grained, moderate calcite cement, with brown oxidized carbonaceous lamination at base (Figure A-27).

Following the coring program at Mine Unit 1, five observation wells were installed; four at the aquifer exemption boundary adjacent to DG core holes and one within the monitor well ring (Figure A-18). The wells were completed in a method which minimized the effects on the groundwater by the completion materials. Each well was first piloted with a 5 5/8" drill bit through the production Q Sand, geophysically logged then reamed with an 8 3/4" drill bit. The completion intervals, or screened intervals, in each well were picked from the geophysical log to include the entire Q Sand thickness and are the logs are displayed in Figures A-24 through A-28. The wells were then cased with 5" outside diameter SDR17 Certa-Lok PVC casing, including 5" slotted casing through the completion intervals. The wells were gravel packed on the outside of the screened interval with 1/4" diameter gravel. The annular space above the gravel pack was filled with a grout consisting of 3/8" bentonite chips to ground surface and topped off with cement. The wells were then developed with the drill rig by air lifting water to the surface. After the surface was reclaimed at each well location, a locking 6" steel monument was installed. Table A-2 lists each observation well with corresponding drill depths and well construction information.

The observation wells, monitor ring wells and core holes and their location relative to the Mine Unit 1 roll-front system are seen in Figure A-29. The oxidized appearance of one core sample from downgradient hole DG-5 can be explained by the location of the core hole relative to the roll-front, which is likely on the oxidized side of the roll-front trend. Additionally, the flow paths utilized in the groundwater transport model (Appendices B and C) are shown relative to the Mine Unit 1 roll-fronts.

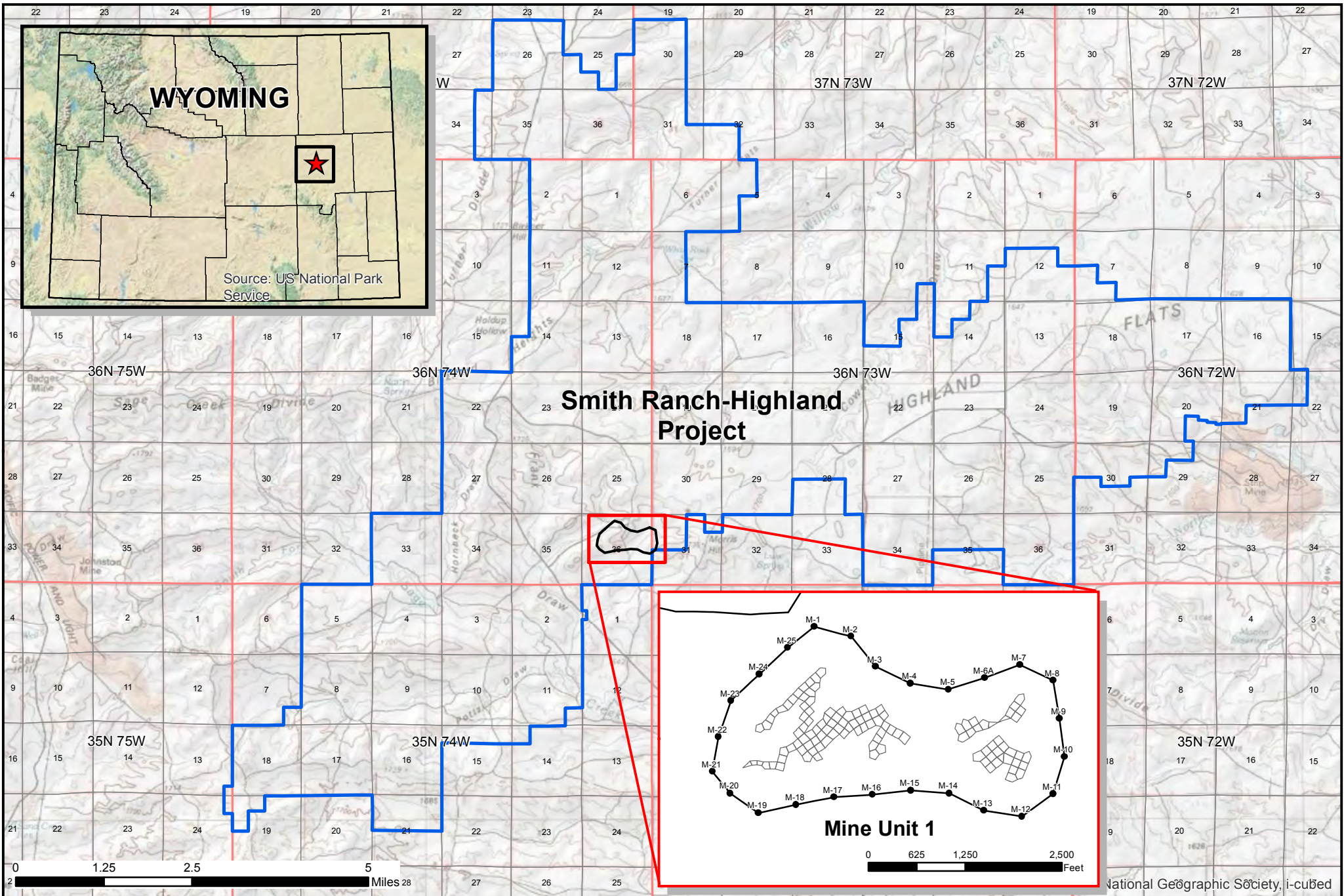
References

PRI, 1997. Power Resources, Inc. dba Cameco Resources, Smith Ranch-Highland Uranium Project. Wyoming Department of Environmental Quality / Land Quality Division Permit No. 633, Volume III-A, 1 Wellfield Pre-operational Data Submittal, March 15, 1997.

PRI, 2014. Power Resources, Inc. dba Cameco Resources, Smith Ranch-Highland Uranium Project. Wyoming Department of Environmental Quality / Land Quality Division Permit No. 633-A2, Volume II-D, Appendix D-5 Geology, March 10, 2014.

Swapp, Susan M., 2016. MU1 Core Description and Analysis Including MU1-DG, MU1-ST, & MU1-UG. Report for Cameco Resources, Department of Geology and Geophysics, University of Wyoming, Laramie, April 10, 2016.

FIGURES



Legend

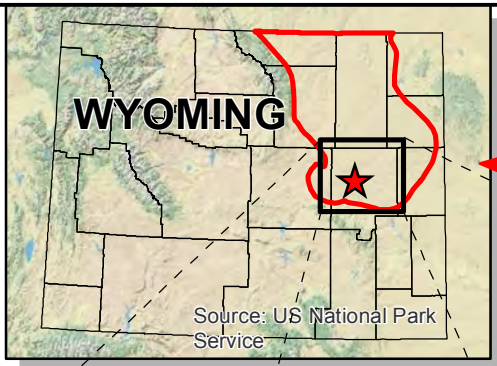
-  Mine Unit
-  Township
-  Smith Ranch-Highland Permit Boundary

 Cameco Resources
 P.O. Box 1210
 Glenrock, WY 82637
 Telephone: (307) 358-6541

Figure A-1
Location Map
Smith Ranch-Highland Project
Converse County, Wyoming
Mine Unit 1 ACL Application

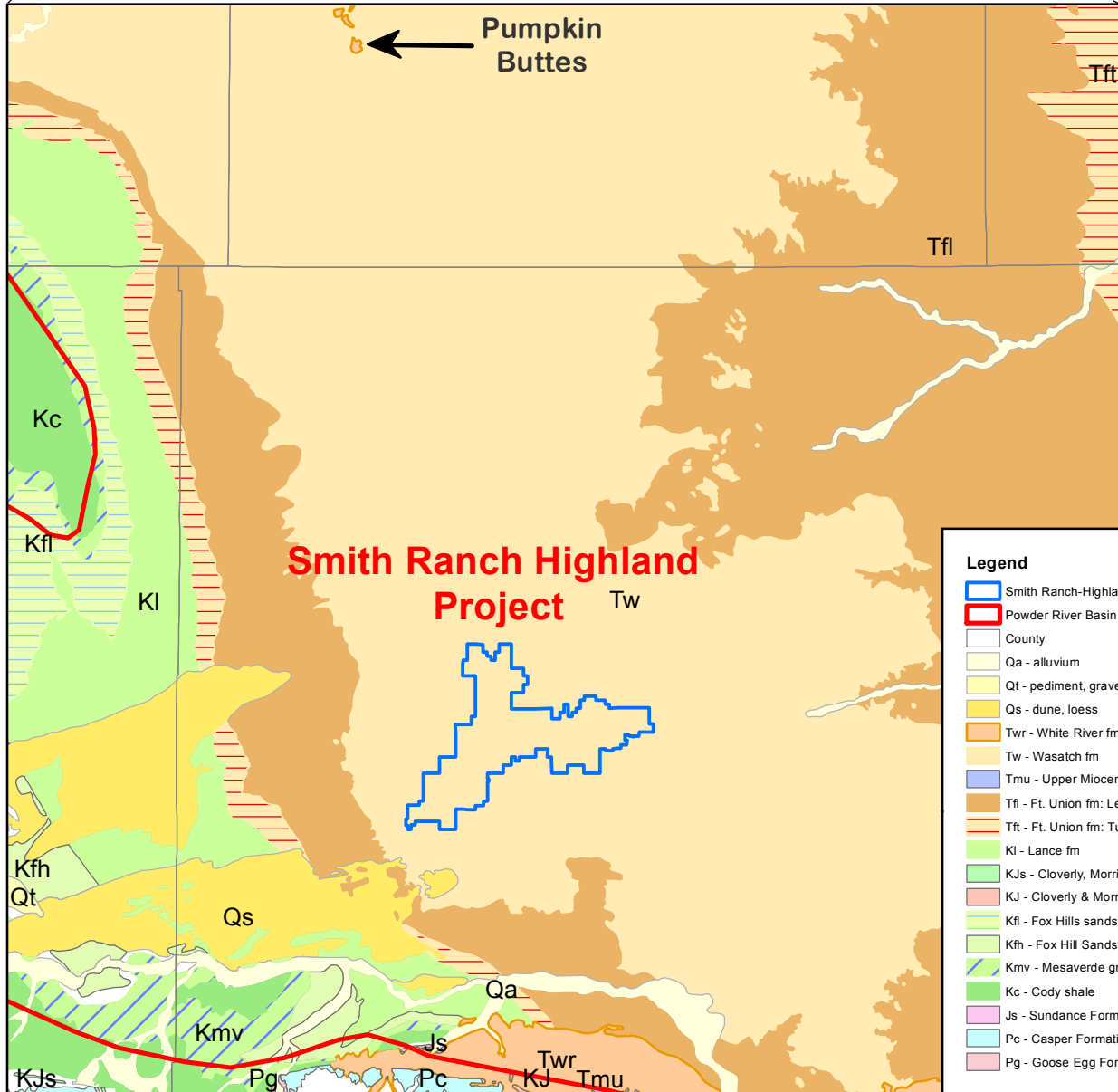


DATE: 6/2/2017	DEPARTMENT: Geology	COORDINATE SYSTEM: NAD 1983 StatePlane Wyoming East FIPS 4901	REV:
SOURCE: O:\GEOLOGY\MU_1\MU-1_GIS_Mapping\MU-1 ACL Application\Maps\Figure A-1 Location Map.mxd			



POWDER RIVER BASIN

Source: US National Park Service



Legend

- Smith Ranch-Highland Permit Boundary
- Powder River Basin Boundary
- County
- Qa - alluvium
- Qt - pediment, gravel
- Qs - dune, loess
- Twr - White River fm
- Tw - Wasatch fm
- Tmu - Upper Miocene Rocks
- Tfi - Ft. Union fm: Lebo member
- Tft - Ft. Union fm: Tullock member
- Kl - Lance fm
- KJs - Cloverly, Morrison, & Sundance Formations
- KJ - Cloverly & Morrison Formation
- Kfi - Fox Hills sandstone; Lewis shale
- Kfh - Fox Hill Sandstone
- Kmv - Mesaverde group
- Kc - Cody shale
- Js - Sundance Formation
- Pc - Casper Formation
- Pg - Goose Egg Formation



Cameco Resources
 P.O. Box 1210
 Glenrock, WY 82637
 Telephone: (307) 358-6541

**Figure A-2
 Geologic Map
 Smith Ranch-Highland Project
 Converse County, Wyoming
 Mine Unit 1 ACL Application**



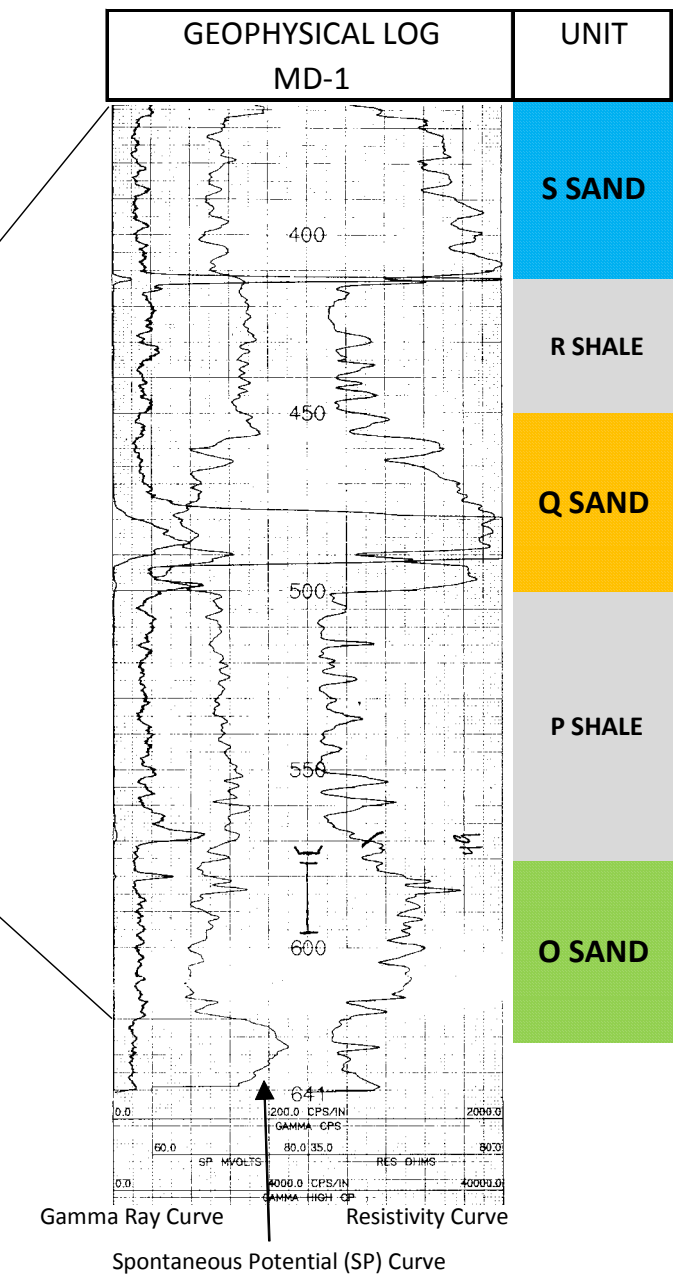
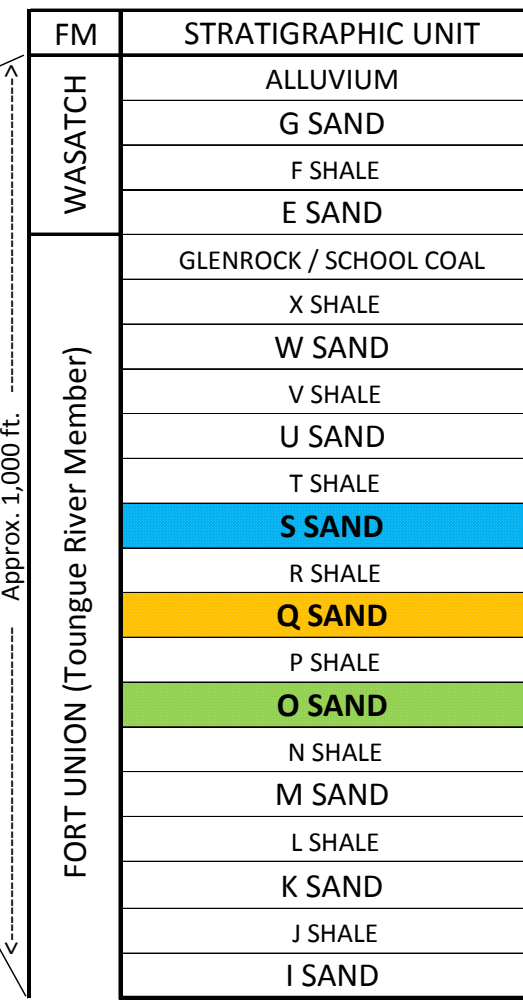
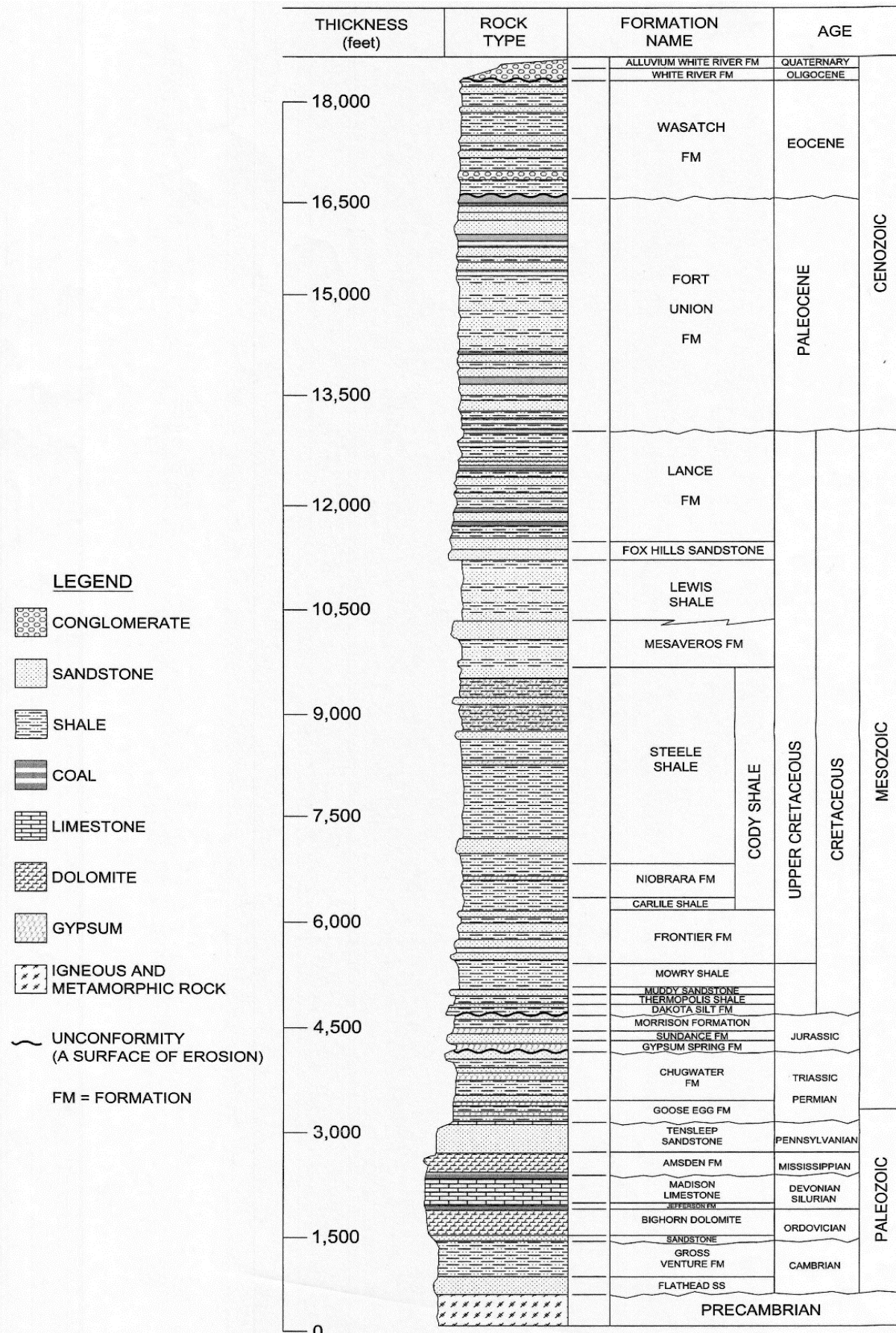
STRATIGRAPHIC COLUMN

GENERALIZED STRATIGRAPHIC SECTION

WESTERN POWDER RIVER BASIN

SMITH RANCH HIGHLAND PERMIT AREA

MINE UNIT 1 SITE



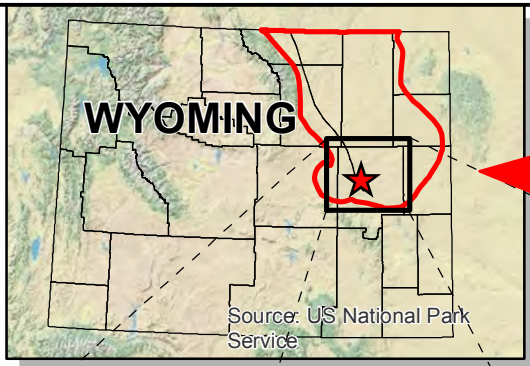
- LEGEND**
- CONGLOMERATE
 - SANDSTONE
 - SHALE
 - COAL
 - LIMESTONE
 - DOLOMITE
 - GYPSUM
 - IGNEOUS AND METAMORPHIC ROCK
 - UNCONFORMITY (A SURFACE OF EROSION)
 - FM = FORMATION

Cameco Resources
P.O. Box 1210
Glenrock, WY 82637
Telephone: (307) 358-6541

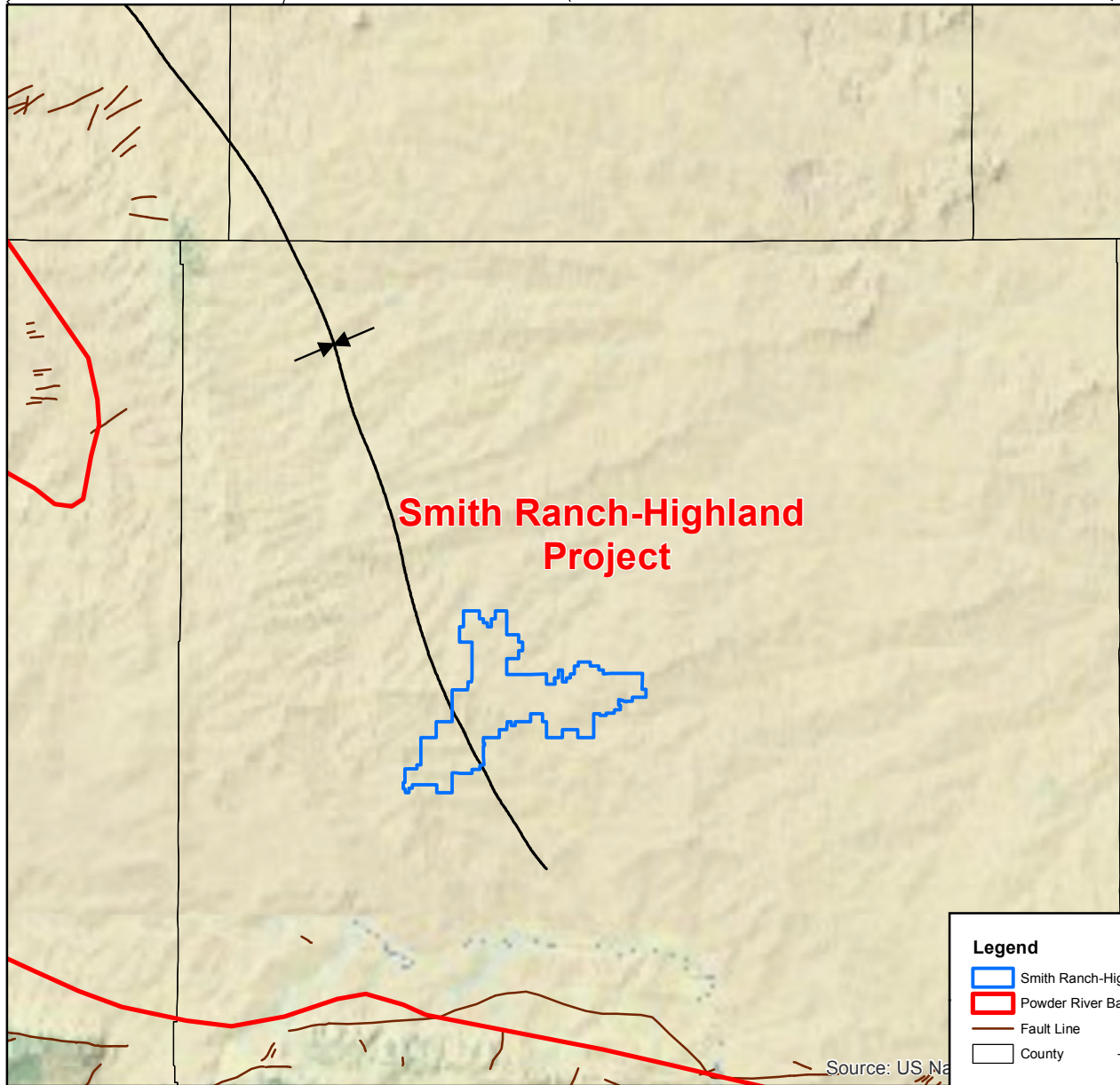
Figure A-3
Regional Stratigraphic Column & Generalized Stratigraphic Section for SRH & Mine Unit 1 Mine Unit 1 ACL Application

Coordinate System: _____
REV: _____

SIZE: X	DATE: 6/6/2017	DEPARTMENT: Geology
DRAWING LOCATION: O:\GEOLOGY\MU_1\MU-1_GIS_Mapping\MU-1 ACL Application\Maps\Figure A-3 Strat Chart.mxd		



POWDER RIVER BASIN



Legend

-  Smith Ranch-Highland Permit Boundary
-  Powder River Basin Boundary
-  Fault Line
-  County
-  Syndinal Axis



Cameco Resources
 P.O. Box 1210
 Glenrock, WY 82637
 Telephone: (307) 358-6541

Figure A-4
Regional Structure Map
Smith Ranch-Highland Project
Converse County, Wyoming



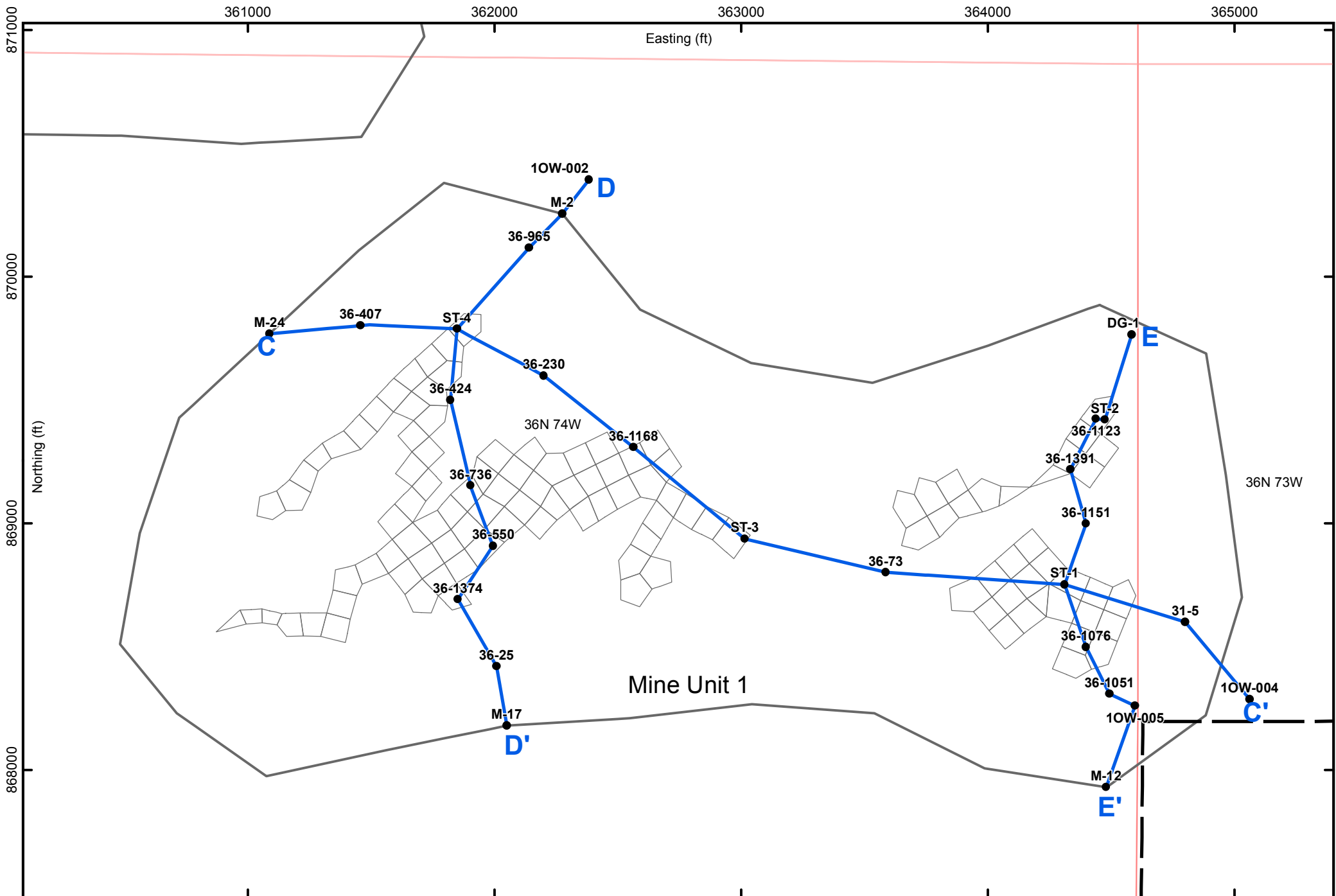
SIZE: X DATE: 6/5/2017

DEPARTMENT: Geology

Coordinate System:
 NAD 1927 StatePlane Wyoming East FIPS 4901
 Datum: North American 1927

REV:

OVERSIZE FIGURES A-6 THROUGH A-11 IN SEPARATE FILE



Legend

- MU-1 Transect Well/Hole
- MU-1 Cross Section Transect
- ▭ Permit Boundary
- ▭ Township



Cameco Resources
P.O. Box 1210
Glenrock, WY 82637
Telephone: (307) 358-6541

**Figure A-12
Mine Unit 1
Cross Section Index Map
Mine Unit 1 ACL Application**

N

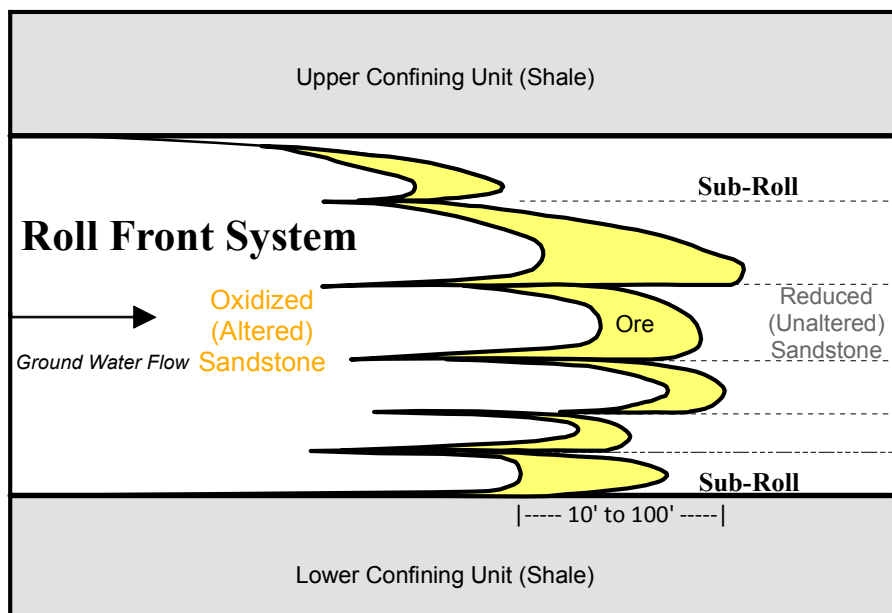
1" = 500 feet

SIZE: X	DATE: 5/25/2017	DEPARTMENT: Geology	Coordinate System: NAD 1983 StatePlane Wyoming East FIPS 4901 Datum: North American 1927	REV:
---------	-----------------	---------------------	---	------

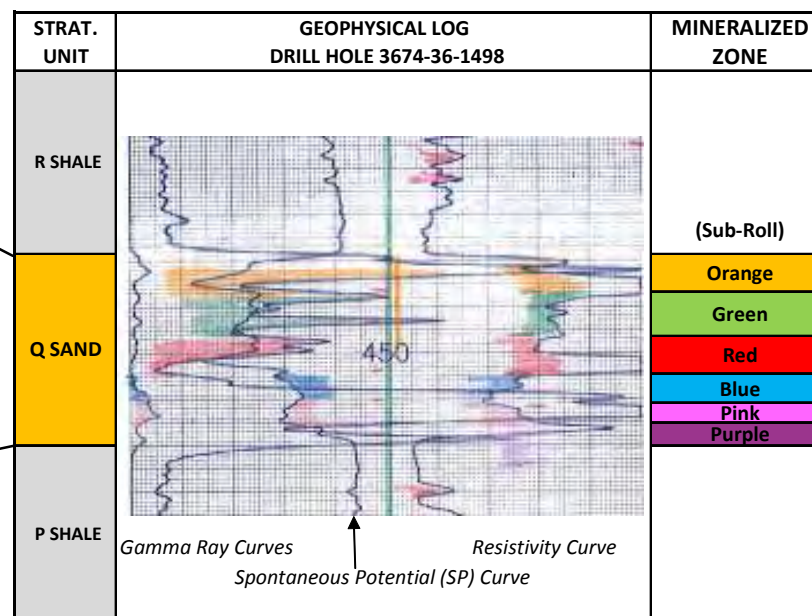
\\GEOLOGY\MU_1\MU-1_GIS_Mapping\MU-1 ACL Application\Maps\Figure A-12 Mine Unit 1 Cross Section Index Map.mxd

OVERSIZE FIGURES A-13 THROUGH A-15 IN SEPARATE FILE

GENERALIZED ROLL FRONT SCHEMATIC



MINE UNIT 1 Q-SAND ROLL FRONT SYSTEM



Cameco Resources
P.O. Box 1210
Glenrock, WY 82637
Telephone: (307) 358-6541

Figure A-16
Roll Front Schematic and
Q-Sand Roll Front System
Mine Unit 1 ACL Application

SIZE:
X

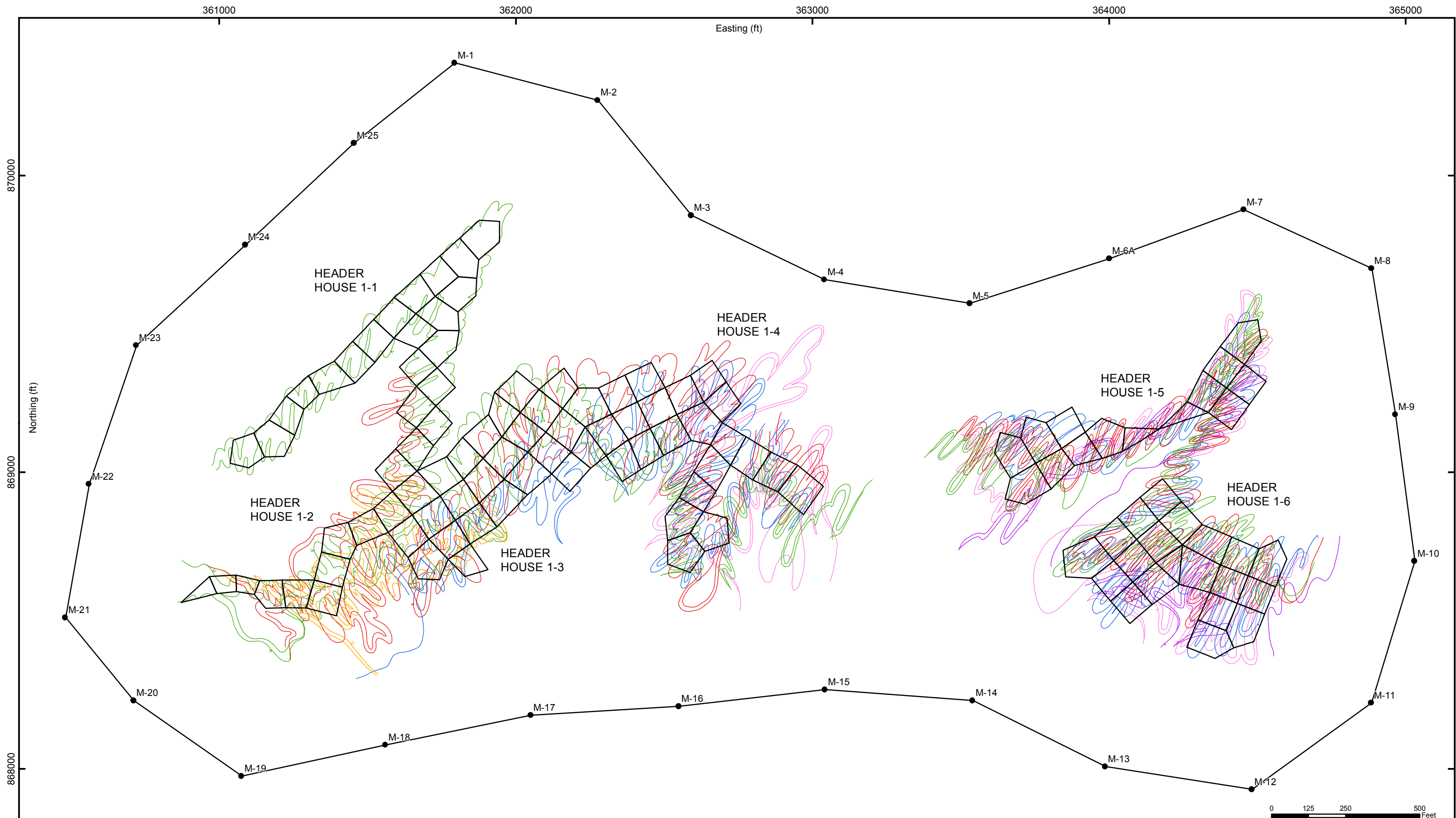
DATE:
5/25/2017

DEPARTMENT:
Geology

Coordinate System:

REV:

DRAWING LOCATION: O:\GEOLOGY\MU_1\MU-1_GIS_Mapping\MU-1 ACL Application\Maps\Figure A-16 Roll Front Schematic.mxd



Legend

Mineralization Horizon

Orange Zone	Red Zone	Pink Zone	Monitor Well
Green Zone	Blue Zone	Purple Zone	Wellfield Pattern



Cameco Resources
P.O. Box 1210
Glenrock, WY 82637
Telephone: (307) 358-6541

SIZE	DATE	DEPARTMENT
X	6/6/2017	Geology

COORDINATE SYSTEM: NAD 1983 StatePlane Wyoming East FIPS 4901
DATUM: North American 1983

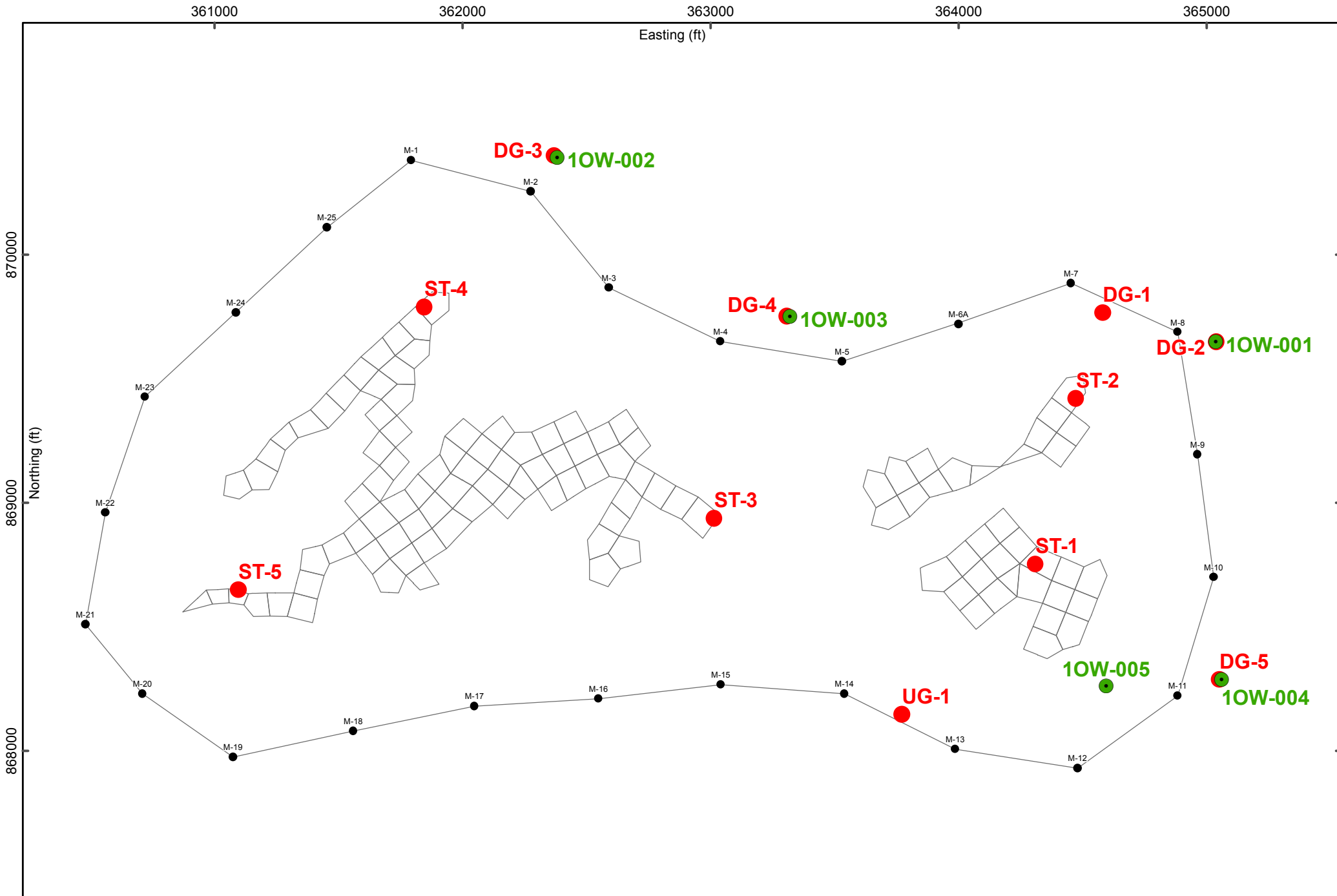
FILE LOCATION: O:\GEOLOGY\MU_1\MU-1_GIS_Mapping\MU-1 ACL Application\Maps\Figure A-17 Mine Unit 1 Roll front Map.mxd

Figure A-17
Mine Unit 1 Roll Front Map
Mine Unit 1 ACL Application

N



1:3,500



- Legend**
- Core Hole
 - Observation Well
 - MU-1 Monitor Well


 Cameco Resources
 P.O. Box 1210
 Glenrock, WY 82637
 Telephone: (307) 358-6541

Figure A-18
Core Hole and
Observation Well Location Map
Mine Unit 1 ACL Application

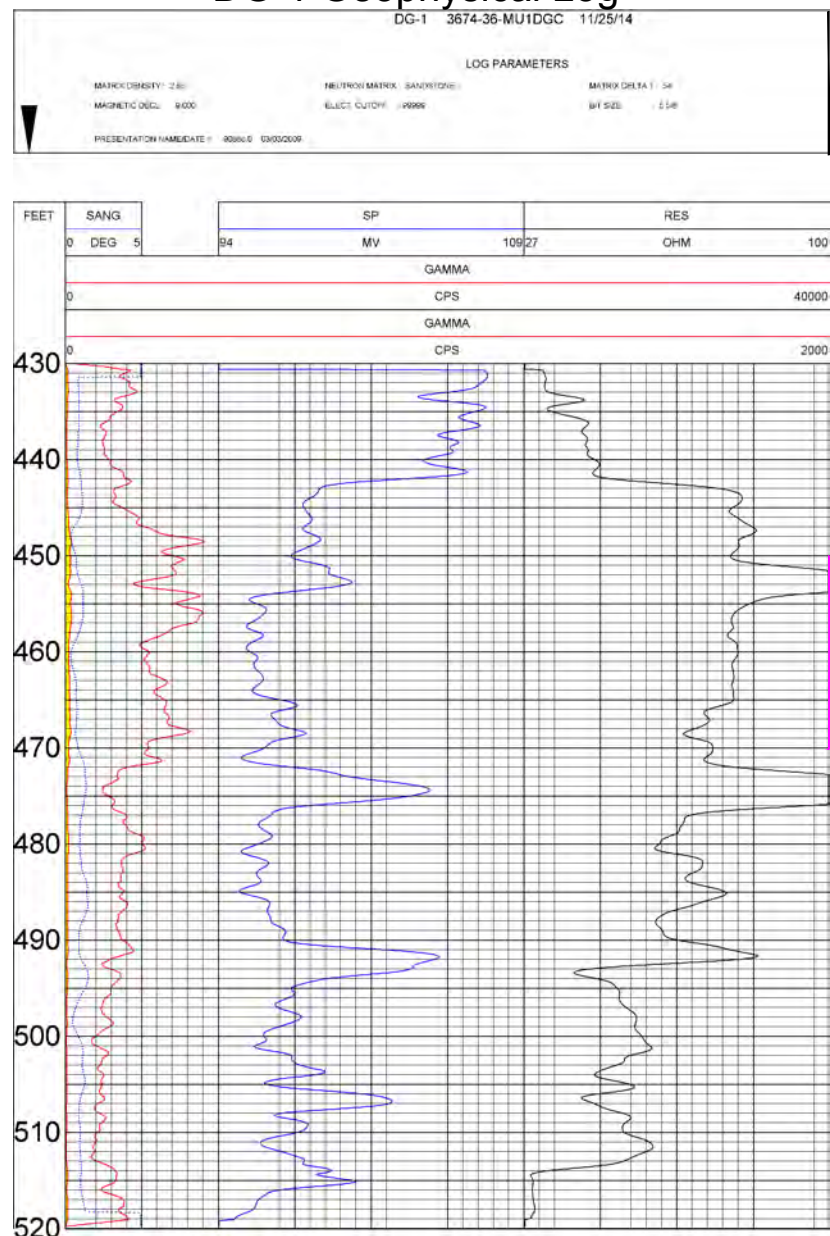
N

 1" = 500 feet

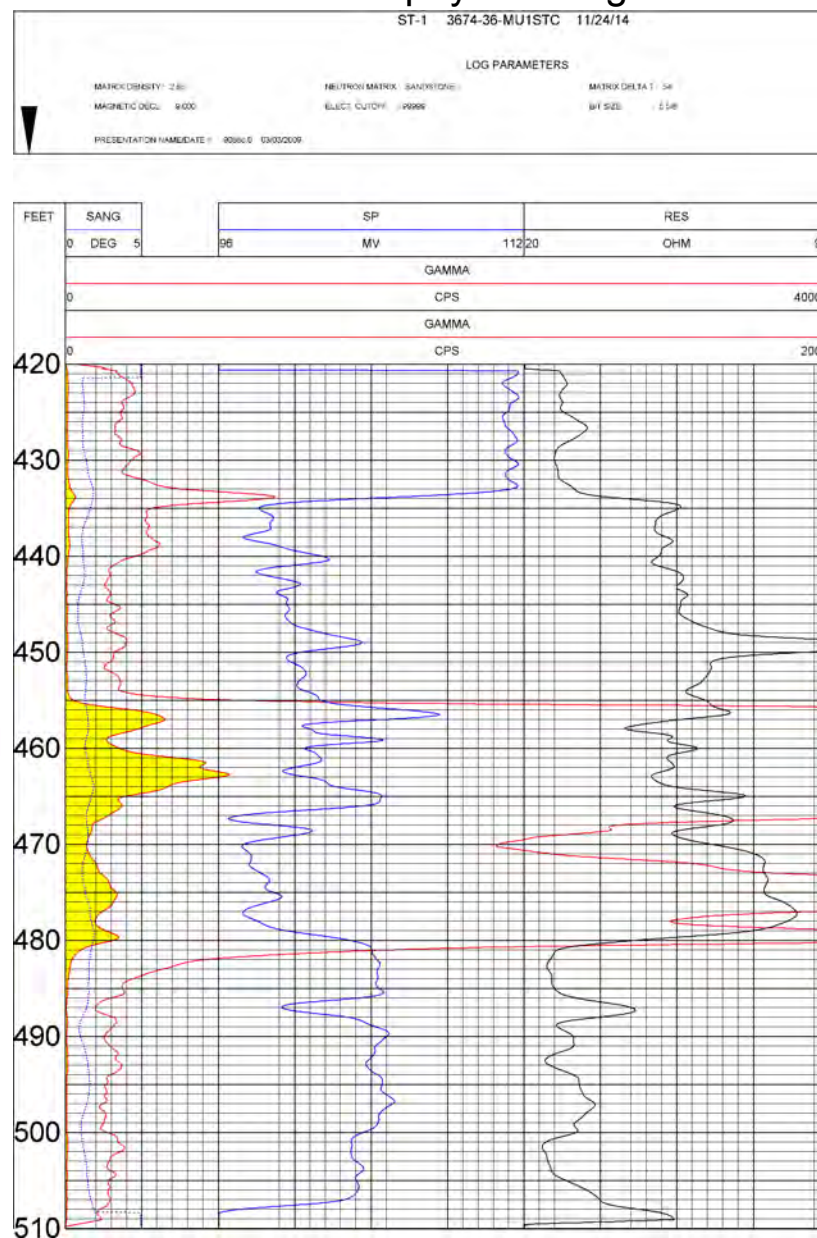
SIZE: X	DATE: 5/24/2017	DEPARTMENT: Geology	<small> Coordinate System: NAD 1983 StatePlane Wyoming East FIPS 4901 Datum: North American 1927 </small>	REV:
<small> SOURCE LOCATION: O:\GEOLOGY\MU_1\MU-1_GIS_Mapping\MU-1 ACL Application\Maps\Figure A-16 Core Hole and Observation Well Location Map.mxd </small>				

Core Holes DG-1, ST-1, and UG-1

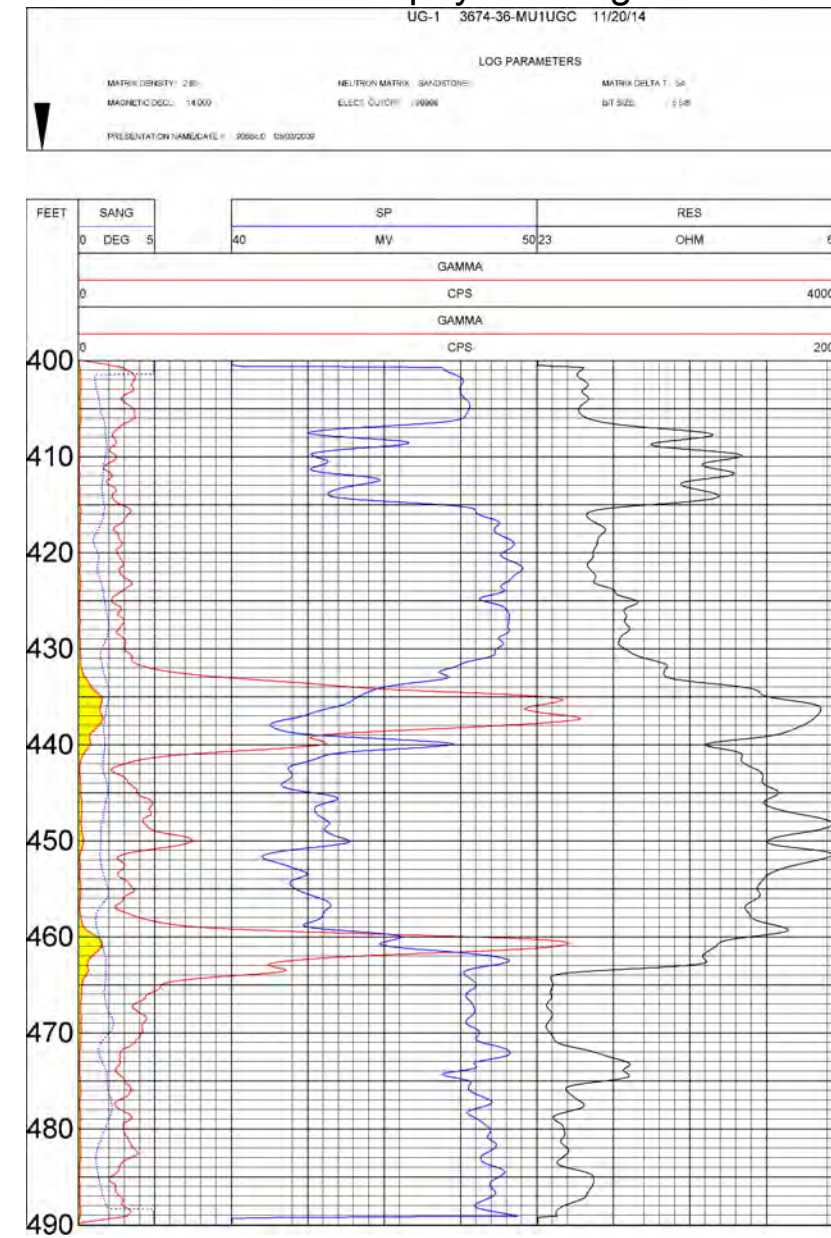
DG-1 Geophysical Log



ST-1 Geophysical Log



UG-1 Geophysical Log

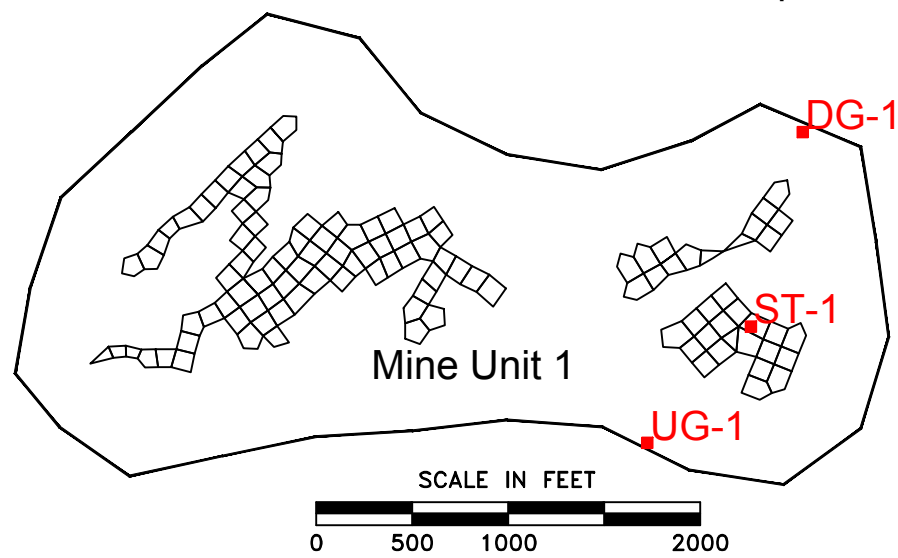


DG-1 Cored Interval: 450'-470'

ST-1 Cored Interval: 457'-477'

UG-1 Cored Interval: 438'-458'

DG-1, ST-1, and UG-1 Location Map

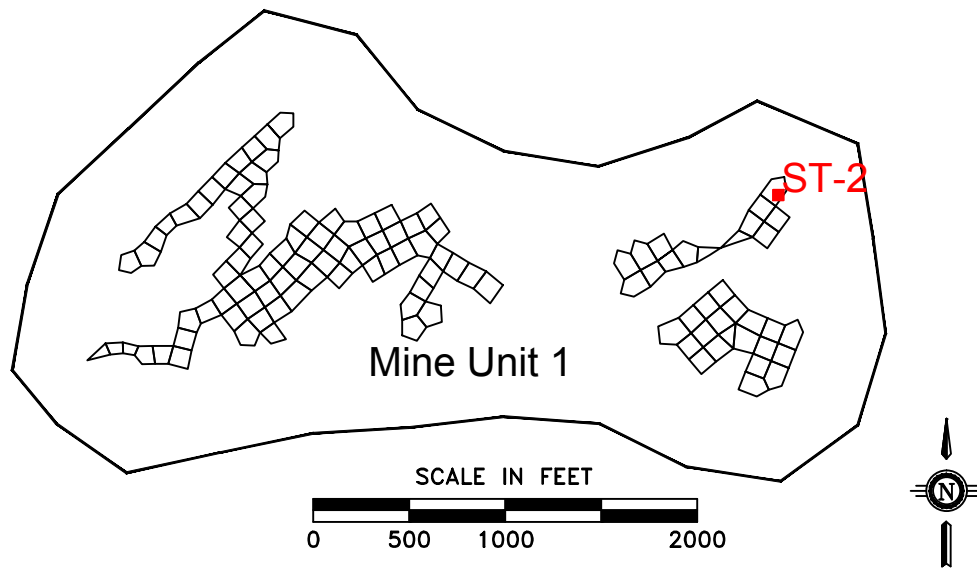


	Cameco Resources Smith Ranch-Highland Operation P.O. Box 1210 Casper, WY 82637 Telephone: (307) 358-6541		Figure A-19 Core Holes DG-1, ST-1 and UG-1 Geophysical Logs and Cored Intervals Mine Unit 1 ACL Application
	SIZE 11x17	DATE 4/19/2017	

Drawing Location: C:\GEOLOGY\MU-1 ACL\CL CORE LOG FILES AND PHOTOS(GEOPHYSICAL LOGS)\DG-1,ST-1,UG-1.DWG

Core Hole ST-2

ST-2 Location Map



ST-2 Core Sample Photos

463'

464'

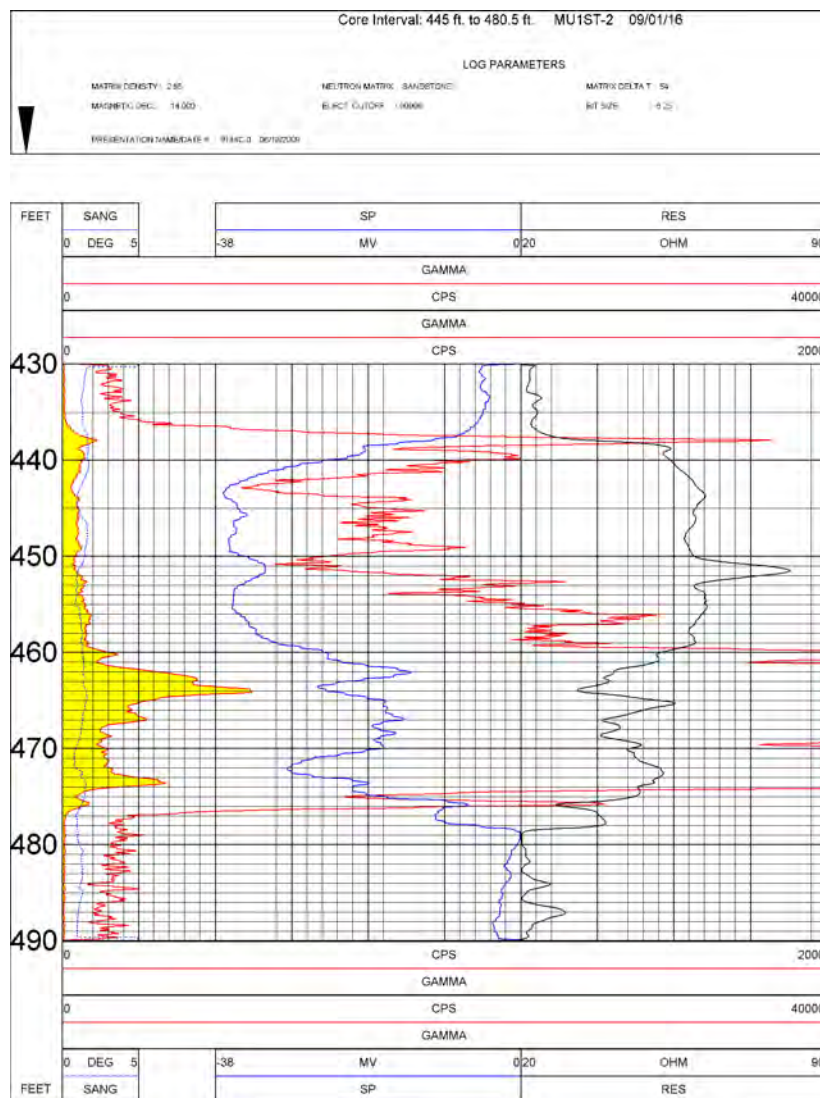


472'

473'



ST-2 Geophysical Log



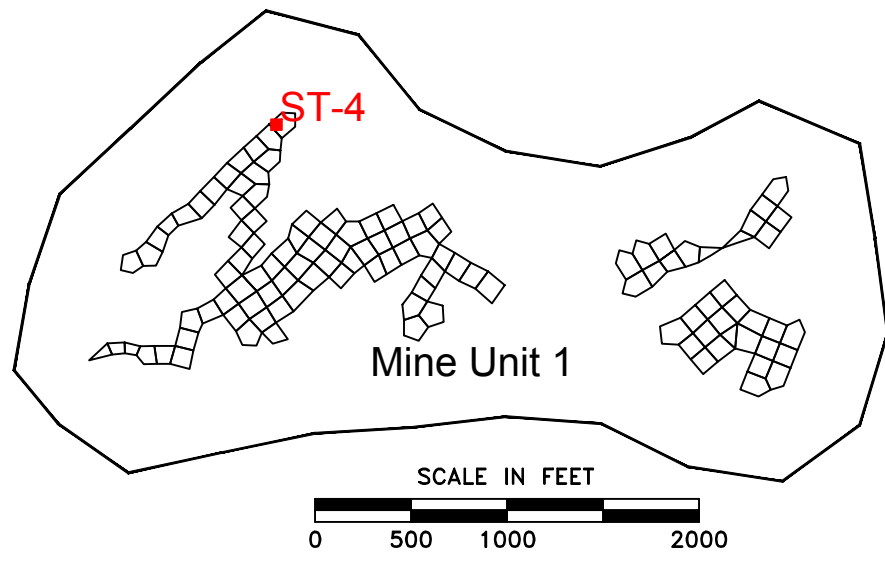
Core Sampled Intervals:
463'-464'
472'-473'

ST-2 Cored Interval:
445'-480.5'

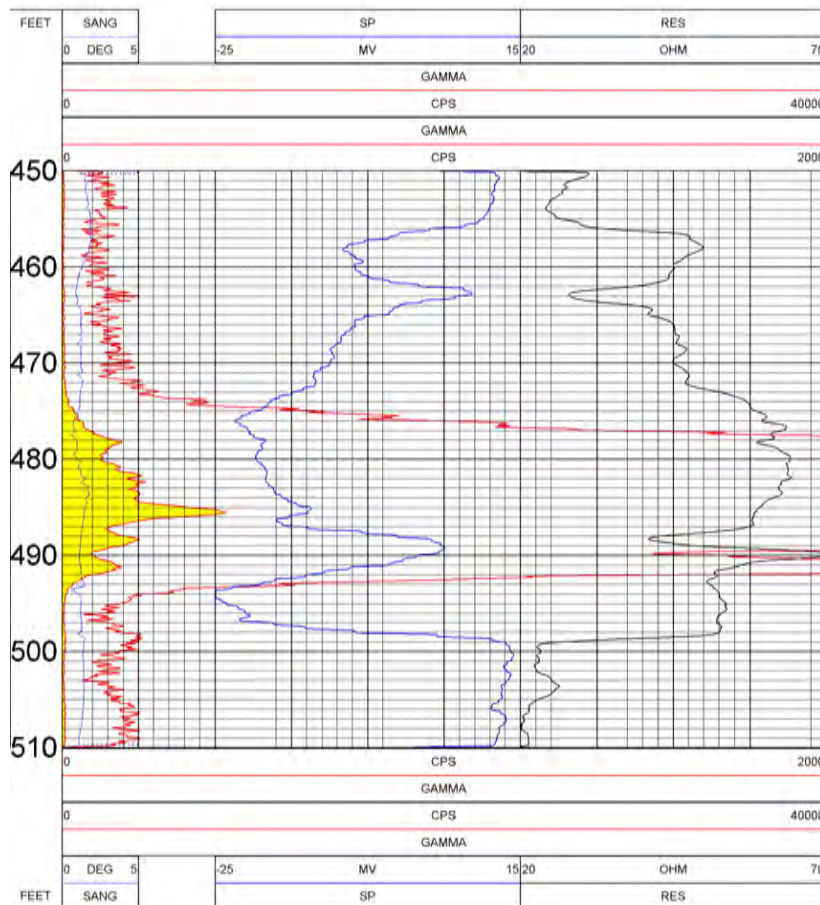
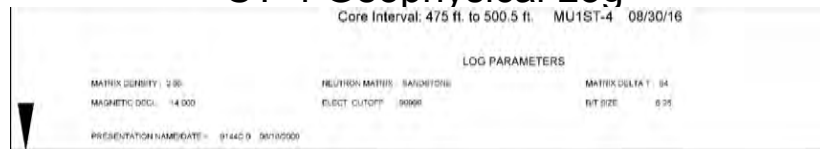
	Cameco Resources Smith Ranch-Highland Operation P.O. Box 1210 Casper, WY 82637 Telephone: (307) 358-6541		Figure A-20 Core Hole ST-2 Geophysical Log, Cored Interval and Core Photographs Mine Unit 1 ACL Application
	SIZE 11x17	DATE 4/19/2017	
Drawing Location: C:\GEOLOGY\MU_1 ACL\ACL CORE LOG FILES AND PHOTOS(GEOPHYSICAL LOGS)\ST-2.DWG			

Core Hole ST-4

ST-4 Location Map



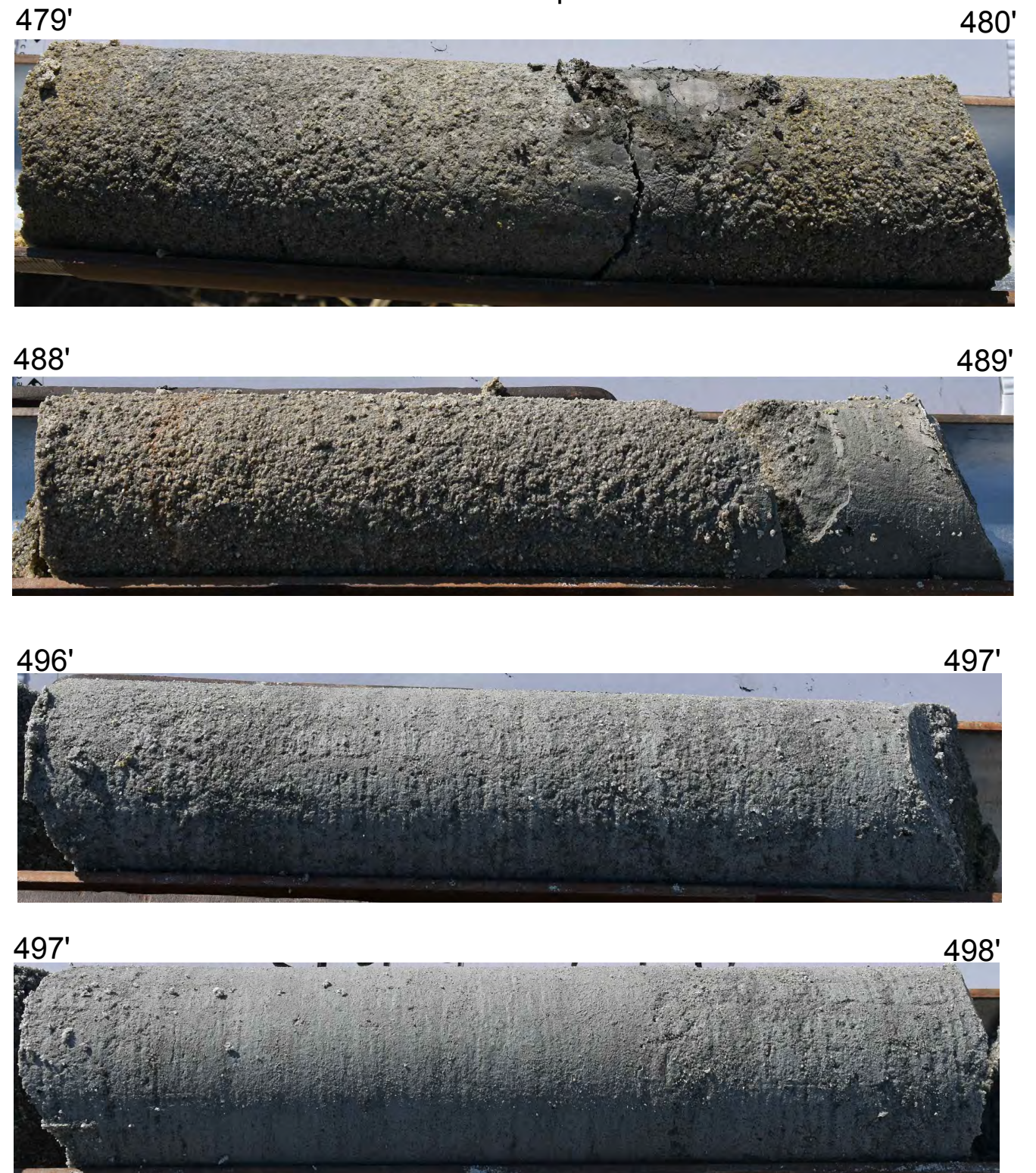
ST-4 Geophysical Log



Core Sampled Intervals:
 479'-480'
 488'-489'
 496'-497'
 497'-498'

ST-4 Cored Interval:
 475'-500.5'

ST-4 Core Sample Photos

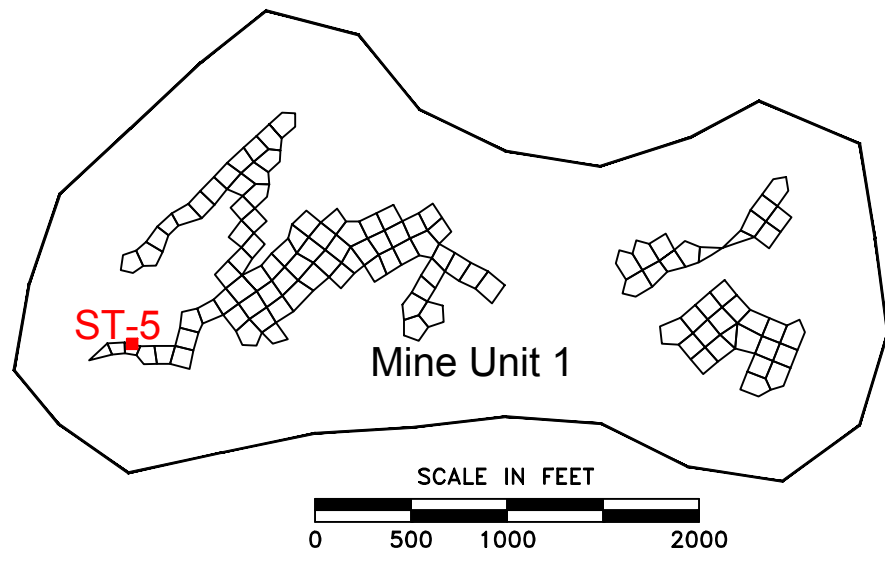


	Cameco Resources Smith Ranch-Highland Operation P.O. Box 1210 Casper, WY 82637 Telephone: (307) 358-6541	Figure A-22 Core Hole ST-4 Geophysical Log, Cored Interval and Core Photographs Mine Unit 1 ACL Application
	SIZE: 11x17 DATE: 4/19/2017 DEPARTMENT: Geology	Drawing Location: O:\GEOLOGY\MU-1\ACL\CL CORE LOG FILES AND PHOTOS\GEOPHYSICAL LOGS\ST-4LOG

Core Hole ST-5

ST-5 Core Sample Photos

ST-5 Location Map

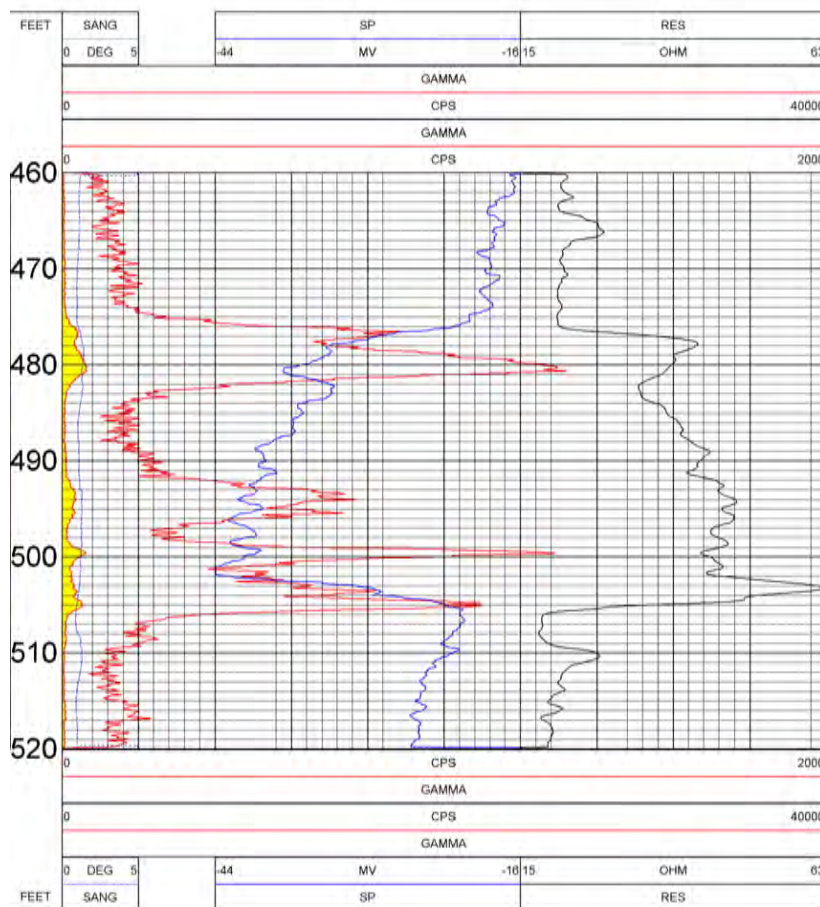


ST-5 Geophysical Log

CORE INTERVAL: 485-505.5 MU1ST-5 08/23/16

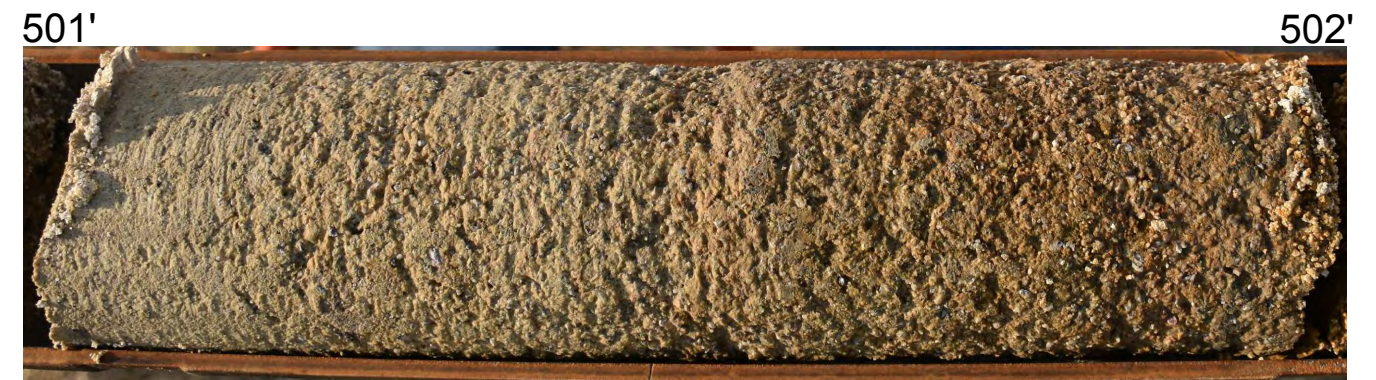
LOG PARAMETERS

MATRIX DENSITY: 2.65	NEUTRON MATRIX: SANDSTONE	MATRIX CORRECTION: 0.9
MAGNETIC DECL.: 14.000	ELECT. CUTOFF: 0.000	BIT SIZE: 8.25
PRESENTATION NAME/DATE: 0144C 0 30/16/2000		



Core Sampled Intervals:
 494'-495'
 499'-500'
 501'-502'
 503'-503.5'

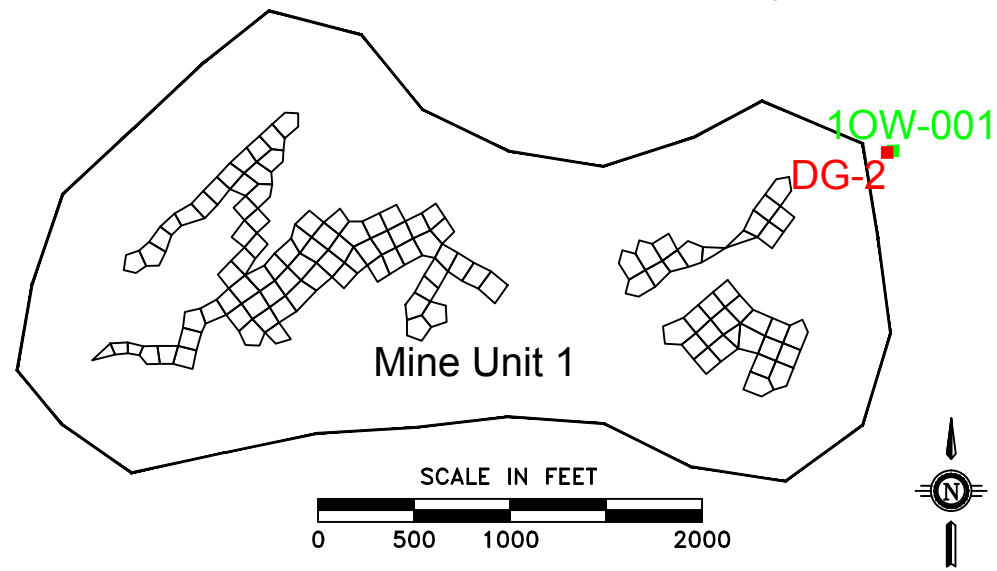
ST-5 Cored Interval:
 485'-505.5'



	Cameco Resources Smith Ranch-Highland Operation P.O. Box 1210 Casper, WY 82637 Telephone: (307) 358-6541		Figure A-23 Core Hole ST-5 Geophysical Log, Cored Interval and Core Photographs Mine Unit 1 ACL Application
	SIZE 11x17	DATE 4/19/2017	
Drawing Location: G:\GEOLOGY\MU-1 ACL\ACL CORE LOG FILES AND PHOTOS\GEOLOGICAL LOGS\ST-5LOG			

Core Hole DG-2 and Observation Well 1OW-001

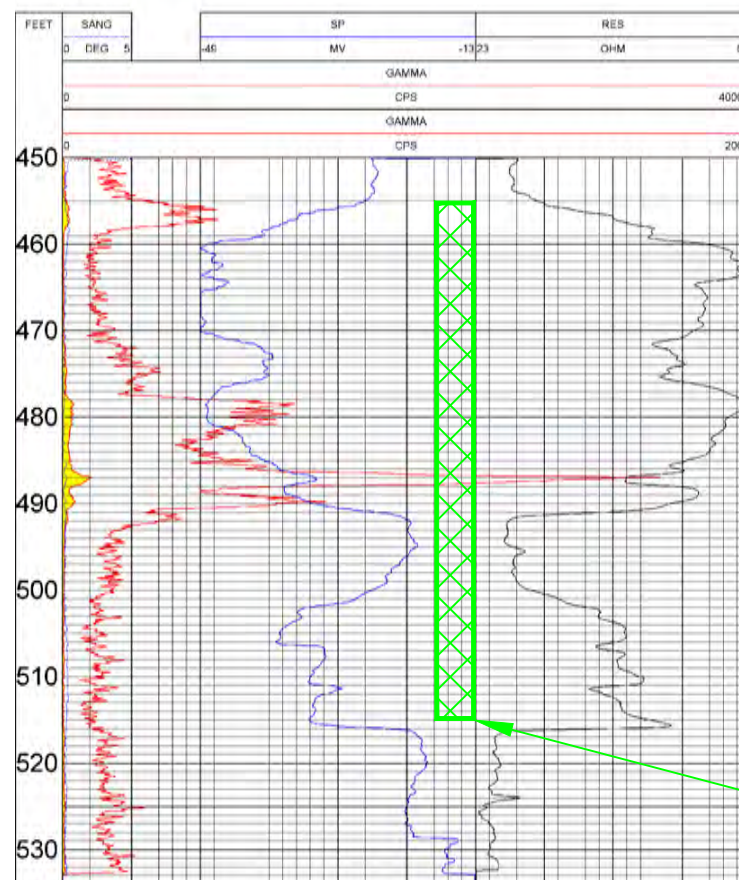
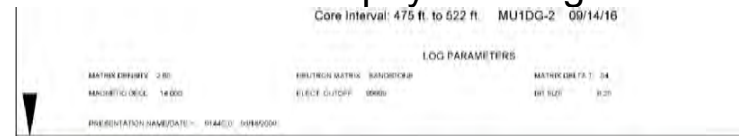
DG-2 and 1OW-001 Location Map



DG-2 Core Sample Photo



DG-2 Geophysical Log



Core Sampled Intervals:

- 477'-478' (No Photo Available)
- 482'-483' (No Photo Available)
- 487.5'-488.5' (No Photo Available)
- 504'-505'

DG-2 Cored Interval: 475'-522'

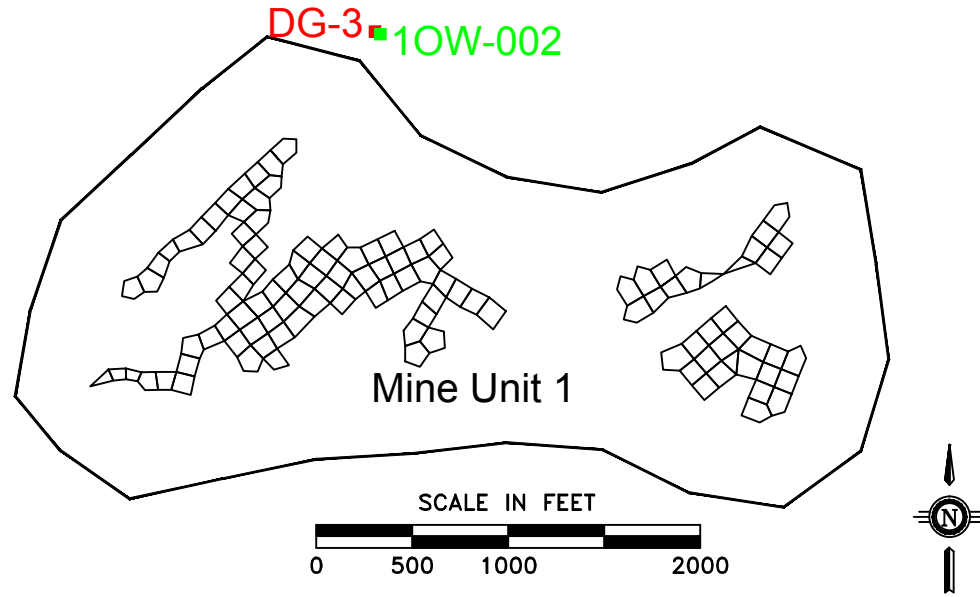
1OW-001 Screened Interval: 455'-515'
(Well is located about 4' East of Core Hole DG-2)

	Cameco Resources Smith Ranch-Highland Operation P.O. Box 1210 Casper, WY 82637 Telephone: (307) 358-6541	Figure A-24 Core Hole DG-2 Geophysical Log, Cored Interval, Core Photographs and Observation Well 1OW-001 Screened Interval Mine Unit 1 ACL Application
	SIZE: 11x17 DATE: 4/25/2017 DEPARTMENT: Geology	

Drawing Location: O:\GEOLOGY\MU-1\ACL\CL CORE LOG FILES AND PHOTOS\GEOPHYSICAL LOGS\DG-2 AND 1OW-001.DWG

Core Hole DG-3 and Observation Well 1OW-002

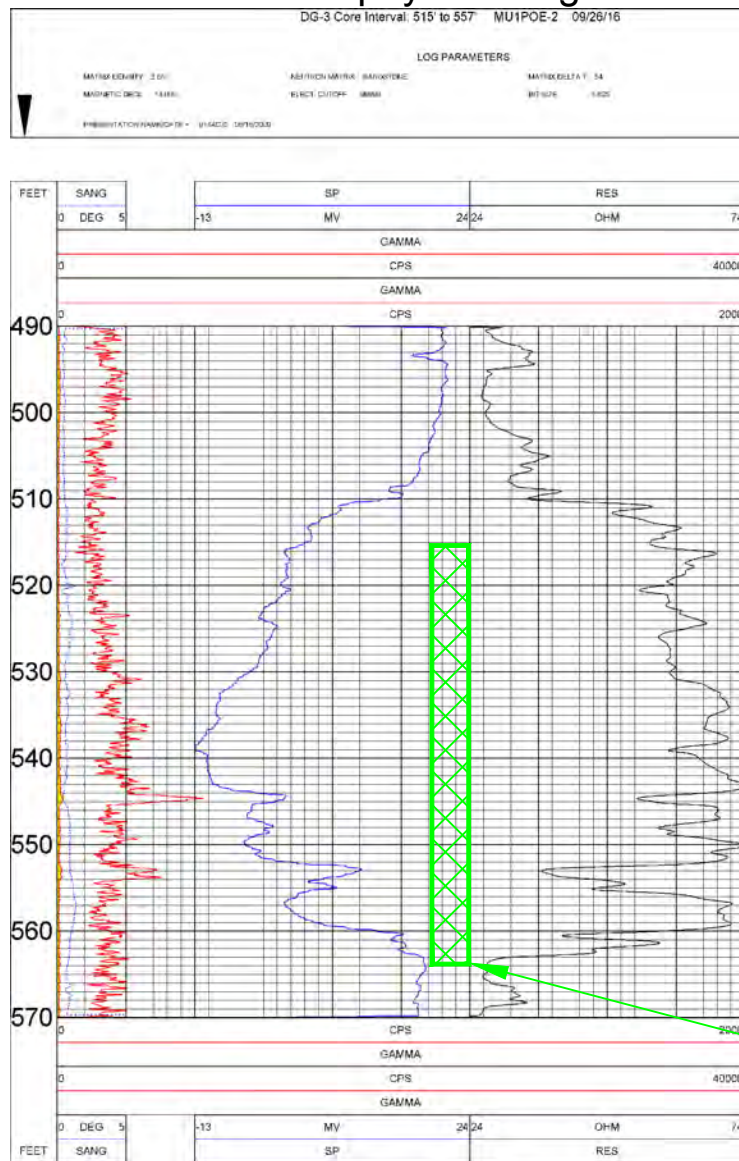
DG-3 and 1OW-002 Location Map



DG-3 Core Sample Photos



DG-3 Geophysical Log



Core Sampled Intervals:
524'-525'
543'-544'
551'-551.7'

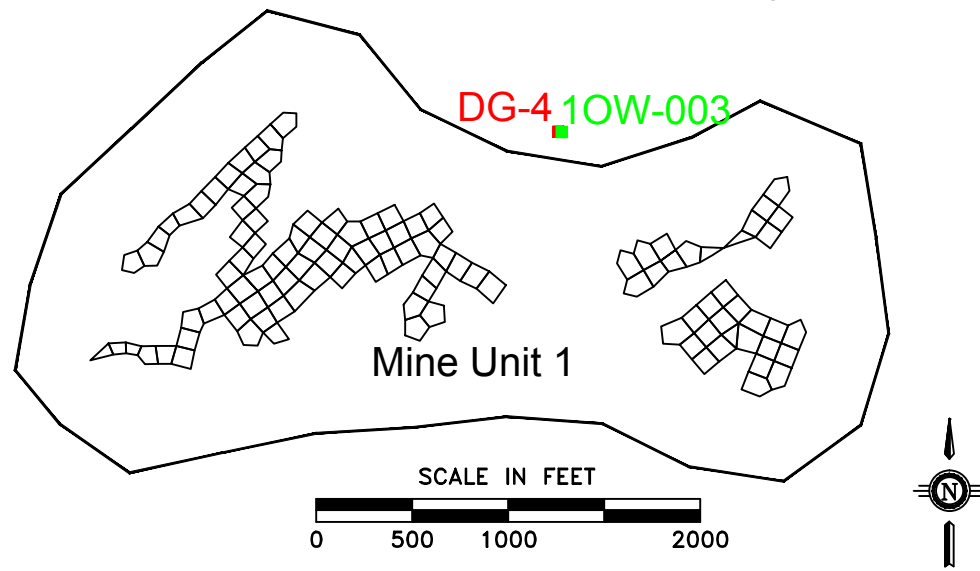
DG-3 Cored Interval:
515'-557'

1OW-002 Screened Interval:
510'-563'
(Well is located about 24' East of Core Hole DG-3)

	Cameco Resources Smith Ranch-Highland Operation P.O. Box 1210 Casper, WY 82637 Telephone: (307) 358-6541		Figure A-25 Core Hole DG-3 Geophysical Log, Cored Interval, Core Photographs and Observation Well 1OW-002 Screened Interval Mine Unit 1 ACL Application
	SIZE 11x17	DATE 4/25/2017	
Drawing Location: G:\GEOLOGY\MU-1 ACL\ACL CORE LOG FILES AND PHOTOS(GEOPHYSICAL LOGS)\DG-3 AND 1OW-002.DWG			

Core Hole DG-4 and Observation Well 1OW-003

DG-4 and 1OW-002 Location Map

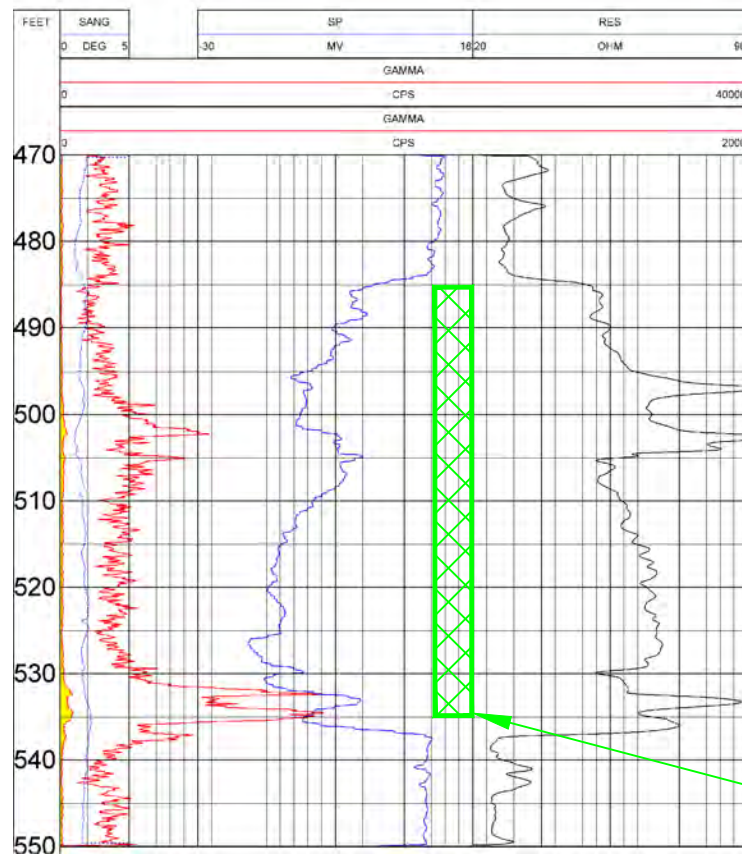


DG-4 Core Sample Photo



DG-4 Geophysical Log

LOG PARAMETERS	
MAGNETIC DEVIATION	3.00
MAGNETIC DEVIATION	14.00
INSTRUMENTATION	10/18/18



Core Sampled Interval:
516'-517'

DG-4 Cored Interval:
495'-535'

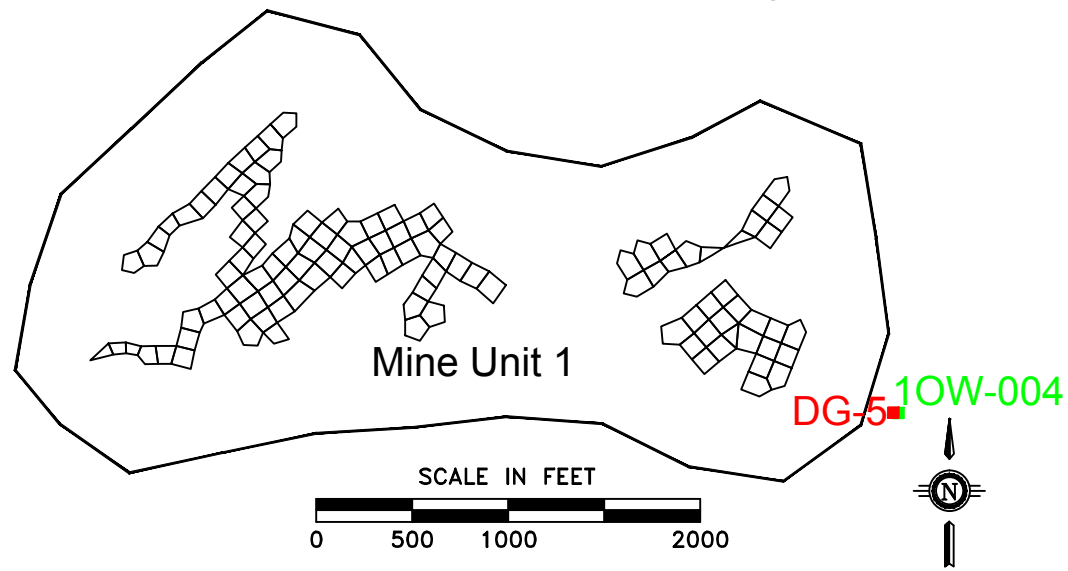
1OW-003 Screened Interval:
485'-535'
(Well is located about 10' East of
Core Hole DG-4)

	Cameco Resources Smith Ranch-Highland Operation P.O. Box 1210 Casper, WY 82637 Telephone: (307) 358-6541	Figure A-26 Core Hole DG-4 Geophysical Log, Cored Interval, Core Photographs and Observation Well 1OW-003 Screened Interval Mine Unit 1 ACL Application
	SIZE: 11x17 DATE: 4/25/2017 DEPARTMENT: Geology	

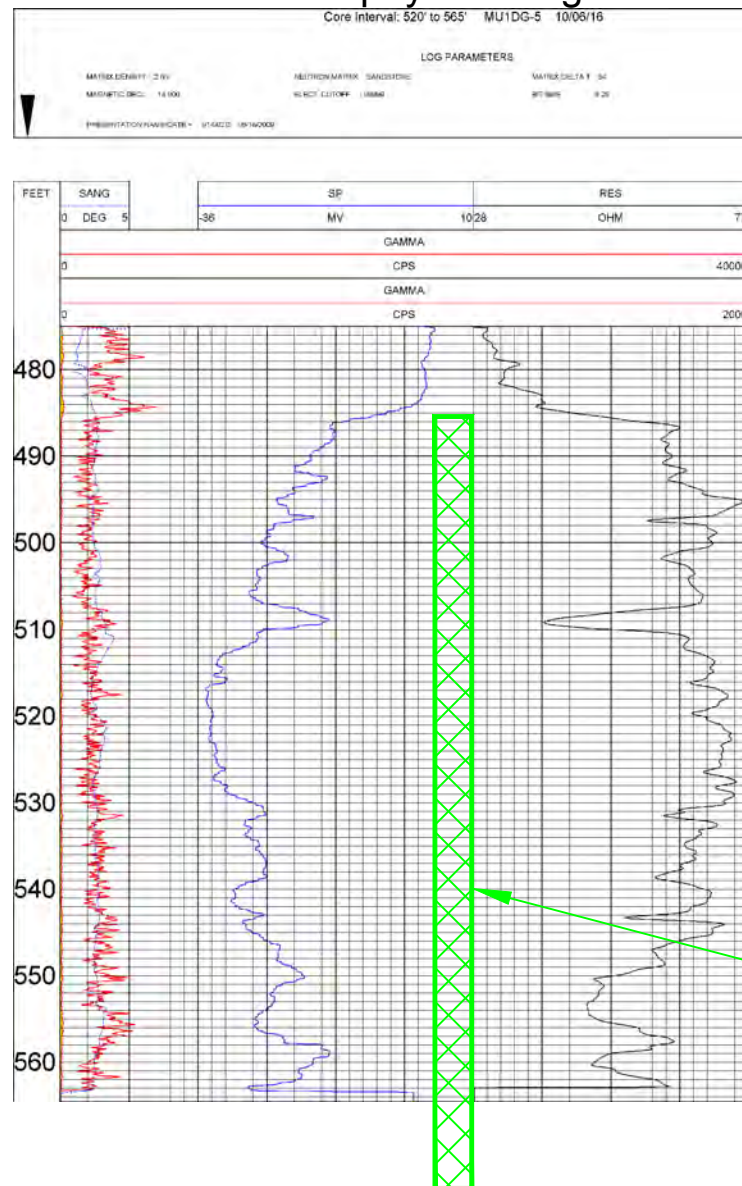
Core Hole DG-5 and Observation Well 1OW-004

DG-5 Core Sample Photos

DG-5 and 1OW-004 Location Map



DG-5 Geophysical Log



Cameco Resources
Smith Ranch-Highland Operation
P.O. Box 1210
Casper, WY 82637
Telephone: (307) 358-6541

Figure A-27

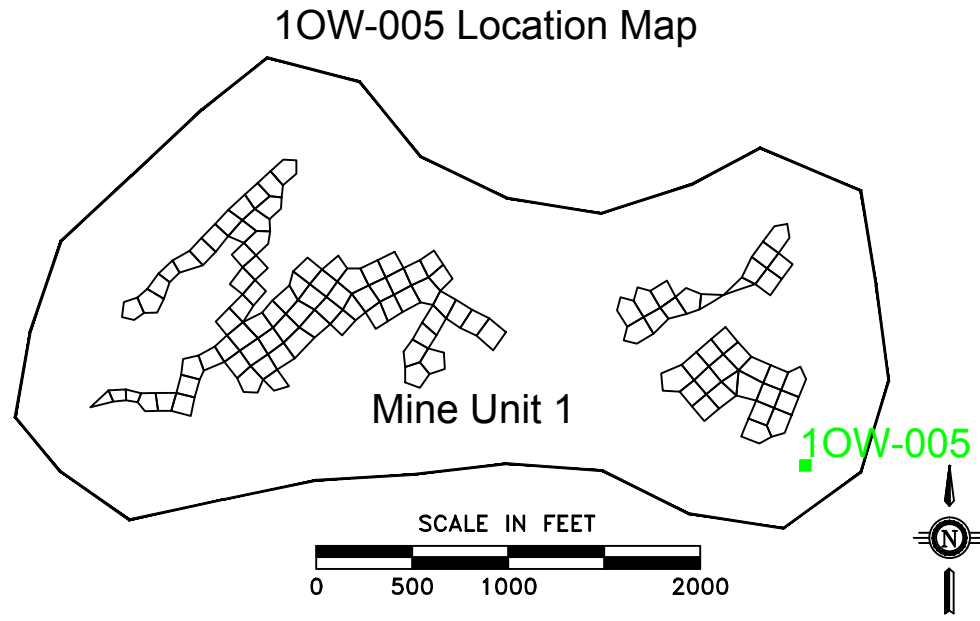
Core Hole DG-5 Geophysical Log, Cored Interval, Core Photographs and Observation Well 1OW-004 Screened Interval Mine Unit 1 ACL Application

SIZE	DATE	DEPARTMENT:
11x17	4/25/2017	Geology

Drawing Location: G:\GEOLOGY\MU_1 ACL\CL CORE LOG FILES AND PHOTOS(GEOPHYSICAL LOGS)\DG-5 AND 1OW-004.DWG

Observation Well 1OW-005

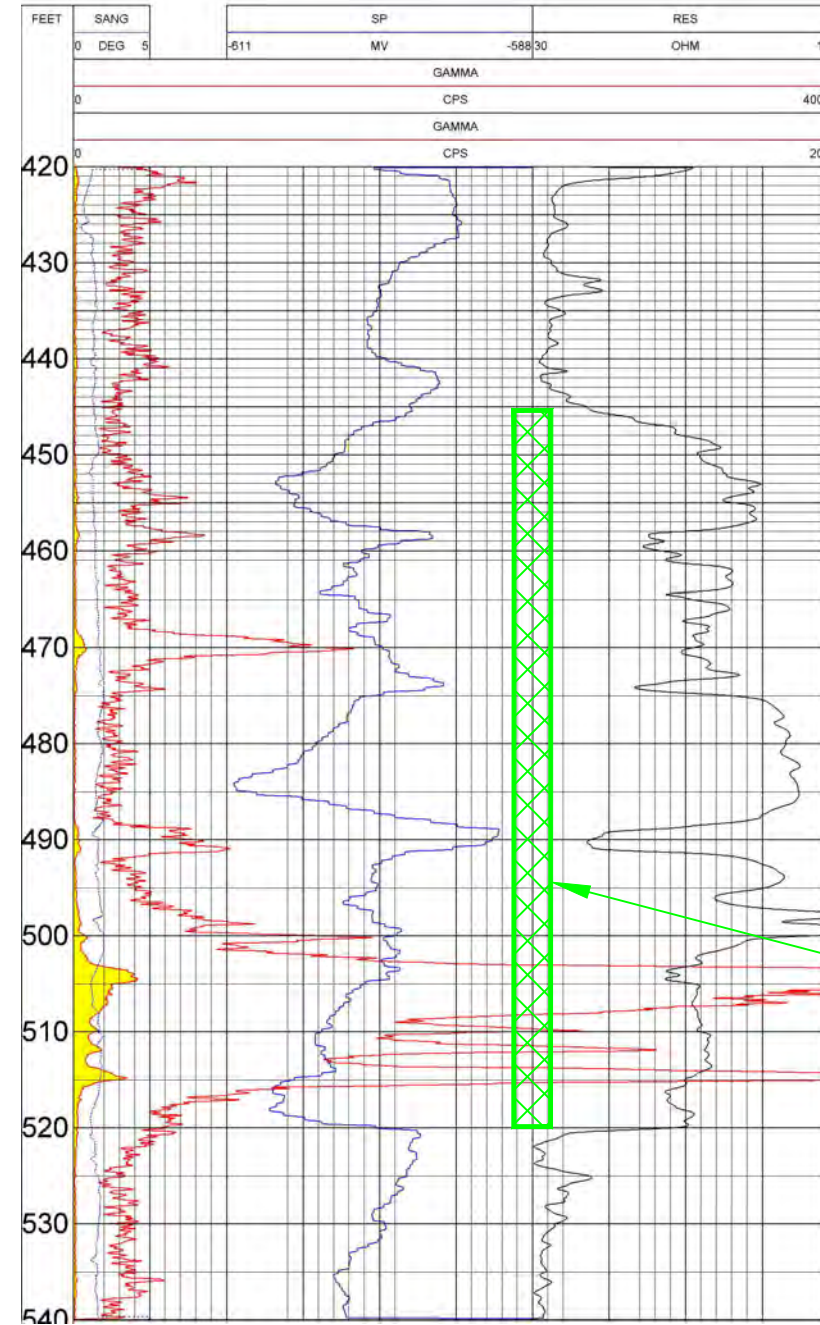
1OW-005 Geophysical Log



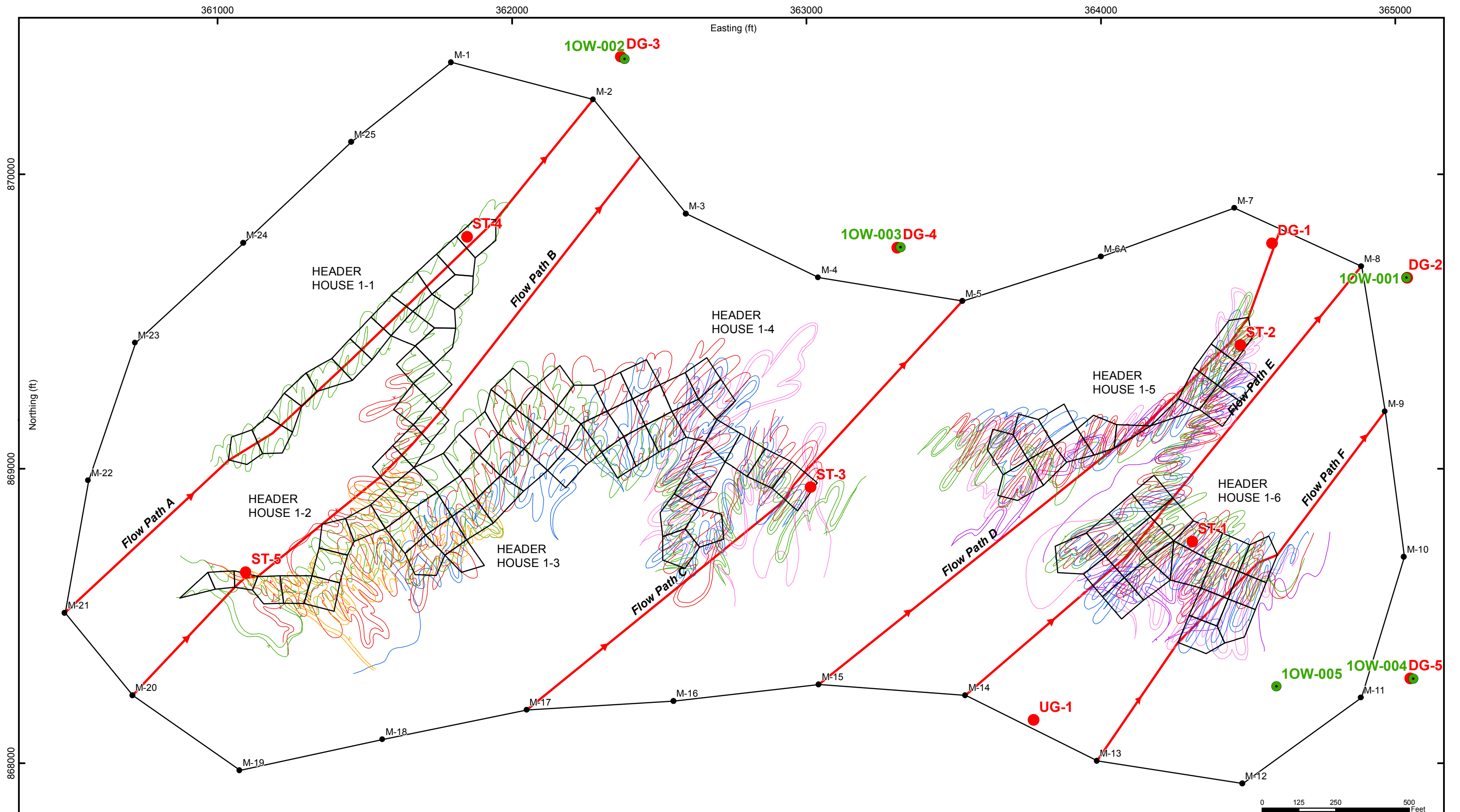
3674-36-1OW-005 10/13/16

LOG PARAMETERS

MATRIX DENSITY: 2.65	NEUTRON MATRIX: SANDSTONE	MATRIX DELTA T: 54
MAGNETIC DGL: 14.000	ELECT. CUT/OFF: /WWW	BIT SIZE: 1.500
PRESENTATION NAME/DATE: IP14C3EST/0 06/16/2009		



<p>Cameco Resources Smith Ranch-Highland Operation P.O. Box 1210 Casper, WY 82637 Telephone: (307) 358-6541</p>	<p>Figure A-28 Observation Well 1OW-005 Geophysical Log and Screened Interval Mine Unit 1- ACL Application</p>	
	<p>SIZE: 11x17</p>	<p>DATE: 4/25/2017</p>
<p>Drawing Location: C:\GEOLOGY\MU_1\ACL\ACL CORE LOG FILES AND PHOTOS\GEOPHYSICAL LOGS\1OW-005.DWG</p>		



Legend

Mineralization Horizon

- Orange Zone
- Red Zone
- Pink Zone
- Green Zone
- Blue Zone
- Purple Zone
- Monitor Well
- Observation Well
- Core Hole
- MU1_FlowPath
- Wellfield Pattern



Cameco Resources
P.O. Box 1210
Glenrock, WY 82637
Telephone: (307) 358-6541

SIZE	DATE	DEPARTMENT	
X	6/13/2017	Geology	

Location System: NAD 1983 StatePlane Wyoming East FIPS 4901
Datum: North American 1983

Figure A-29
Roll Front & Flow Path Map
Mine Unit 1 ACL Application


 1:3,500

Location System: NAD 1983 StatePlane Wyoming East FIPS 4901
Datum: North American 1983

Pathing Location: O:\GEOLOGY\MU_1\MU-1_GIS_Mapping\MU-1 ACL Application\Maps\Figure A-29 Mine Unit 1 Flow Path Map.mxd

TABLES

**TABLE A-1
MINE UNIT 1 CORE HOLE INFORMATION SUMMARY
MINE UNIT 1 ACL APPLICATION**

CORE HOLE	NORTHING (FT)*	EASTING (FT)*	GROUND LEVEL ELEVATION IN MSL (FT)	TWN	RNG	QTR/QTR SEC	GEOPHYSICAL LOG DATE	6 1/4" TOTAL DRILL DEPTH (FT)	CORE INTERVAL (FT.)
DG-1	869765	364582	5514	36N	74W	NE/NE 36	11/26/2014	520	450-470
DG-2	869649	365040	5524	36N	73W	NW/NW 31	9/14/2016	560	475-522
DG-3	870399	362369	5575	36N	74W	NW/NE 36	9/21/2016	600	515-557
DG-4	869751	363309	5550	36N	74W	NE/NE 36	10/19/2016	580	495-535
DG-5	868287	365052	5577	36N	73W	SW/NW 31	10/6/2016	600	520-565
ST-1	868752	364311	5511	36N	74W	SE/NE 36	11/24/2014	520	457-477
ST-2	869420	364474	5501	36N	74W	SE/NE 36	9/1/2016	540	445-480.5
ST-3	868937	363014	5511	36N	74W	SW/NE 36	8/25/2016	520	455-483
ST-4	869788	361847	5533	36N	74W	NE/NW 36	8/30/2016	540	475-500.5
ST-5	868662	361096	5558	36N	74W	SE/NW 36	8/23/2016	560	485-505.5
UG-1	868146	363772	5494	36N	74W	NE/SE 36	11/20/2014	500	438-458

* COORDINATE SYSTEM: NAD27 US STATE PLANE: WY EAST 4901

**TABLE A-2
MINE UNIT 1 OBSERVATION WELL SUMMARY
MINE UNIT 1 ACL APPLICATION**

WELL	NORTHING (FT)*	EASTING (FT)*	GROUND LEVEL ELEVATION IN MSL (FT)	CASING STICK-UP (FT)	TWN	RNG	QTR/QTR SEC	GEOPHYSICAL LOG DATE	5 5/8" PILOT DRILL DEPTH (FT)	8 3/4" REAM DRILL DEPTH (FT)	SCREENED INTERVAL (FT.)	CASING TYPE	GRAVEL PACK TYPE	GROUT INTERVAL (FT)	GROUT TYPE
1OW-001	869648.93	365037.21	5524.26	2.26	36N	73W	NW/NW 31	9/28/2016	540	515	455-515	5" PVC, SDR17	1/4" Diameter Pea Gravel	0-455	3/8" Bentonite Chips
1OW-002	870392.81	362382.36	5575.70	1.38	36N	74W	NW/NE 36	9/26/2016	580	563	510-563	5" PVC, SDR17	1/4" Diameter Pea Gravel	0-510	3/8" Bentonite Chips
1OW-003	869751.97	363319.89	5550.14	2.33	36N	74W	NE/NE 36	10/11/2016	580	485	485-535	5" PVC, SDR17	1/4" Diameter Pea Gravel	0-485	3/8" Bentonite Chips
1OW-004	868286.46	365061.23	5577.85	1.35	36N	73W	SW/NW 31	10/3/2016	600	575	485-575	5" PVC, SDR17	1/4" Diameter Pea Gravel	0-485	3/8" Bentonite Chips
1OW-005	868259.95	364595.98	5546.05	1.59	36N	74W	SE/NE 36	10/13/2016	580	520	445-520	5" PVC, SDR17	1/4" Diameter Pea Gravel	0-485	3/8" Bentonite Chips

* COORDINATE SYSTEM: NAD27 US STATE PLANE: WY EAST 4901

ATTACHMENT A-1

MU1 CORE DESCRIPTION AND ANALYSIS
Including MU1-DG, MU1-ST, & MU1-UG

Dr. Susan M. Swapp

Department of Geology and Geophysics

University of Wyoming

Laramie, Wyoming

April 10, 2016

TABLE OF CONTENTS

Methods

Sample Selection and Preparation..... 4

Hand Sample Petrography 4

Optical Petrography 4

Scanning Electron Microscopy 4

X-Ray Diffraction 5

Bulk Chemical Analysis..... 5

Whole Rock Chemistry..... 5

Petrography 5

Hand Sample Observations..... 5

Electron Microscopy Observations..... 9

Map Interpretation Consideration..... 9

Common Characteristics of all Samples..... 9

MU1-DG Samples..... 10

MU1-ST Samples..... 10

MU1-UG Samples..... 10

Clay Mineralogy 11

Modal Analysis 12

Summary 12

Figures 13 - 34

Appendix A 35

TABLES AND FIGURES

Table 1	Samples in this study	4
Table 2	MU1-DG Whole Rock Chemical Analyses	6
Table 3	MU1-ST Whole Rock Chemical Analyses	7
Table 4	MU1-UG Whole Rock Chemical Analyses	8
Figure 1	MU1-DG Composite Backscattered Electron Images	13
Figure 2	MU1-DG-451-452 X-Ray Maps.....	14
Figure 3	MU1-DG-456-457 X-Ray Maps.....	15
Figure 4	MU1-DG-460-461 X-Ray Maps.....	16
Figure 5	MU1-DG-465-466 X-ray Maps	17
Figure 6	MU1-DG-469-470 X-ray Maps	18
Figure 7	MU1-ST Composite Backscattered Electron Maps.....	19
Figure 8	MU1-ST-457-458 X-ray Maps.....	20
Figure 9	MU1-ST-463-464 X-ray Maps.....	21
Figure 10	MU1-ST-470-471 X-ray Maps.....	22
Figure 11	MU1-ST-473-474 X-ray Maps.....	23
Figure 12	MU1-ST-478-477 X-ray Maps.....	24
Figure 13	MU1-UG Composite Backscattered Electron Maps.....	25
Figure 14	MU1-UG-438-439 X-ray Maps	26
Figure 15	MU1-UG-442-443 X-ray Maps	27
Figure 16	MU1-UG-446-447 X-ray Maps	28
Figure 17	MU1-UG-452-453 X-ray Maps	29
Figure 18	MU1-UG-454-455 X-ray Maps	30
Figure 19	Clay Mineralogy, MU1-DG	31
Figure 20	Clay Mineralogy, MU1-ST	32
Figure 21	Clay Mineralogy, MU1-UG	33
Figure 22	Modal Analysis, All Samples.....	34

Table 1: Samples in this report.

MU1-DG	MU1-ST	MU1-UG
438' - 439'	457' - 458'	451' - 452'
442' - 443'	463' - 464'	456' - 457'
446' - 447'	470' - 471'	460' - 461'
452' - 453'	473' - 474'	465' - 466'
454' - 455'	476' - 477'	469' - 470'

This report describes mineralogy, petrography, petrofabrics, and whole rock chemistry of fifteen samples from three cores from MU1 (Table 1). This material was delivered to the University of Wyoming on Dec. 9, 2014. These samples were collected after mining operations were completed.

I. METHODS:

Sample Selection and Preparation: 1" – 2" sections of core were selected from each of the 15 intervals. A thin section billet approximately 20 mm X 40mm X 8 mm was cut from the core for use in preparing polished petrographic thin sections. The balance of the selected portion was powdered for whole rock chemical analysis and for powder X-Ray diffraction analysis.

Standard polished petrographic thin sections were prepared for each sample by Vancouver Petrographics (30 µm thick, polished to 0.25 µm diamond surface). Some samples are so poorly indurated that they partially disaggregated during cutting. In order to preserve the original petrofabric character of the samples to the maximum extent possible, all 15 samples were vacuum impregnated with epoxy before sending them out for thin section preparation.

Sample not sent for thin section preparation was powder in a tungsten carbide shatter box. A 10 – 15 gram aliquot of the powdered material was sent to ALS for bulk chemical analysis. Samples with known compositions were included as checks on the accuracy of the analyses.

Remaining powdered samples were used for X-ray diffraction study. Details of instrumentation, sample preparation, and operating conditions are discussed below in the X-ray diffraction section.

Conventional Hand Sample Petrography: Core samples were examined in their entirety using hand lens and dilute hydrochloric acid. The advantage of this approach is that it enables examination of the largest possible fraction of the available material, and it also allows observation of properties that may not be apparent using more technologically sophisticated methods (e.g., color, degree of induration, and large-scale fabric features).

Optical Petrography: Petrographic thin sections were examined in a polarizing microscope. This examination confirmed quality of sample preparation, degree of heterogeneity of the samples, and general petrofabric features of the sample. Images of each thin section were created for use in recording details of later observations.

Scanning Electron Microscopy: Polished samples were analyzed using two electron microscopes at the University of Wyoming. Both methods utilize polished samples of rock from the cores; all samples are necessarily carbon-coated for conductivity prior to analysis.

Quanta 450 Field Emission Scanning Electron Microscope: This instrument is equipped with an Oxford Energy Dispersive Light-Element X-Ray Spectrometer and is capable of spatial resolution on the order of 20 nanometers. The principle advantage of this instrument is high spatial resolution.

JEOL JXA-8900R Superprobe: This instrument is an electron probe microanalyzer and is equipped with a Thermo NSS EDS system and with 5 wavelength dispersive x-ray spectrometers. This instrument is capable of spatial resolution on the order of 2 microns. The advantage of this instrument is the full integration of stage automation with EDS analysis, advanced EDS data processing capabilities, and the availability of wavelength dispersive x-ray spectrometers that enable resolution of characteristic x-ray peaks that overlap severely in EDS analysis.

X-Ray Diffraction: Powdered aliquots of each sample were analyzed for identification and quantification of crystalline phases (minerals) using the Scintag XDS2000 powder x-ray diffractometer at the University of Wyoming. This instrument is equipped with a copper x-ray tube. Data were acquired using 40 KeV, 30 mA tube settings and various scanning rates. Bulk samples were examined to determine abundances of constituent phases, and clay separates were examined to identify clay species present.

Bulk Chemical Analysis: Major, minor, and trace element concentrations for bulk samples were acquired from powdered aliquots of each sample. We used the ALS commercial laboratory to acquire these data.

II. WHOLE-ROCK CHEMISTRY

Powdered samples were sent to ALS-Global for whole-rock chemical analysis (Tables 2, 3, and 4). Major elements were analyzed as oxides using inductively coupled plasma – atomic emission spectroscopy (ICP-AES, ALS Process ME_ICP06), and trace elements were analyzed using inductively coupled plasma – mass spectrometry (ICP-MS, ALS Process ME-MS81). See Appendix A for method details.

The data are typical of immature arkosic sediments and are consistent with observed mineralogy (see below). High tungsten values are certainly a consequence of powdering the samples for analysis in a tungsten carbide shatter box. None of the samples show significant uranium enrichment, although samples from the UG hole have uranium concentrations approximately 10 times higher than the other two cores.

III. PETROGRAPHY

a. Hand Sample Observations

All samples examined in this study are drill core materials. They are uniformly gray, coarse-grained, homogeneous samples that are poorly indurated and that tend to disaggregate if not handled with extreme care. All samples are arkosic sandstones with obvious feldspar, quartz, and clay components. Calcite was recognized in one sample in hand sample (MU1-DG 451'-452') where it occurs as pervasive cement. Pyrite was not recognized in any of the hand samples. Organic material was tentatively identified in one sample (MU1-DG-451-452) and confirmed in microscopic examination.

Table 2(a): Major and minor element concentrations, in weight percent oxides. (LOI = Loss on Ignition)

Oxide Weight Percent					
Depth (ft)	451'-452'	456'-457'	461'-462'	465'-466'	469'-470'
SiO ₂	60.8	82.2	81.7	82	83.7
Al ₂ O ₃	5.61	9.19	10.75	10.10	9.27
Fe ₂ O ₃	1.16	1.06	0.57	0.48	0.74
CaO	15.70	0.62	0.41	0.40	0.49
MgO	0.36	0.44	0.28	0.24	0.32
Na ₂ O	0.81	1.66	2.05	1.90	1.68
K ₂ O	1.98	2.91	4.38	4.56	3.52
Cr ₂ O ₃	n.d.	0.01	n.d.	n.d.	n.d.
TiO ₂	0.09	0.11	0.06	0.05	0.12
MnO	0.18	0.01	0.01	n.d.	0.01
P ₂ O ₅	0.02	0.01	0.02	0.01	0.02
SrO	0.01	0.01	0.01	0.01	0.01
BaO	0.04	0.07	0.07	0.08	0.06
LOI	13.90	2.06	1.45	0.91	1.51
Total	100.66	100.36	101.76	100.74	101.45

Table 2: Bulk chemical analyses for 5 samples from MU1-DG. These data were acquired by ALS-Global, using their processes ME-ICP06 and ME-MS81. See Appendix A for analytical details.

Table 2(b): Trace element concentrations, in parts per million.

Elements, Parts per Million					
Depth (ft)	451'-452'	456'-457'	461'-462'	465'-466'	469'-470'
Ba	366	659	649	669	572
Ce	23.4	25.3	26.9	22.3	41.7
Cr	10	40	10	10	20
Cs	0.75	0.35	0.95	0.72	0.71
Dy	1.37	1.62	1.25	1.23	1.81
Er	0.86	1.1	0.69	0.73	0.93
Eu	0.38	0.35	0.33	0.39	0.44
Ga	6.9	10.7	12.3	11.1	11.2
Gd	1.36	1.84	1.43	1.4	2.22
Hf	2.3	2.6	2.2	2.2	3.4
Ho	0.28	0.34	0.27	0.24	0.39
La	13.5	14.9	15.3	12.9	23.1
Lu	0.12	0.15	0.1	0.08	0.17
Nb	3.3	3.6	3	2.4	3.9
Nd	9.8	10.8	11.1	9.7	16.2
Pr	2.67	3.02	3.15	2.68	4.68
Rb	61.7	79.5	137.5	131	105
Sm	1.8	2.04	2.19	1.89	2.78
Sn	1	19	4	4	14
Sr	80.4	108.5	91.5	95	90.2
Ta	0.7	1.2	1	1.4	1.5
Tb	0.21	0.26	0.2	0.18	0.31
Th	4.88	7.86	6.44	6.24	12.45
Tm	0.11	0.19	0.09	0.09	0.15
U	7.39	6.97	8.43	5.51	5.92
V	15	85	8	6	11
W	148	442	366	567	483
Y	8.1	10.6	6.5	6.4	10.4
Yb	0.79	1.16	0.66	0.66	1.03
Zr	84	88	72	68	110

Table 3(a): Major and minor element concentrations, in weight percent oxides. (LOI = Loss on Ignition)

Oxide Weight Percent						
Depth (ft)	442'-443'	457'-458'	463'-464'	470'-471'	473'-474'	476'-477'
SiO2	81.4	79.6	79.3	82.2	81.1	81.9
Al2O3	9.33	9.95	11.35	10.25	10.10	10.35
Fe2O3	1.68	1.21	1.10	0.76	0.79	0.63
CaO	0.50	0.48	0.43	0.50	0.48	0.46
MgO	0.62	0.32	0.40	0.29	0.37	0.27
Na2O	1.17	1.64	1.74	1.86	1.71	1.88
K2O	2.63	3.85	4.20	3.96	3.55	4.02
Cr2O3	n.d.	0.01	n.d.	n.d.	n.d.	n.d.
TiO2	0.20	0.35	0.10	0.09	n.d.	0.07
MnO	0.01	0.02	n.d.	0.01	0.01	n.d.
P2O5	0.03	0.05	0.02	0.02	0.02	0.02
SrO	0.01	0.01	0.01	0.01	0.01	0.01
BaO	0.06	0.07	0.08	0.08	0.07	0.08
LOI	3.04	1.98	2.78	1.65	2.05	1.56
Total	100.68	99.54	101.51	101.68	100.36	101.25

Table 3: Bulk chemical analyses for 6 samples from MU1-ST. These data were acquired by ALS-Global, using their processes ME-ICP06 and ME-MS81. See Appendix for analytical details.

Table 3(b): Trace element concentrations, in parts per million.

Elements, Parts per Million						
Depth (ft)	442'-443'	457'-458'	463'-464'	470'-471'	473'-474'	476'-477'
Ba	590	675	731	676	696	729
Ce	32.5	232	27.9	26.6	27.3	23.1
Cr	30	60	20	20	20	10
Cs	1.18	0.66	1.11	0.62	0.61	0.57
Dy	1.72	7.73	1.62	1.47	1.3	1.26
Er	1.1	4.16	0.99	0.8	0.71	0.77
Eu	0.64	0.87	0.48	0.46	0.45	0.48
Ga	10.7	12.3	12.9	11.3	11.7	11.8
Gd	2.26	11.2	1.69	1.63	1.72	1.46
Hf	3.3	16.4	2.8	2.3	2.3	2.3
Ho	0.41	1.59	0.32	0.27	0.25	0.28
La	18.2	122.5	15.3	15.1	15.7	13.9
Lu	0.16	0.62	0.14	0.12	0.12	0.12
Nb	5.1	7.2	3.4	2.6	2.9	2.5
Nd	14.2	87.9	12.1	11.4	12.1	10.4
Pr	3.93	25.3	3.38	3.31	3.33	2.83
Rb	79.8	110.5	121.5	108	98.8	112
Sm	2.71	15.9	2.54	2.15	2.07	1.85
Sn	12	12	1	12	36	13
Sr	81.8	94.8	104	100.5	99.4	104
Ta	0.8	2.8	1	1.1	1.4	1
Tb	0.36	1.43	0.29	0.23	0.27	0.24
Th	6.46	75.1	6.89	6.98	6.45	5.43
Tm	0.18	0.62	0.13	0.16	0.11	0.11
U	4.91	25.8	24.4	12.85	10.9	7.1
V	45	21	18	12	17	10
W	230	794	389	398	549	411
Y	10.6	42.2	8.2	8	7.3	7.2
Yb	1.11	4.03	0.9	0.8	0.73	0.82
Zr	119	633	86	77	75	76

Table 4(a): Major and minor element concentrations, in weight percent oxides. (LOI = Loss on Ignition)

Oxide Weight Percent			
Depth (ft)	438'-439'	446'-447'	454'-455'
SiO ₂	83.8	83.1	82.2
Al ₂ O ₃	8.31	8.60	9.51
Fe ₂ O ₃	1.64	1.13	0.80
CaO	0.53	0.47	0.57
MgO	0.62	0.46	0.47
Na ₂ O	1.05	1.22	1.78
K ₂ O	2.32	2.64	3.06
Cr ₂ O ₃	0.01	n.d.	n.d.
TiO ₂	0.29	0.19	0.09
MnO	0.01	0.01	0.01
P ₂ O ₅	0.04	0.03	0.01
SrO	0.01	0.01	0.01
BaO	0.06	0.06	0.07
LOI	2.43	2.24	1.68
Total	101.12	100.16	100.26

Table 4: Bulk chemical analyses for 3 samples from MU1-UG. These data were acquired by ALS-Global, using their processes ME-ICP06 and ME-MS81. See Appendix for analytical details.

Table 4(b): Trace element concentrations, in parts per million.

Elements, Parts per Million			
Depth (ft)	438'-439'	446'-447'	454'-455'
Ba	537	577	690
Ce	41.8	33.5	17.7
Cr	40	30	30
Cs	1.09	0.87	0.4
Dy	2.5	1.65	1.22
Er	1.63	0.89	0.76
Eu	0.62	0.46	0.4
Ga	10	9.7	10.8
Gd	2.69	1.87	1.37
Hf	6.5	3.8	2.1
Ho	0.57	0.36	0.28
La	22.7	18.8	10.4
Lu	0.27	0.16	0.09
Nb	6.6	4.6	2.6
Nd	18.2	14.5	8
Pr	4.93	3.88	2.2
Rb	68.1	74.3	83.6
Sm	3.73	2.61	1.74
Sn	11	29	14
Sr	75.5	80.3	108
Ta	1.7	1.1	0.9
Tb	0.45	0.3	0.22
Th	11.3	8.56	4.57
Tm	0.27	0.17	0.12
U	87.6	4.7	46.5
V	38	41	17
W	540	374	346
Y	15.2	9	7.2
Yb	1.57	1.06	0.83
Zr	244	143	72

b. Electron Microscopy Observations:

Scanning electron microscope (SEM) images of polished thin sections were acquired to enable identification and quantification of minerals and to characterize grain sizes, shapes, and sorting.

Two large-area maps were made for each of the 15 thin sections. These maps are constructed by collecting maps of smaller sub-areas and assembling them into a montage covering the larger area.

1. A backscattered electron (BSE) map covering the largest possible rectangular area on each thin section. BSE images are gray-scale images in which brightness is proportional to average atomic number of the minerals. These maps are useful for showing grain sizes, shapes and sorting, and spatial distribution of compositionally distinct.
2. Characteristic X-ray images covering a representative 15 mm X 10 mm sub-area of the first map. These data are acquired using an energy dispersive X-ray spectrometer and are therefore referred to as EDS maps. They enable positive identification of compositionally distinct minerals based on these images.

Map Interpretation Considerations:

EDS maps are routinely colored according to the element they illustrate, and they are scaled from black for 0 intensity to a bright color for the maximum observed intensity in the field of the map. As a result, these maps always range from black to very bright colors, even if there is no measureable amount of the corresponding element present anywhere on the map. For this reason, the maximum number of counts for each element is listed in the caption for the corresponding map, and these values enable the reader to evaluate the significance of the color variation shown in the map.

BSE and EDS maps were acquired on a stationary sample by rastering the electron beam over the sample. At low magnifications artifacts occur in images because of the inherent variation in signal strength with distance from the detector as the beam rasters across the sample. High magnifications for sub-images address this issue successfully but result in extremely long acquisition times for large maps. The maps in this report were all acquired over an area 1.7 mm X 1.3 mm (70X on this instrument). The maps are of acceptable uniformity, but systematic variation in intensity across the component images is apparent in all of the large-area maps. This periodic variation in intensity is obvious and is not petrographically significant.

Common Characteristics of all Samples:

The primary minerals in all of these samples are quartz, plagioclase feldspar (sodic end member albite), potassium feldspar (much of which is coarsely perthitic), clay minerals, various ferromagnesian minerals (especially ilmenite, chlorite and traces of biotite), and trace amounts of white mica (muscovite). Accessory minerals include pyrite, ilmenite, sphene, apatite, garnet, epidote, calcite, zircon, and monazite. Some of the feldspar is altered to clay; this alteration is clearly post-deposition (authigenic). Most of the clay-size fraction shows no spatial relationship to feldspar and likely did not form from in-situ alteration of feldspar. Relative abundances of all minor and trace minerals are quite variable

between samples and even between subareas of the same sample; this is not surprising for extremely immature sediments such as these. Everything about these samples suggests extremely rapid deposition and burial very close to a granitic source terrain.

Average grain size is highly variable between individual samples. Individual grains are highly angular, and grain size sorting is poor in most samples. These factors suggest deposition close to the sediment source, with minimal sediment transport. Since samples are inclined to disaggregate during sample preparation, some of the pore space is presently filled with epoxy, and virtually all of the black areas in these images are underlain by epoxy. For each sample there is a separate WORD document that contains detailed images and corresponding EDS X-ray spectra.

MU1-DG Samples:

Composite BSE images for all 5 samples show medium to coarse grained, poorly sorted, and poorly rounded arkosic sandstones (Fig. 1). One sample contains appreciable organic material which is obvious as a dark vein in the BSE image (451' – 452').

MU1-DG-451'-452': Identification of major minerals and textural relations between them is facilitated by EDS maps (Fig. 2). Note that this sample has calcite cement, pyrite occurs as framboids and apparently predates the formation of the cement, and biotite/chlorite grains are generally devoid of pyrite in this sample.

MU1-DG-456-457: The EDS maps for this sample are given in Fig. 3. Pyrite is extremely rare in this sample, but small, rounded structures made of iron oxide are common. These are interpreted to be pseudomorphs of iron oxide after pyrite framboids.

MU1-DG-460-461: The EDS maps for this sample are given in Fig. 4. This sample disaggregated during cutting, rendering the textural relations in this slide of questionable value. The rock contains very little pyrite or other high atomic number minerals. Biotite is being replaced by ilmenite and chlorite and locally by chlorite and pyrite. Sphene is common .

MU1-DG-465-466: EDS maps for this sample are given in Fig. 5. This sample has high abundance of heavy minerals, biotite, and chlorite. Pyrite is strongly associated with chlorite where chlorite is replacing biotite. Pyrite always occurs in small spheres (framboids).

MU1-DG-469-470: EDS maps for this sample are given in Fig. 6. Pyrite is present in modest amounts and is usually associated with clay. Ilmenite is also abundant.

MU1-ST Samples:

Composite BSE images for all 5 samples show medium to very coarse grained, poorly sorted, and poorly rounded arkosic sandstones (Fig. 7). All samples contain pyrite as framboids, ilmenite, epidote, and sphene. Pyrite is commonly spatially associated with ilmenite and chlorite/biotite grains.

MU1-ST-457-458: EDS maps for this sample are given in Fig. 8. Pyrite commonly occurs in chlorite and clustered around ilmenite grains. Sphene and epidote are also common.

MU1-ST-463-464: EDS maps for this sample are given in Fig. 9. This sample has abundant pyrite, spatially associated with chlorite. Ilmenite is present but not abundant. Accessory minerals include sphene, apatite, and in one location, xenotime.

MU1-ST-470-471: EDS maps for this sample are given in Fig. 10. Pyrite is spatially associated with ilmenite in this sample. Biotite, chlorite, and pyrite are significantly less abundant in this sample than in the other ST samples. Some feldspar is being replaced authigenically by clay; locally pyrite is associated with this clay. Accessory minerals include muscovite, allanite, and epidote.

MU1-ST-473-474: EDS maps for this sample are given in Fig. 11. Pyrite is spatially associated with ilmenite in this sample. Pyrite is NOT spatially associated with biotite/chlorite in this sample. Pyrite, biotite, and chlorite are all less abundant in this sample than in the other ST samples.

MU1-ST-476-477: EDS maps for this sample are given in Fig. 12. This sample strongly resembles MU1-ST-473-474 in every respect: low abundance of pyrite & chlorite/biotite, pyrite spatially associate with ilmenite but not with chlorite/biotite, and the same suite of accessory minerals.

MU1-UG Samples:

Composite BSE images for all 5 samples show fine to medium grained, moderately well sorted but poorly rounded arkosic sandstones (Fig. 13). Pyrite is absent in all but one sample (438'-439' contains pyrite). Accessory minerals in all samples include iron oxide, zircon, epidote, sphene, and rare barite, monazite, rare chromite, and allanite. Since these samples are so similar, no individual descriptions are given here. EDS maps for these samples are given in Figs. 14-18.

IV. CLAY MINERALOGY

Clay-sized mineral grains make up a small fraction of all samples in this study. The best approach to identification of specific clay minerals is powder X-ray diffraction. We separated the clay fraction from powdered rock samples by suspension in water and then decanting the clay-laden water into filter vessels. We prepared oriented clay mounts and examined them in a Scintag XDS2000 powder X-ray diffractometer running at 40KV, 30 mA, 1 degree 2-theta per minute, using a Cu X-ray tube and a solid state X-ray detector. Results are summarized in Figs. 19 – 21.

All samples included smectite (a swelling clay; peaks marked with red lines), and lesser amounts of kaolinite (green), illite (blue), and chlorite (small peak at $6.6^\circ 2\Theta$). Smectite is confirmed by the presence of a peak near $6^\circ 2\Theta$ that moves to $5.2^\circ 2\Theta$ upon exposure to ethelene glycol (EG). Illite is indicated by a peak near $9^\circ 2\Theta$. Chlorite and kaolinite are confirmed by peaks near $12.4^\circ 2\Theta$ and $24.8^\circ 2\Theta$ and by complementary evidence from SEM/EDS examination of the samples.

All clays are at least in part authigenic, based on textural relations sited above. Smectite is a product of post-depositional weathering of volcanogenic glass, and its presence in these samples indicates some

volcanogenic component in the original detritus. The chlorite may be detrital or it may be a product of post-depositional weathering of detrital biotite, or both.

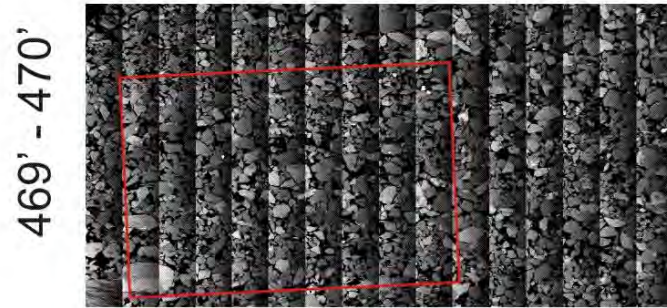
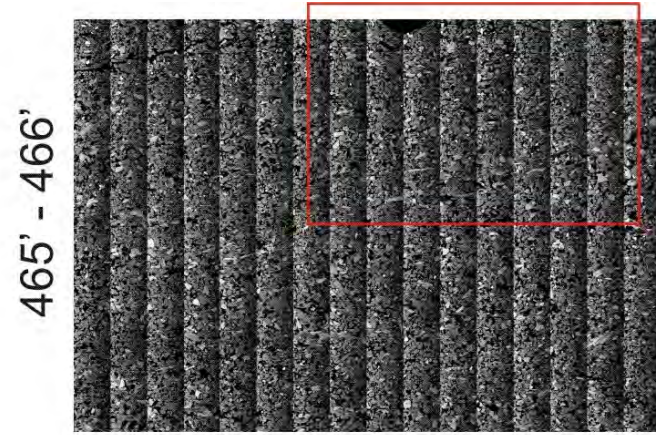
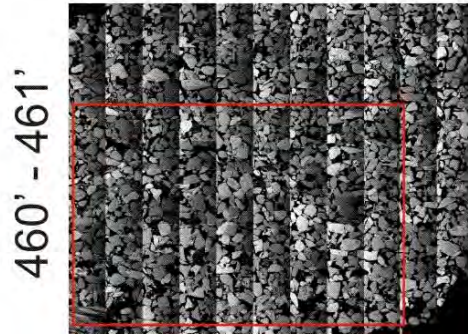
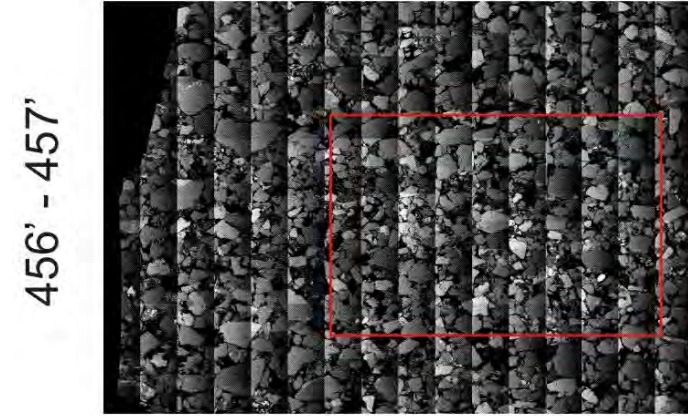
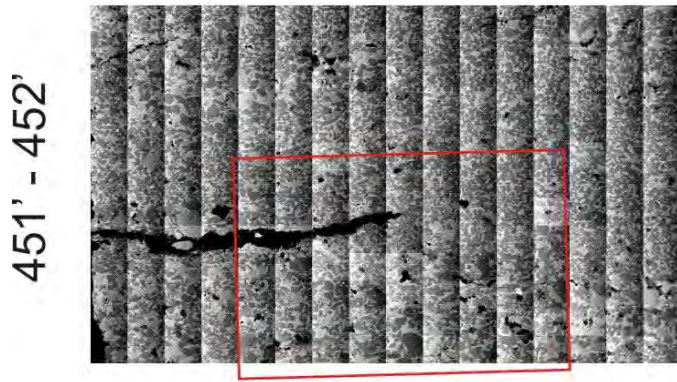
We have not quantified the relative abundances of individual clay species at this time.

V. MODAL ANALYSIS

We used 3 approaches to estimating abundances of major minerals in these samples. The minerals Quartz, Albite, K-feldspar, calcite, and sheet silicates including chlorite, smectite, illite, kaolinite (and biotite) comprise more than 90% of these samples. It is extremely difficult to obtain high-precision measurements of minerals making up less than 5% of a mixture, so we analyzed for the major minerals and normalized the results to 100%. Two X-ray diffraction techniques were employed: classical reference intensity ratio (RIR) measurements were made using corundum as an internal standard, and the whole-pattern fitting (Rietveldt) method was also utilized. In addition, we used knowledge of chemical composition of major phases combined with whole rock chemical analyses to estimate mineral abundances by employing an n-dimensional linear least squares calculation to find the 'best fit' mineral abundances for each sample. Results of the three approaches are illustrated in Figure 22. The results for the RIR X-ray technique and for the "chemical solution" are very comparable and agree well with petrographic observations described above. The whole-pattern solution seems to have overestimated quartz in several cases, so we suggest that those results be considered with caution.

VI. SUMMARY

These samples comprise a set of texturally immature arkosic sandstones. The principal detrital component comes from a proximal quartzo-feldspathic granitic/metamorphic terrain. There is also evidence of a small but significant and persistent volcanogenic detrital component, now largely to completely replaced by smectitic clay. There is significant evidence for post-depositional alteration of feldspars to clays and possibly authigenic alteration of biotite to chlorite. Pyrite is present in all samples except 4 of the 5 UG samples. In all cases it occurs as framboids; the framboids are commonly associated with ilmenite and/or with biotite/chlorite mineral grains. In one DG sample, pyrite framboids were apparently completely replaced by pseudomorphs of iron oxide. No uraninite or other uranium minerals were observed in any of these samples. Trace mineral assemblages are complex and include monazite, zircon, and various ferromagnesian minerals typical of the source terrain described above. It would be informative to examine pre-mining samples from the same localities.



0 5 10 15
Millimeters

Figure 1 Composite backscattered electron images of samples from MU1-DG, illustrating mineralogy, grain sizes, and textures. All images are printed at 3X magnification. Minerals with higher average atomic number appear brighter in these images, while materials with low average atomic number appear darker (e.g., Pyrite (FeS_2) is bright, while organic matter and epoxy showing through holes in the sample are black. Feldspar and quartz are intermediate in brightness.) The rectangle outlines the area of the Xray maps shown in later images.

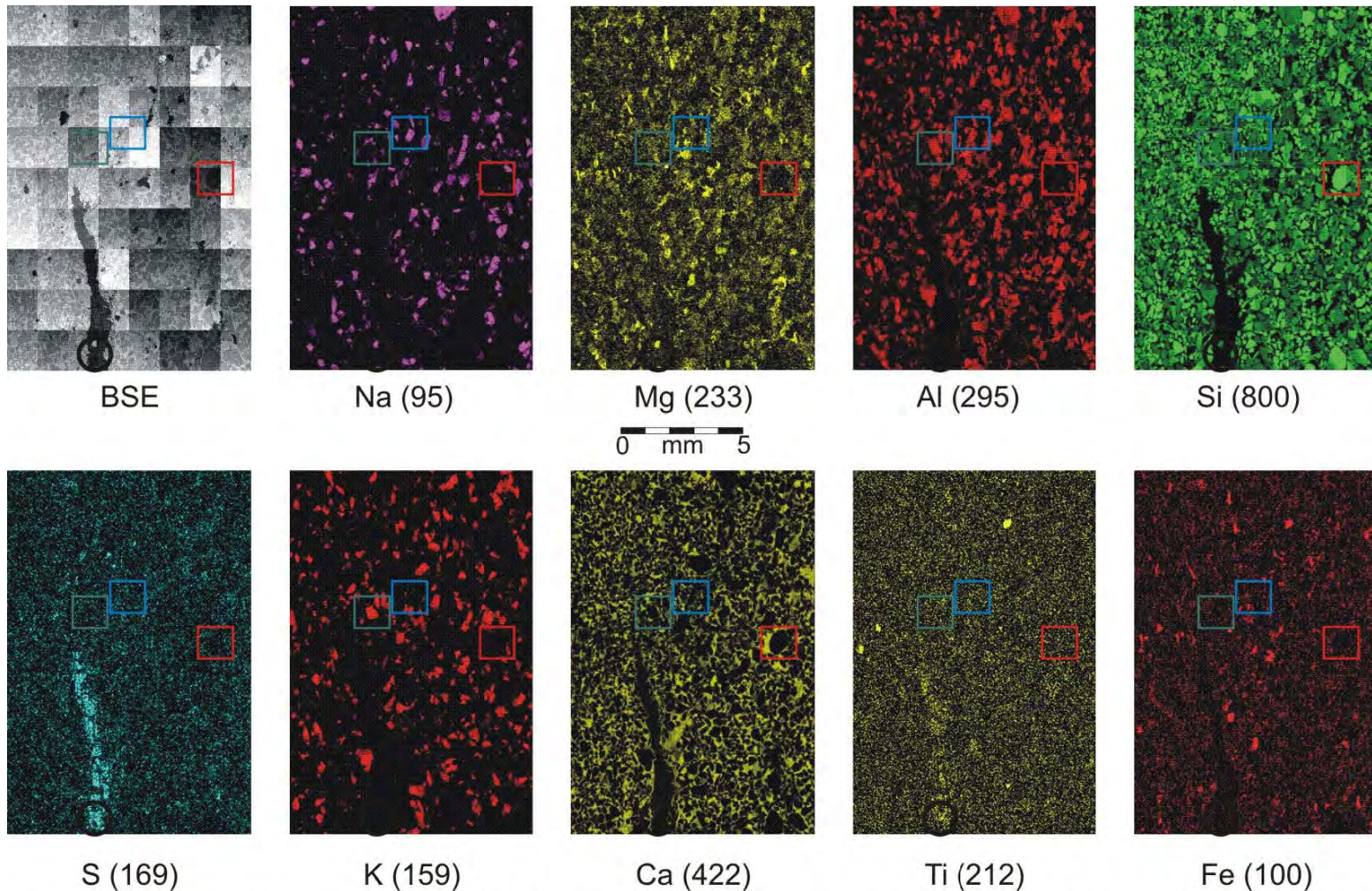


Figure 2: **MU1-DG-451-452** The red boxes show a large quartz grain (SiO_2); the blue boxes show an albite grain ($\text{NaAlSi}_3\text{O}_8$), the green boxes show a potassium feldspar grain (KAlSi_3O_8). The dark sub-vertical strip in the BSE image is organic material, and pyrite (FeS_2) is concentrated along it (e.g., Black circle). The grains are too small to resolve at this scale. The pervasive calcite cement in this sample is obvious in the Ca map. The numbers in parentheses are the maximum number of counts observed for that element in this scan (see text for discussion).

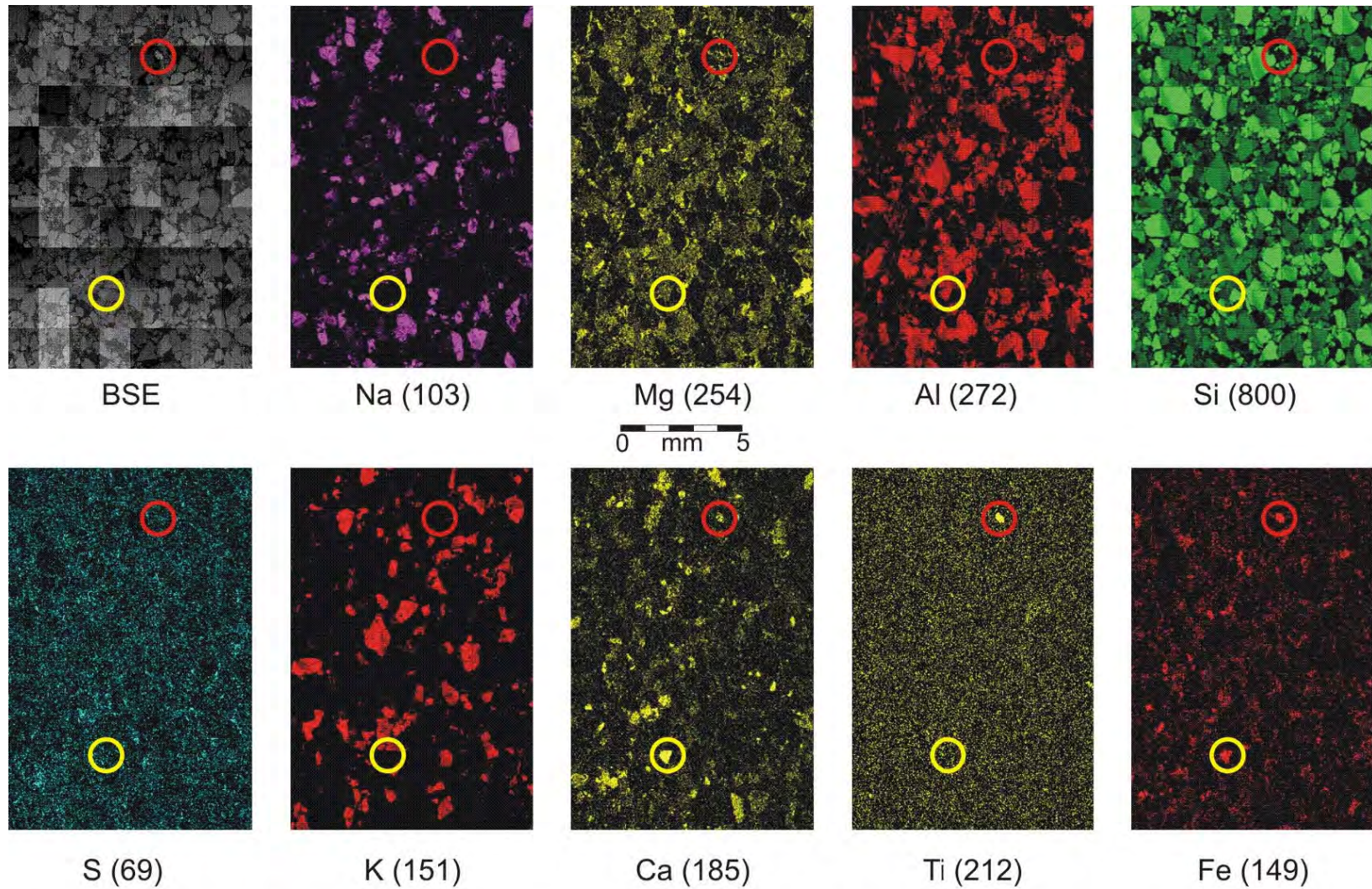


Figure 3: **MU1-DG-456-457** This sample has abundant quartz, albite, and potassium feldspar. It also has abundant epidote ($\text{Ca}_2(\text{Al}, \text{Fe}^{3+})_3\text{Si}_3\text{O}_{12}(\text{OH})$, in the yellow circle). Pyrite is very rare in this sample. Ilmenite (FeTiO_3) and sphene (CaTiSiO_3) are common in this sample (red circle). The numbers in parentheses are the maximum number of counts observed for that element in this scan.

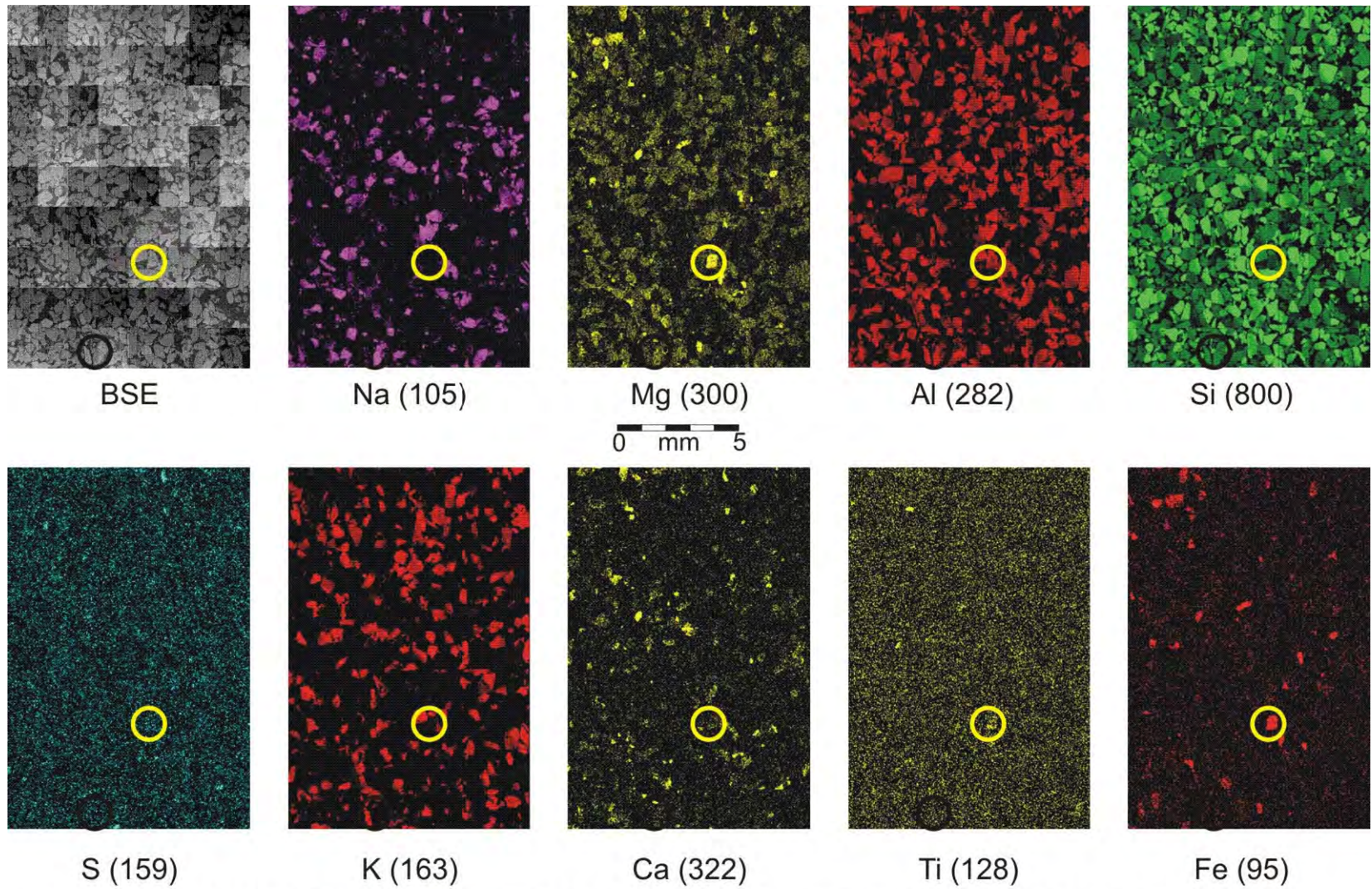


Figure 4: **MU1-DG-460-461** This sample has abundant quartz, albite, and potassium feldspar. Some large flakes of chlorite after biotite are apparent (yellow circle), and epidote is common. The numbers in parentheses are the maximum number of counts observed for that element in this scan.

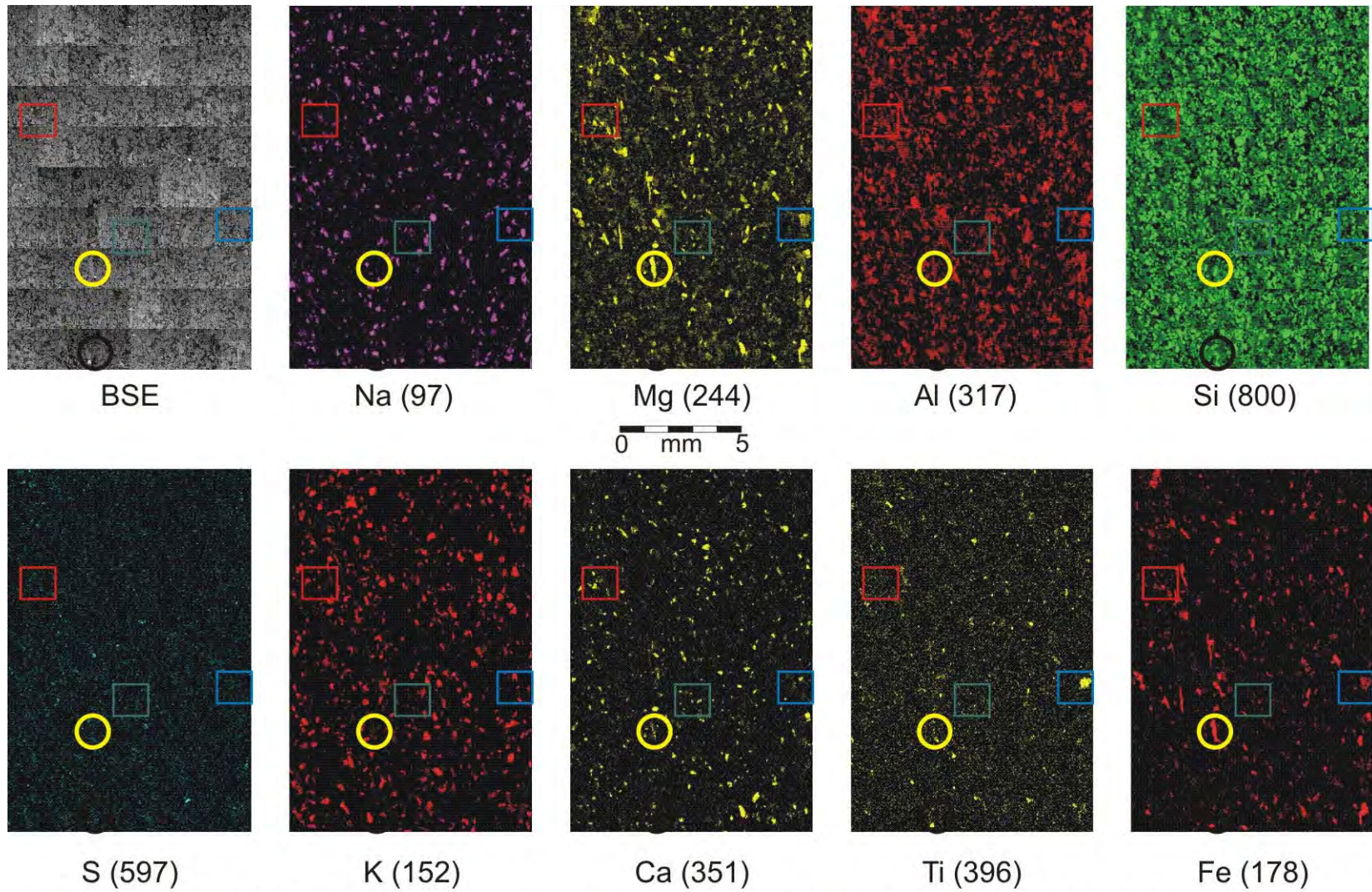


Figure 5: **MU1-DG-465-466** Abundant chlorite (yellow circle), epidote (red box), ilmenite (blue box) and fine-grained pyrite (green box) are apparent in this sample, in addition to quartz, albite, and potassium feldspar. The numbers in parentheses are the maximum number of counts observed for that element in this scan.

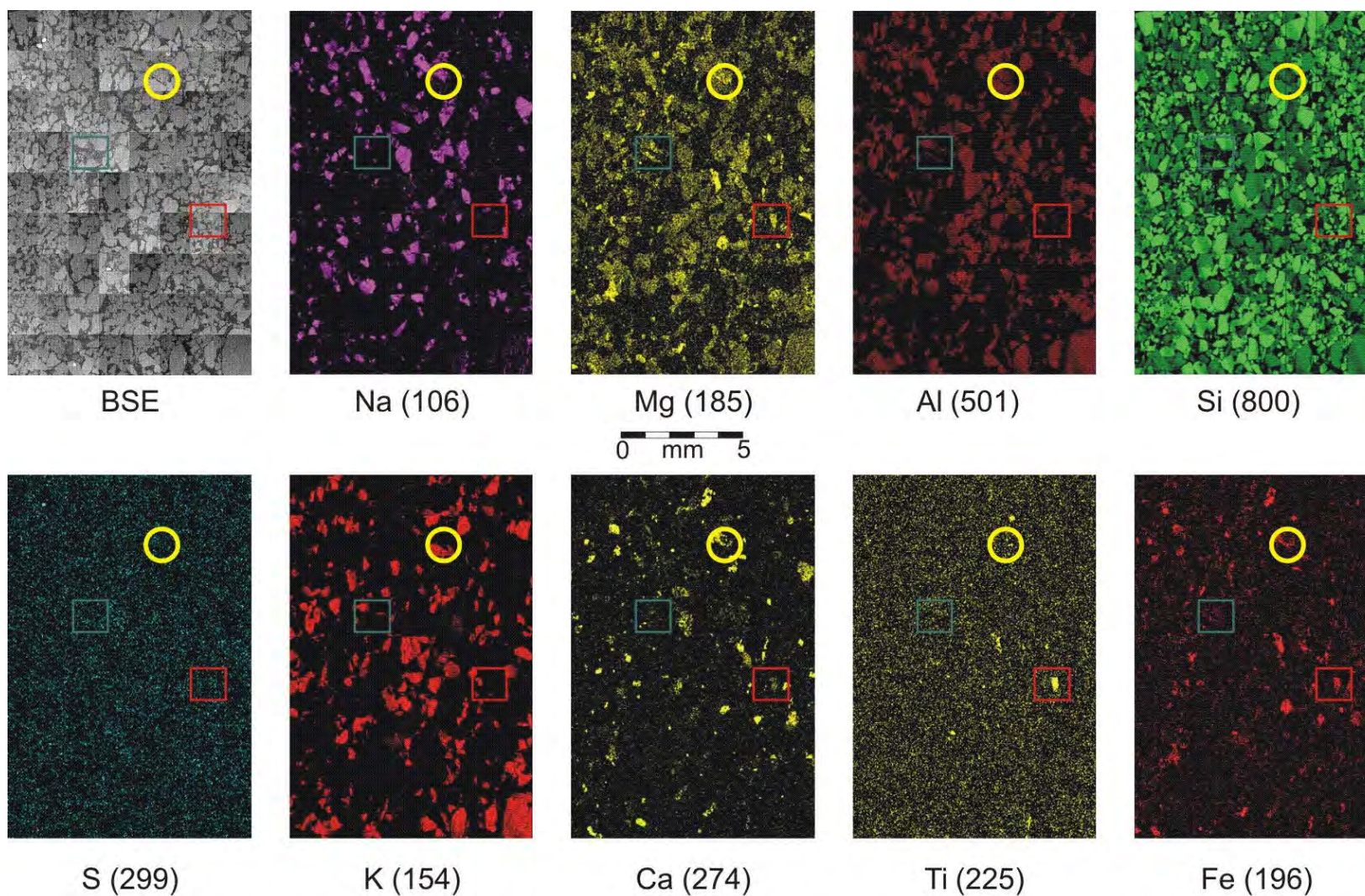


Figure 6: **MU1-DG-469-470** Ilmenite and sphene (red box), epidote (yellow circle), and chlorite (green box) are abundant in this sample, in addition to quartz, albite, and potassium feldspar. Pyrite is too fine-grained to resolve at this scale. The numbers in parentheses are the maximum number of counts observed for that element in this scan.

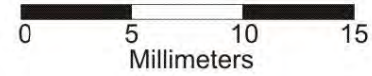
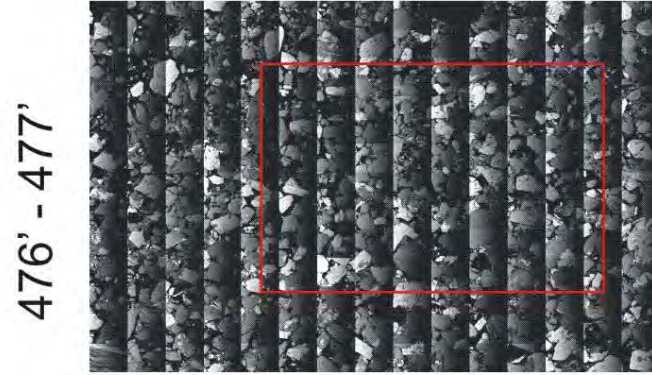
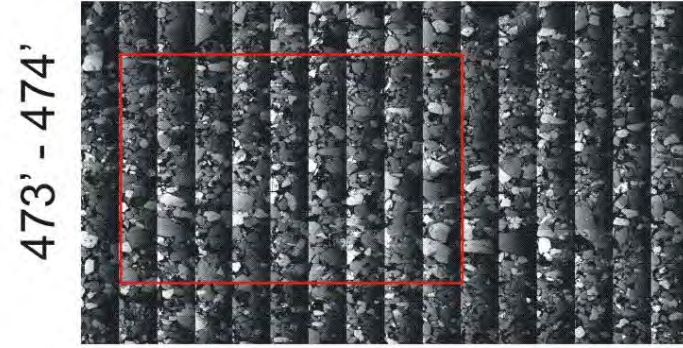
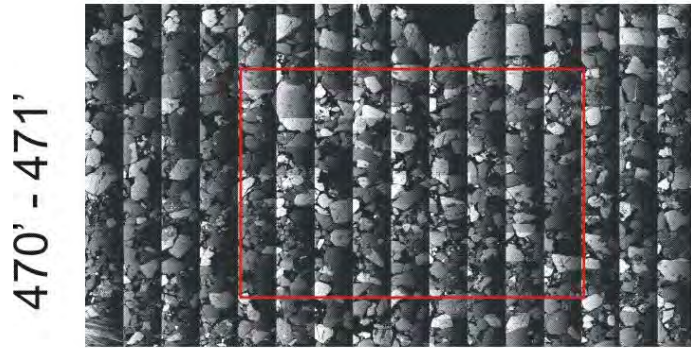
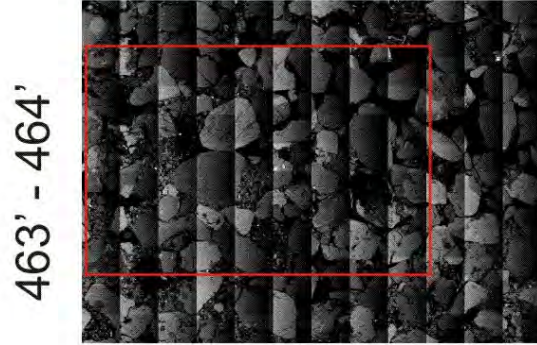
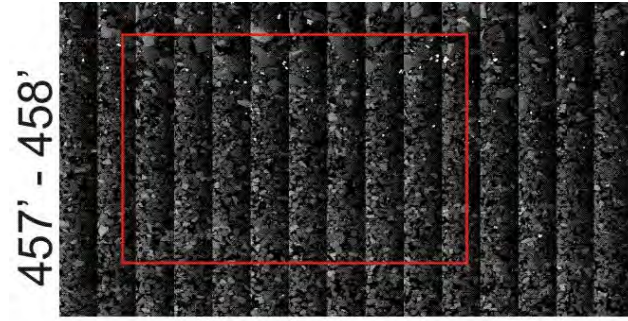


Figure 7 Composite backscattered electron images of samples from MU1-ST, illustrating mineralogy, grain sizes, and textures. All images are printed at 3X magnification. Minerals with higher average atomic number appear brighter in these images, while materials with low average atomic number appear darker (e.g., Pyrite (FeS_2) is bright, while organic matter and epoxy showing through holes in the sample are black. Feldspar and quartz are intermediate in brightness.) The rectangle outlines the area of the Xray maps shown in later images.

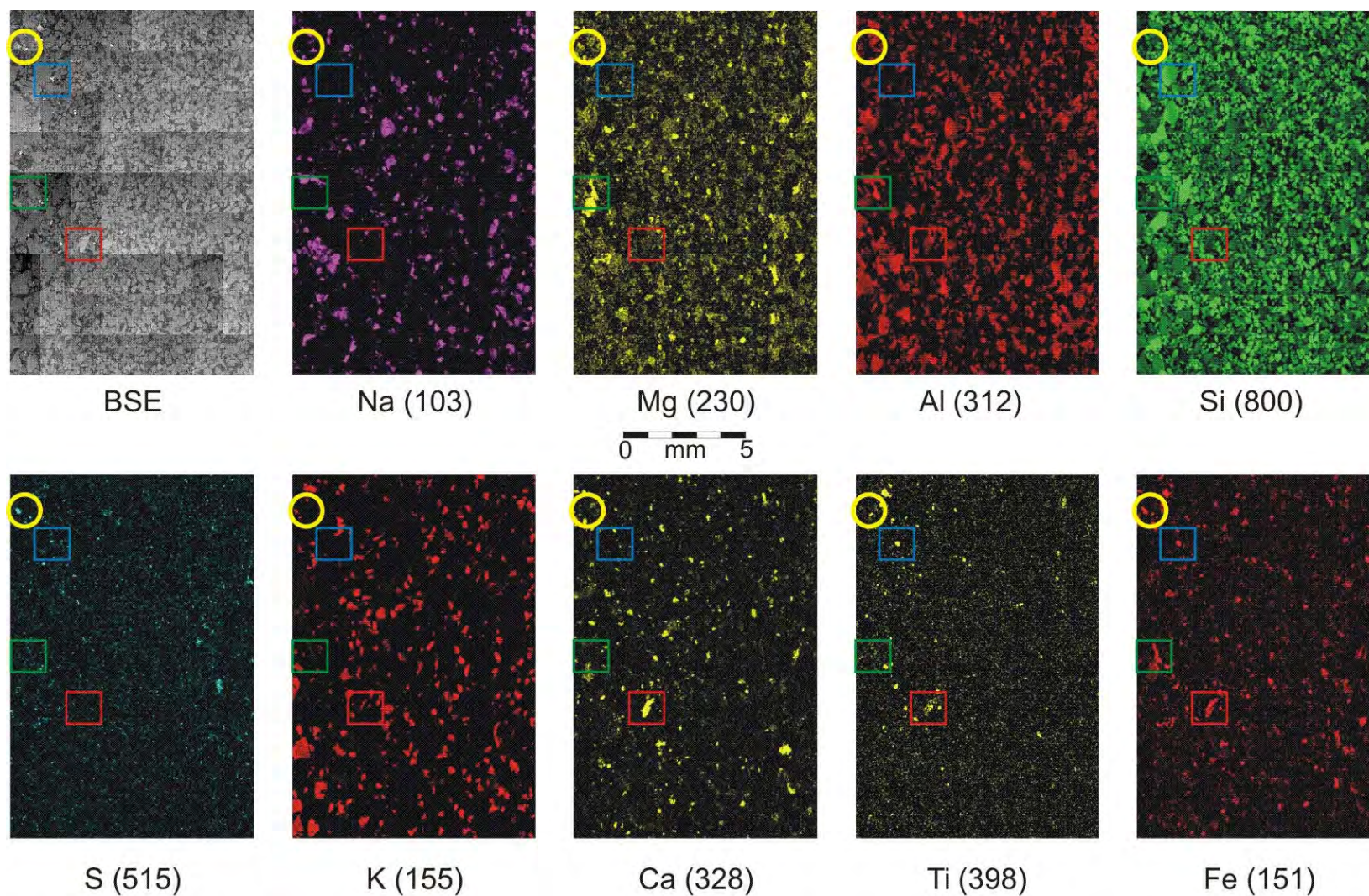


Figure 8: **MU1-ST-457-458** Pyrite (yellow circle), epidote (red box), ilmenite (blue box), and chlorite (green box) are common in this sample, in addition to quartz, albite, and potassium feldspar. Much of the pyrite is too fine-grained to resolve at this scale. The numbers in parentheses are the maximum number of counts observed for that element in this scan.

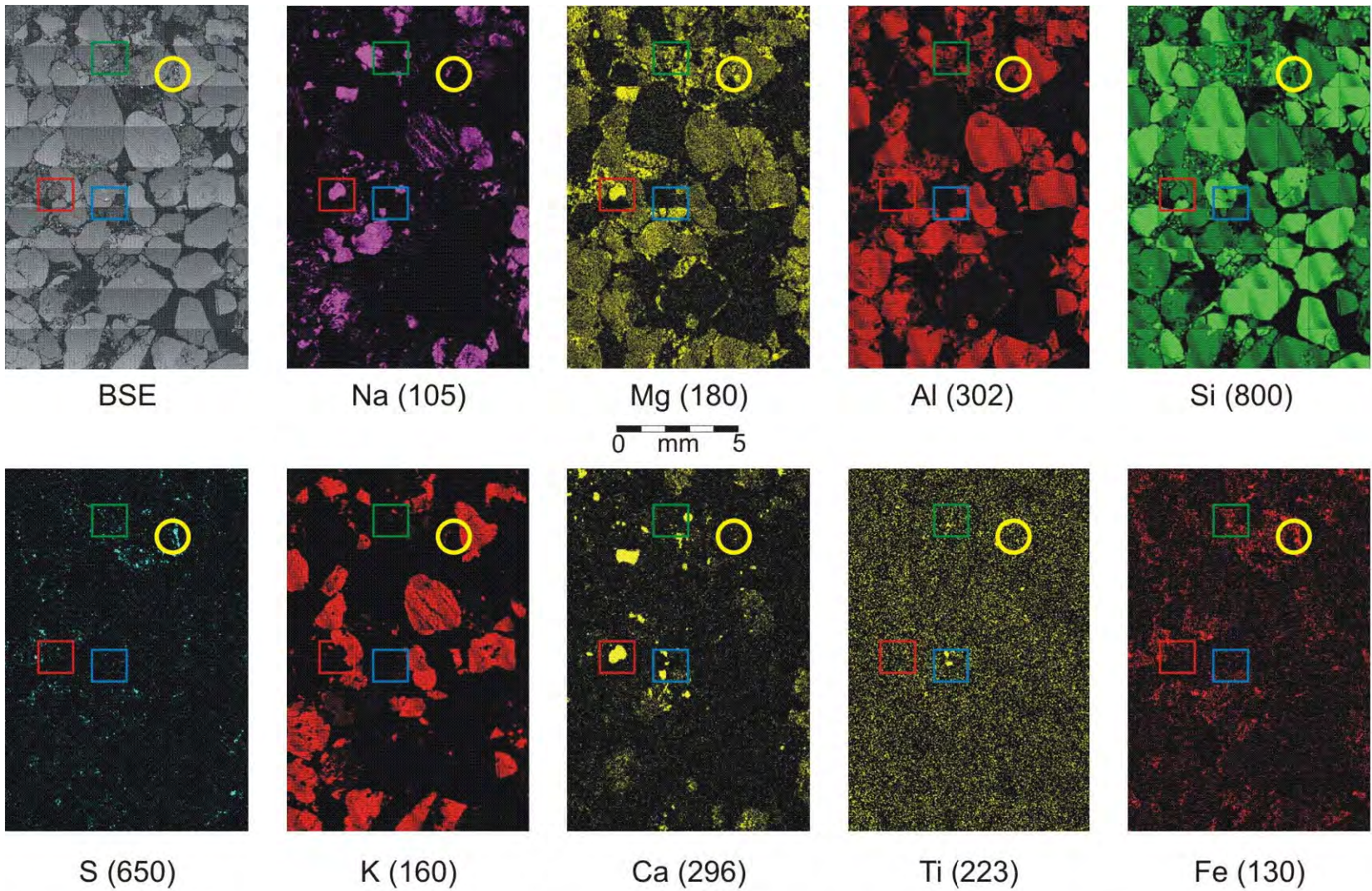


Figure 9: **MU1-ST-463-464** Pyrite (yellow circle), epidote (red box), ilmenite (blue box), and chlorite (green box) are common in this sample, in addition to quartz, albite, and potassium feldspar. The numbers in parentheses are the maximum number of counts observed for that element in this scan.

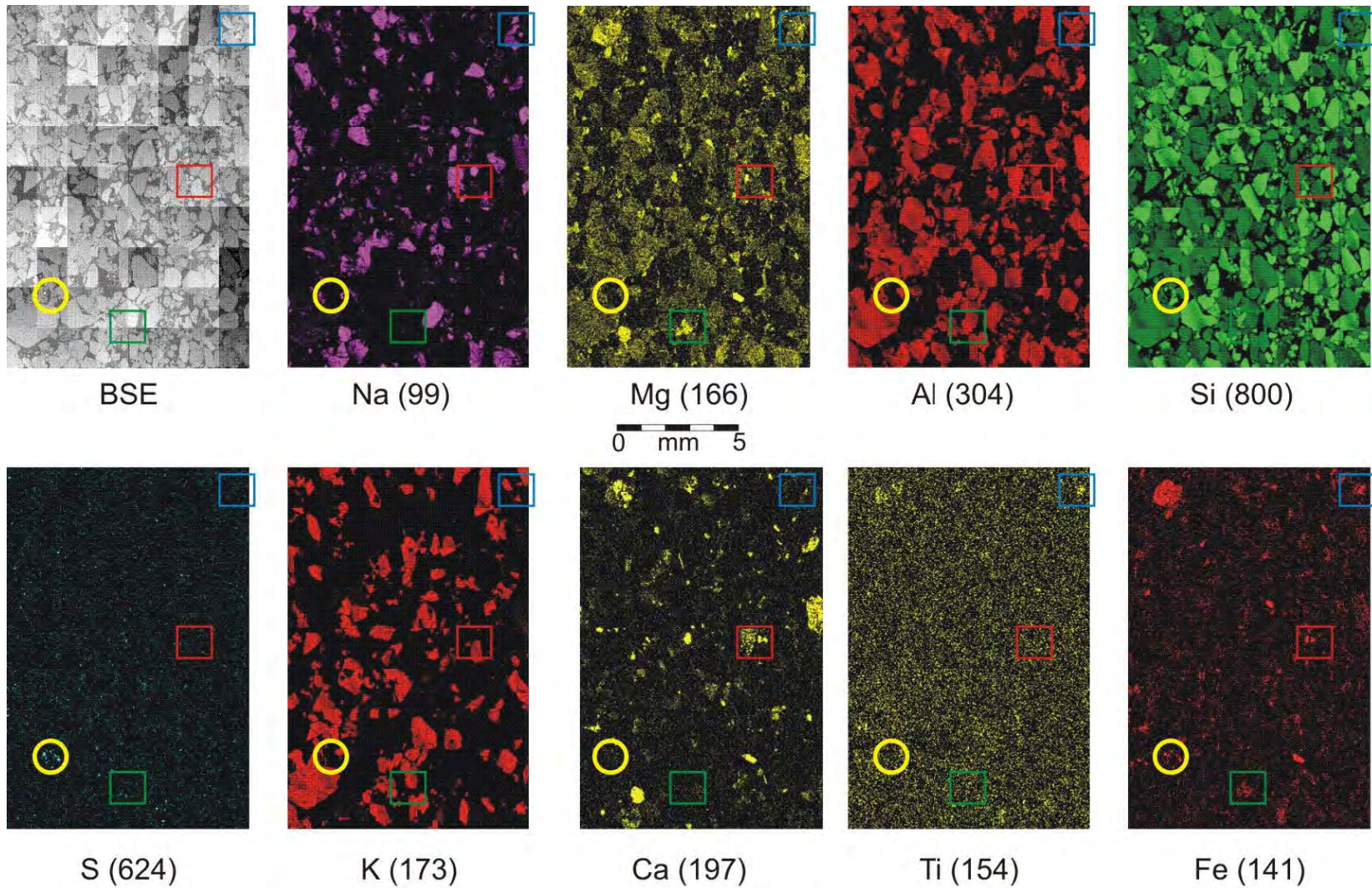


Figure 10: **MU1-ST-470-471** Pyrite (yellow circle), epidote (red box), ilmenite (blue box), and chlorite (green box) are common in this sample, in addition to quartz, albite, and potassium feldspar. Most of the pyrite is too fine-grained to resolve at this scale. The numbers in parentheses are the maximum number of counts observed for that element in this scan.

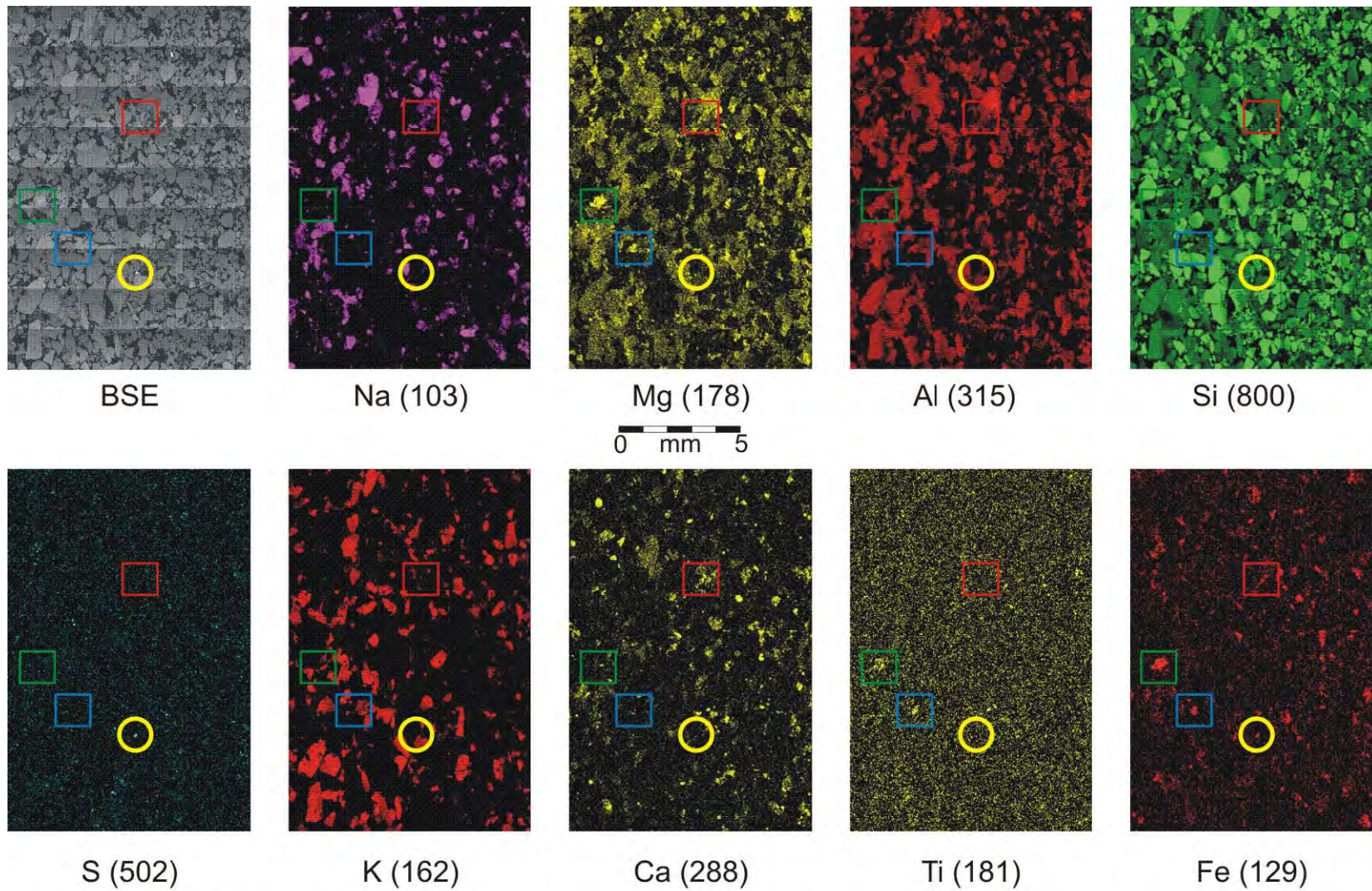


Figure 11: **MU1-ST-473-474** Pyrite (yellow circle), epidote (red box), ilmenite (blue box), and chlorite (green box) are common in this sample, in addition to quartz, albite, and potassium feldspar. The numbers in parentheses are the maximum number of counts observed for that element in this scan.

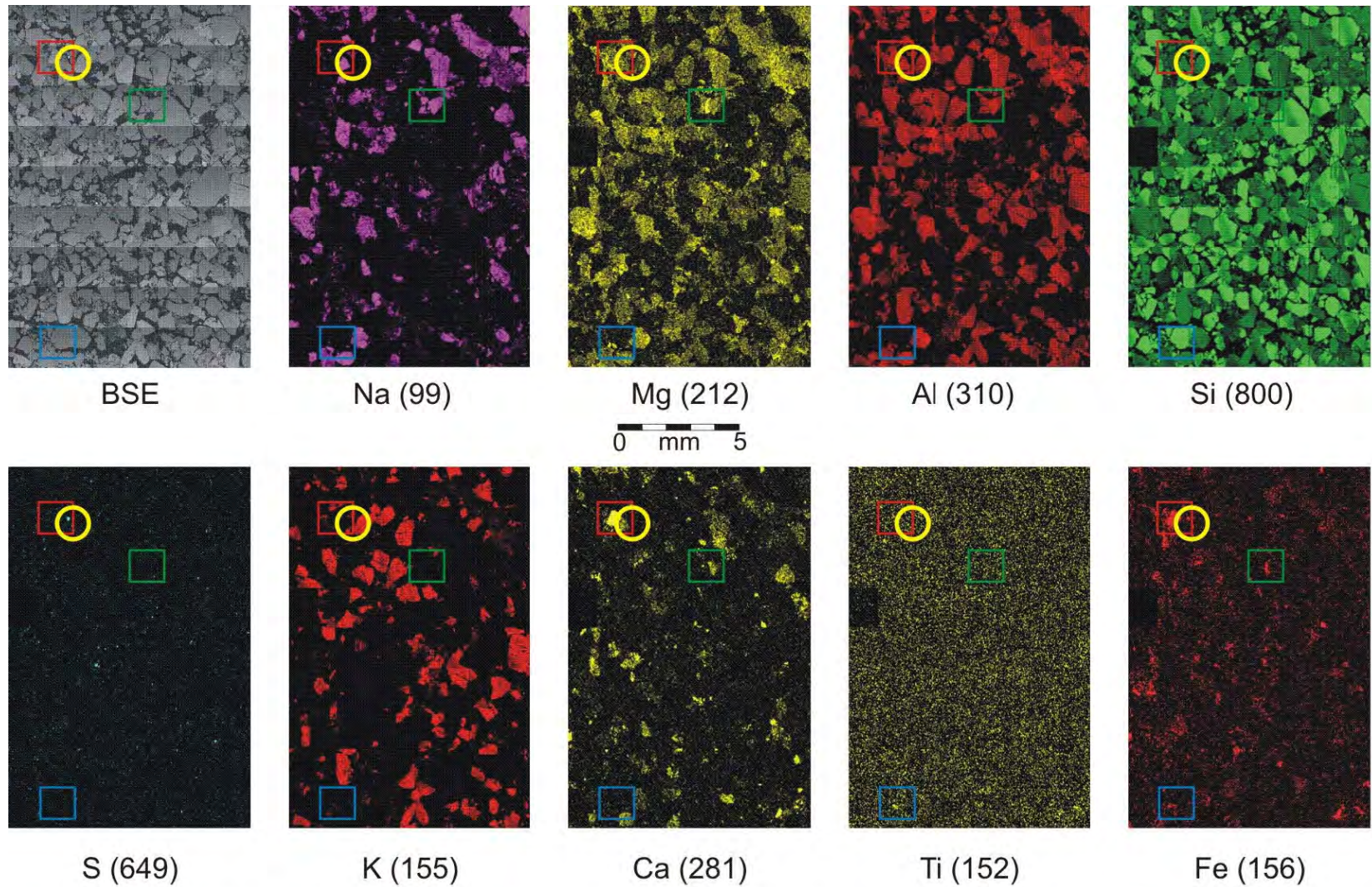


Figure 12: **MU1-ST-476-477** Pyrite (yellow circle), epidote (red box), ilmenite (blue box), and chlorite (green box) are common in this sample, in addition to quartz, albite, and potassium feldspar. Most of the ilmenite is too fine-grained to resolve at this scale. The numbers in parentheses are the maximum number of counts observed for that element in this scan.

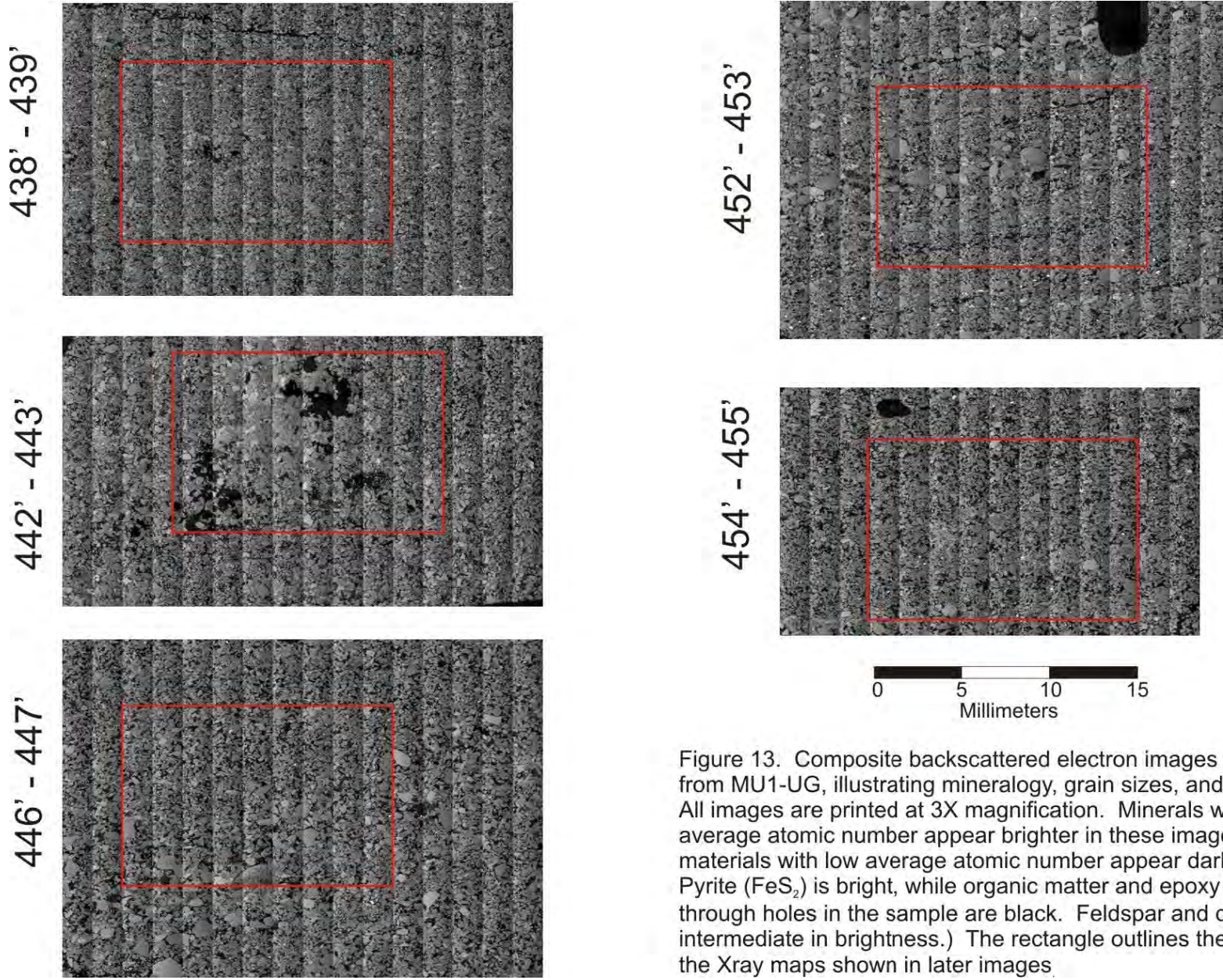


Figure 13. Composite backscattered electron images of samples from MU1-UG, illustrating mineralogy, grain sizes, and textures. All images are printed at 3X magnification. Minerals with higher average atomic number appear brighter in these images, while materials with low average atomic number appear darker (e.g., Pyrite (FeS_2) is bright, while organic matter and epoxy showing through holes in the sample are black. Feldspar and quartz are intermediate in brightness.) The rectangle outlines the area of the Xray maps shown in later images.

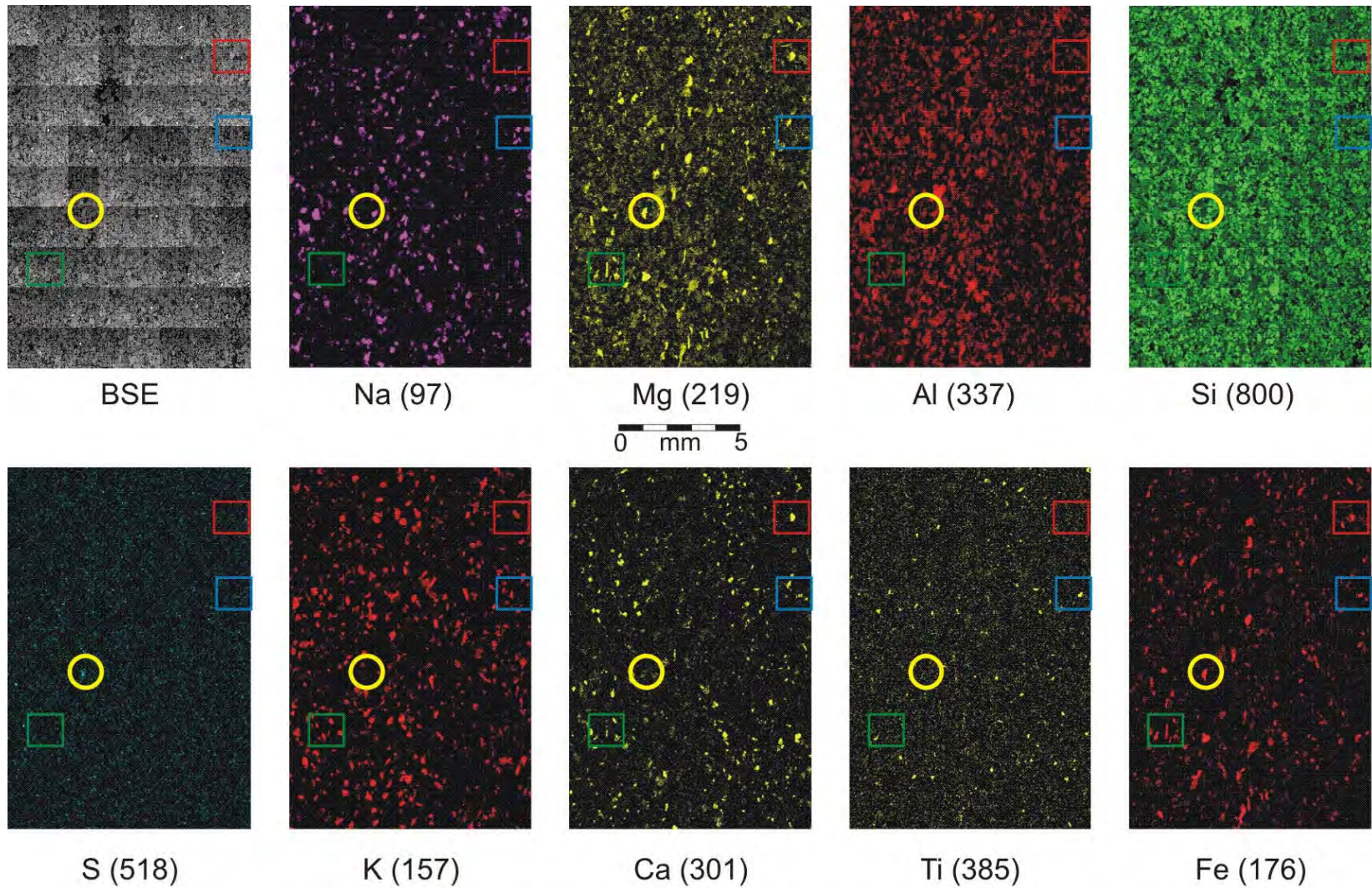


Figure 14: **MU1-UG-438-439** Pyrite (yellow circle), epidote (red **box**), ilmenite (blue box), and chlorite (green box) are common in this sample, in addition to quartz, albite, and potassium feldspar. Most of the pyrite is too fine-grained to resolve at this scale. The numbers in parentheses are the maximum number of counts observed for that element in this scan.

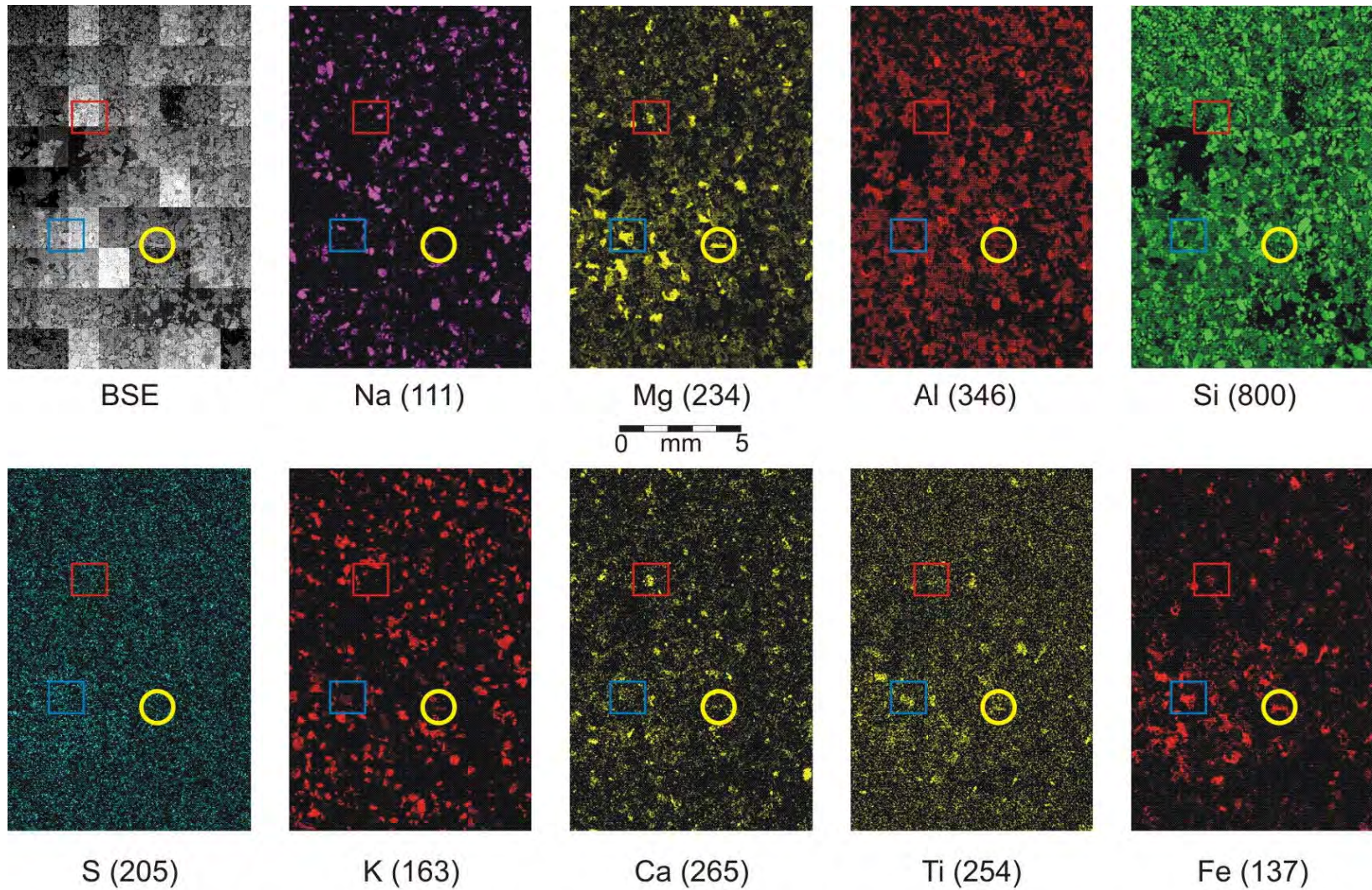


Figure 15: **MU1-UG-442-443** Epidote (red box), ilmenite and sphene (blue box), and chlorite (yellow circle) are common in this sample, in addition to quartz, albite, and potassium feldspar. Pyrite does not occur in this sample. The numbers in parentheses are the maximum number of counts observed for that element in this scan.

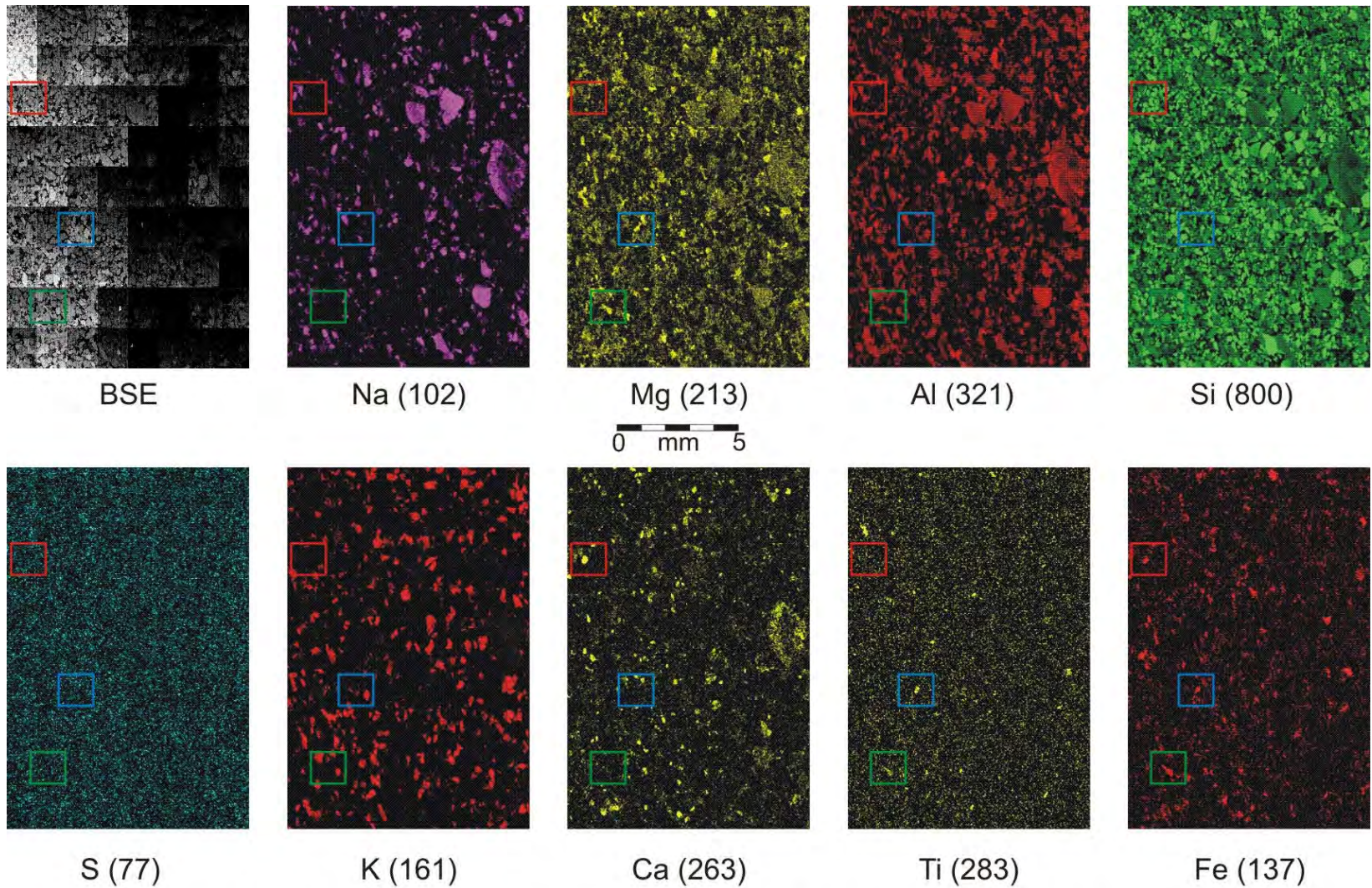


Figure 16: **MU1-UG-446-447** Epidote (red box), ilmenite (blue box), and chlorite (green box) are common in this sample, in addition to quartz, albite, and potassium feldspar. Pyrite is absent in this sample. The numbers in parentheses are the maximum number of counts observed for that element in this scan.

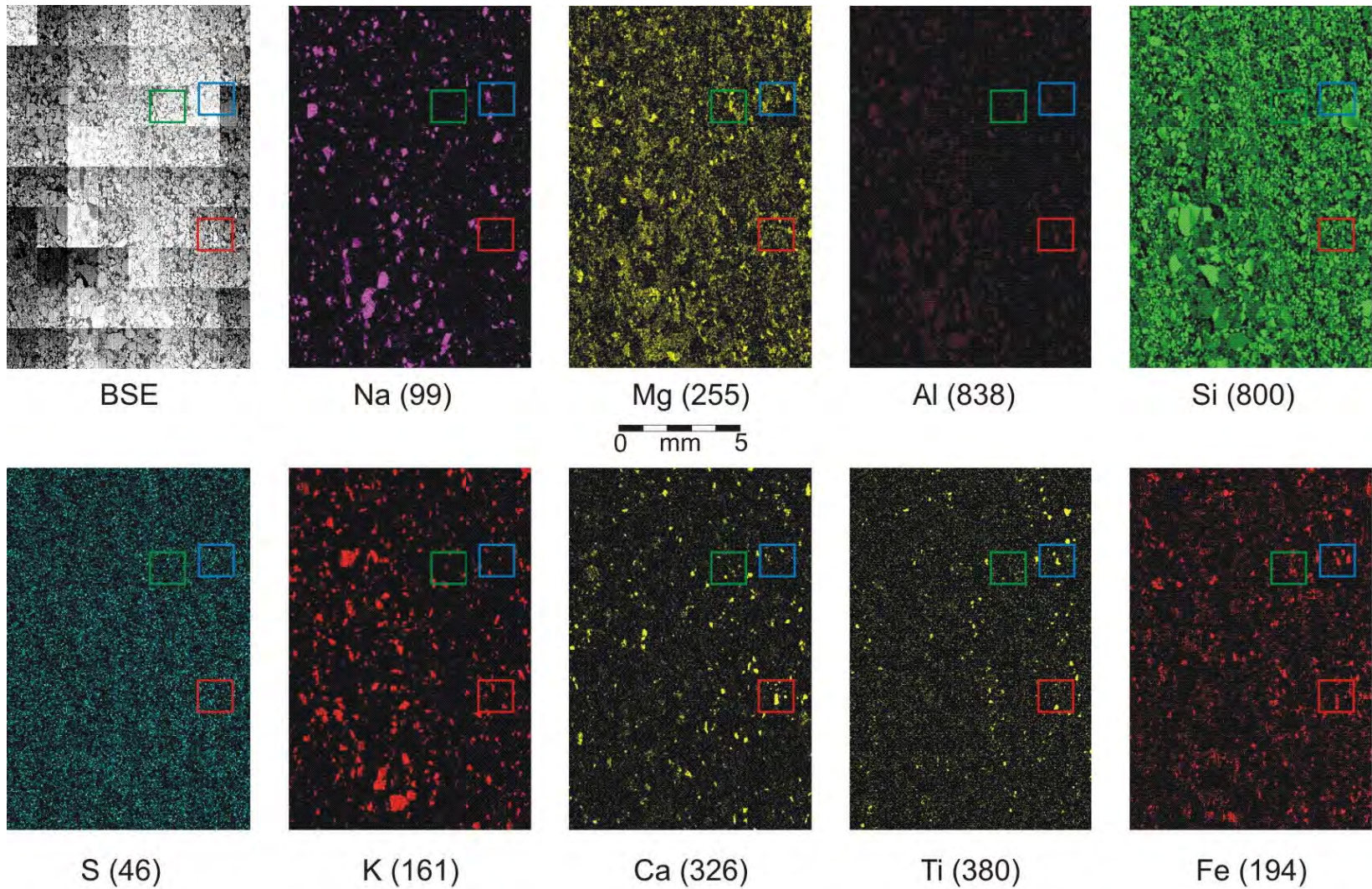


Figure 17: **MU1-UG-452-453** Epidote (red box), ilmenite (blue box), and chlorite (green box) are common in this sample, in addition to quartz, albite, and potassium feldspar. Pyrite is largely absent in this sample. The numbers in parentheses are the maximum number of counts observed for that element in this scan.

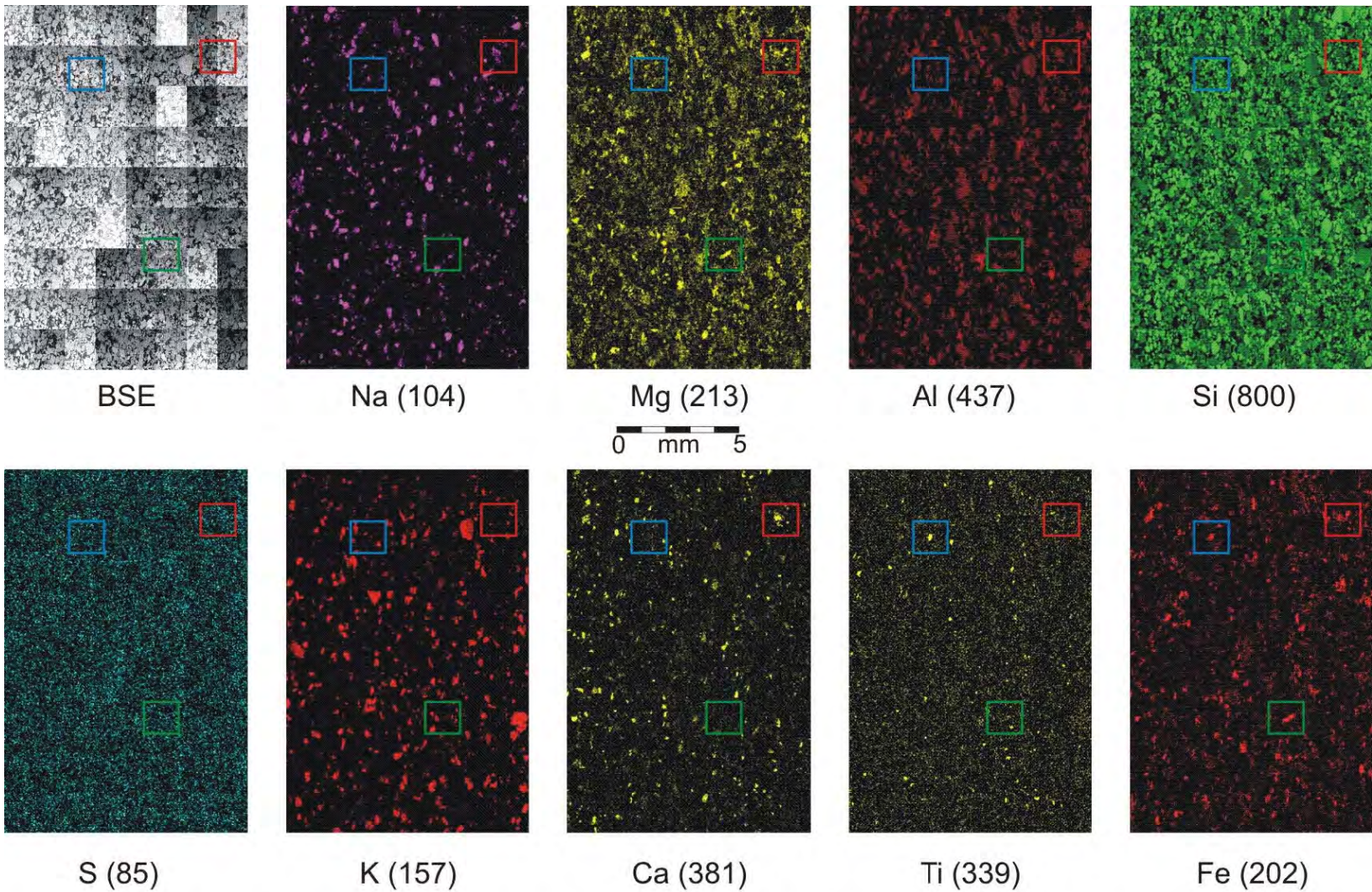


Figure 18: **MU1-UG-454-455** Epidote (red box), ilmenite (blue box), and chlorite (green box) are common in this sample, in addition to quartz, albite, and potassium feldspar. Pyrite is absent in this sample. The numbers in parentheses are the maximum number of counts observed for that element in this scan.

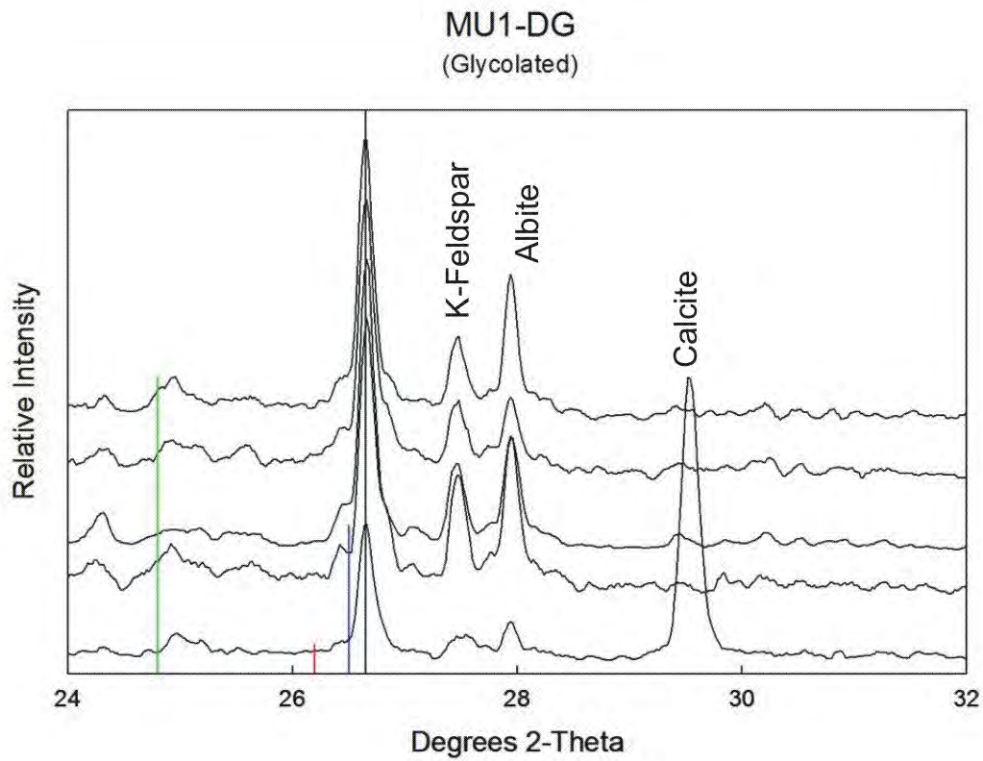
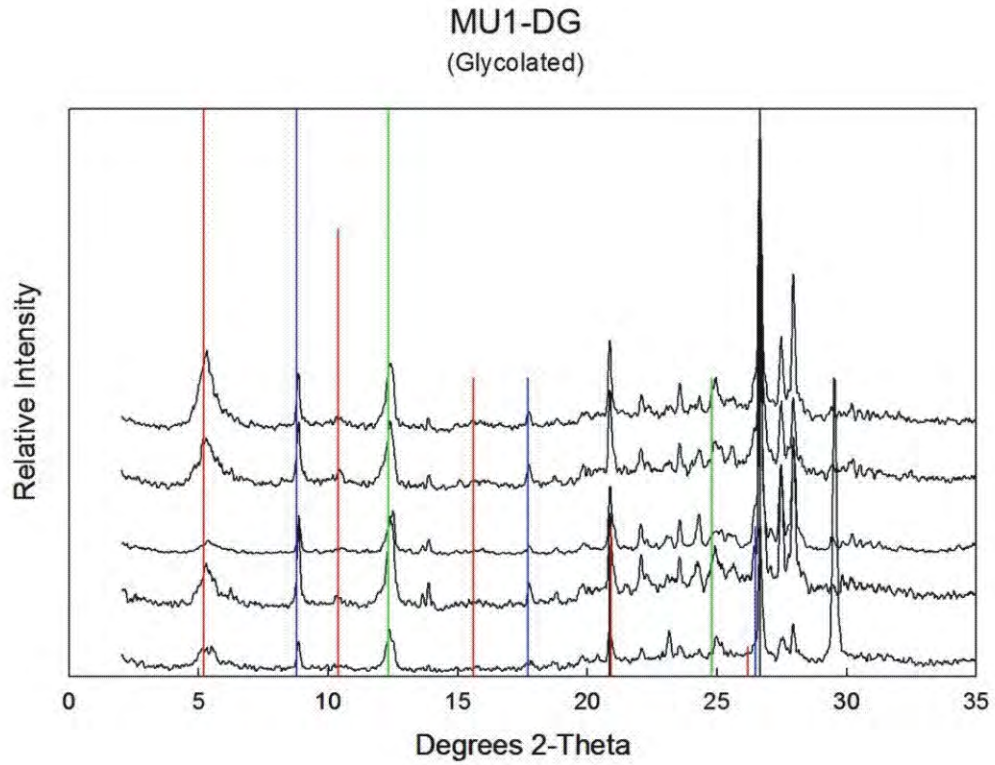


Figure 19: MU1-DG Clay fraction. Red=smeectite, Blue=illite, Green=kaolinite, Black=Quartz. Additional peaks are labelled in diagram above.

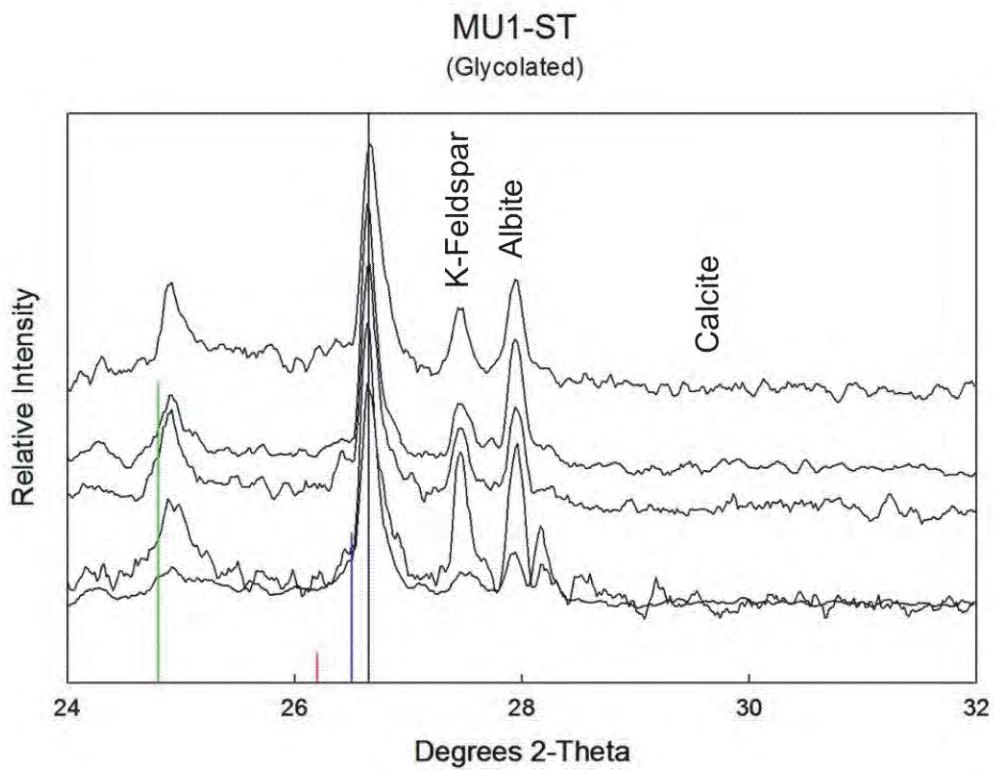
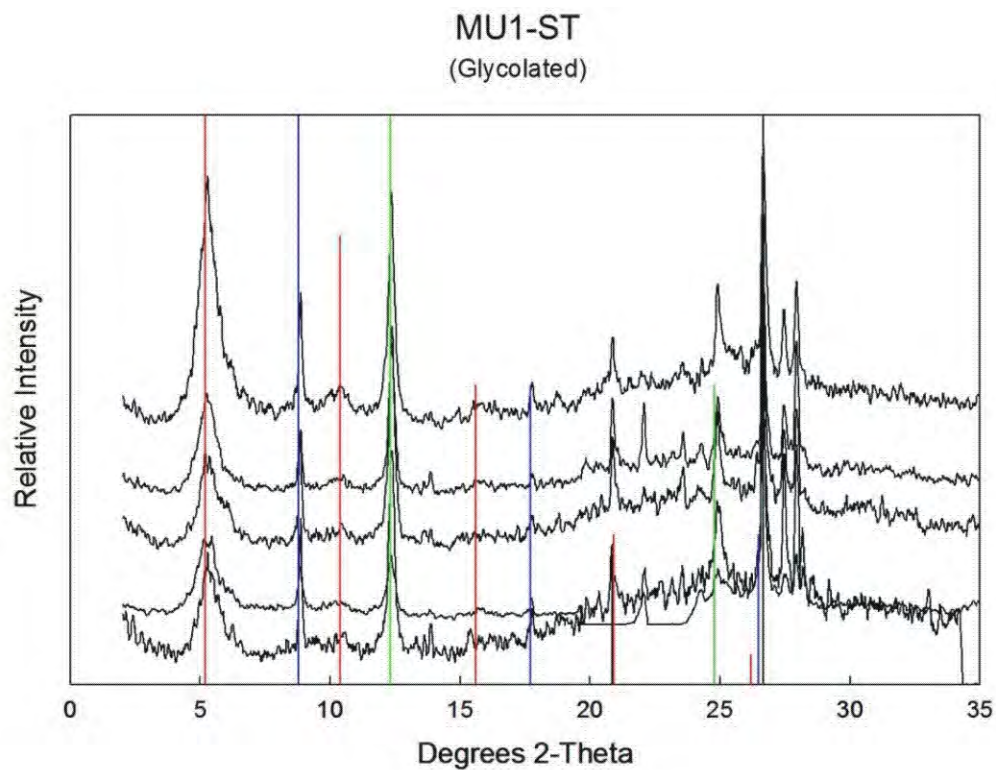


Figure 20: MU1-ST Clay fraction. Red=smeectite, Blue=illite, Green=kaolinite, Black=Quartz. Additional peaks are labeled in diagram above.

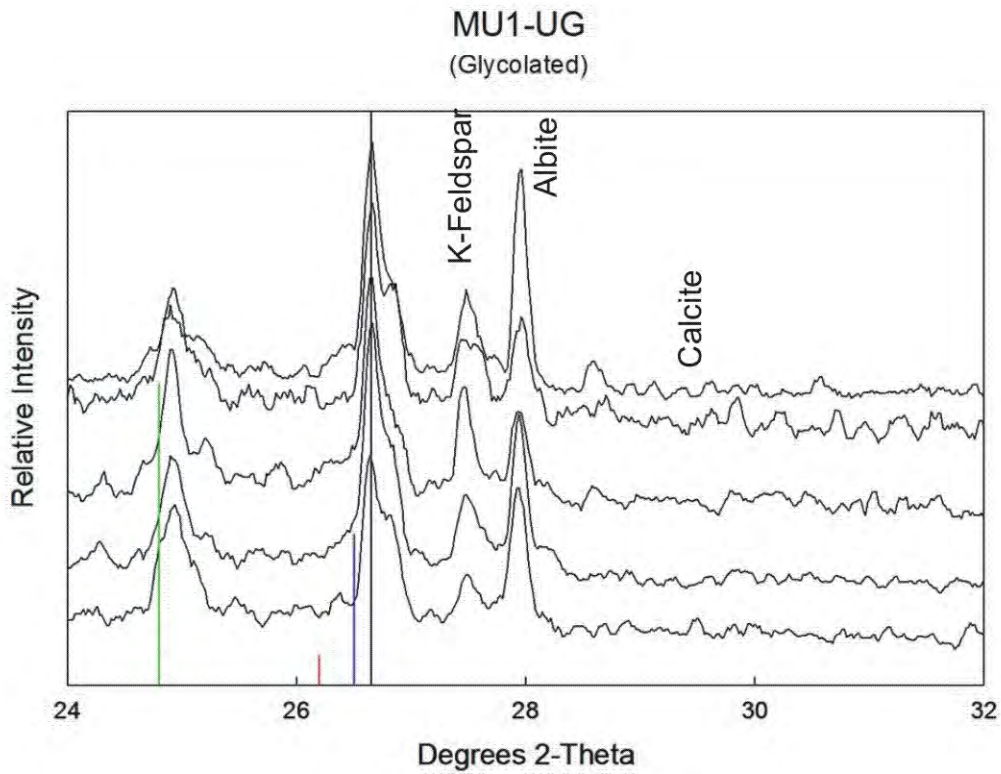
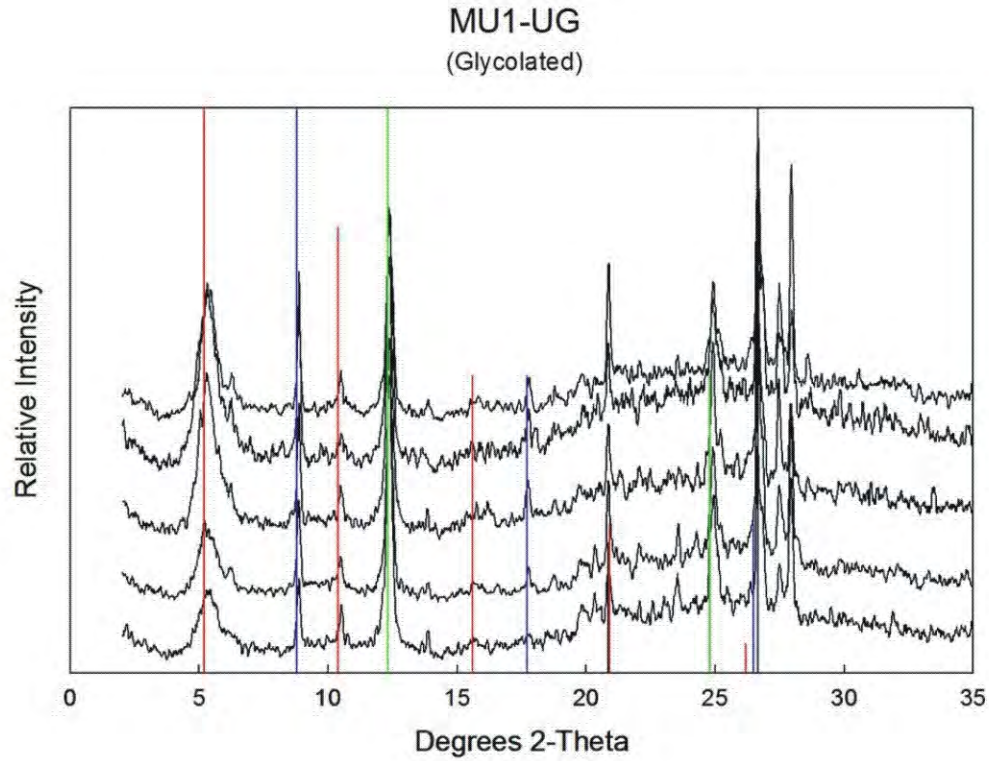


Figure 21: MU1-UG Clay fraction. Red=smeectite, Blue=illite, Green=kaolinite, Black=Quartz. Additional peaks are labeled in diagram above.

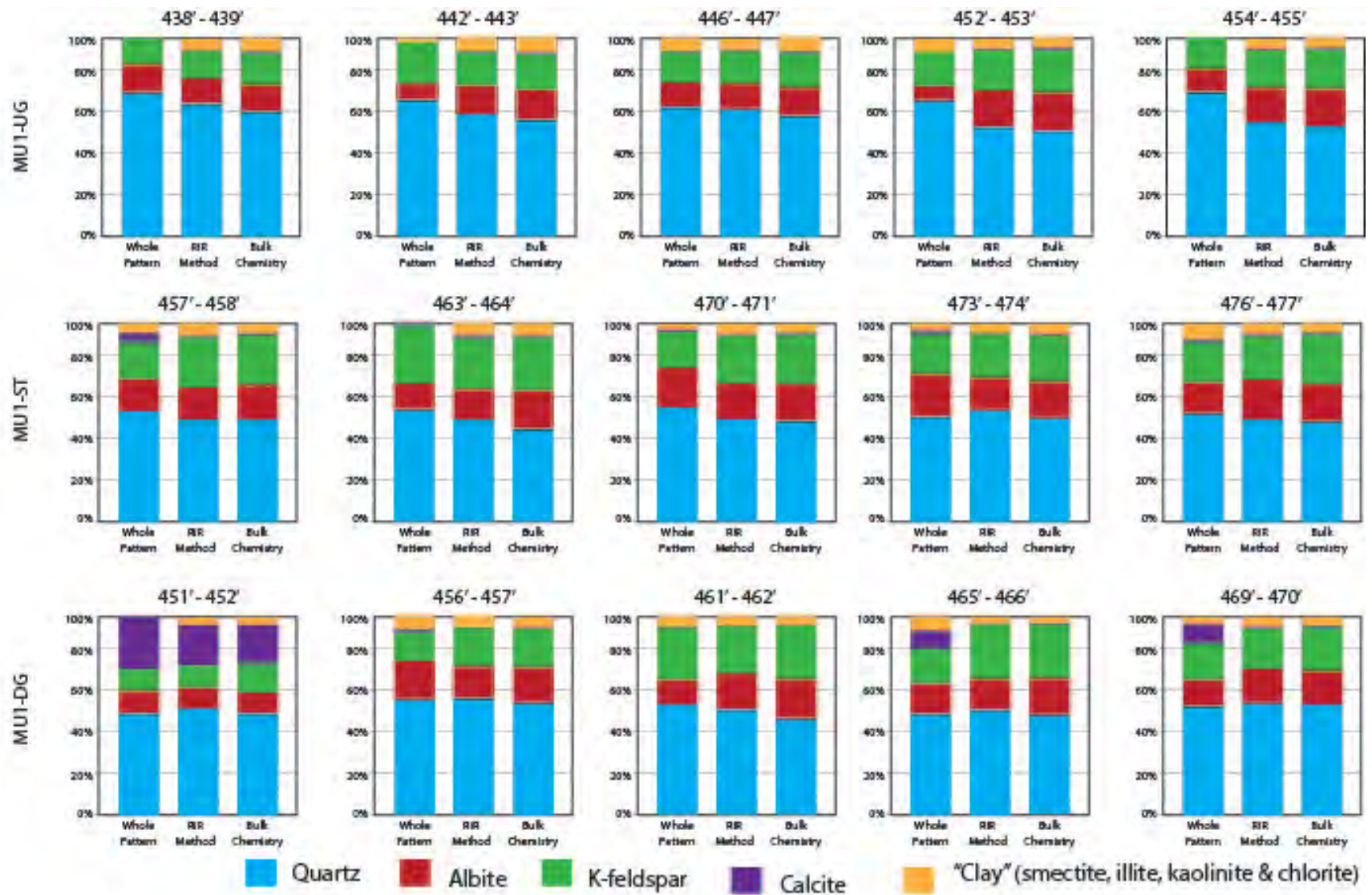


Figure 22: Major mineral modal estimates for all MU1 Samples.



WHOLE ROCK GEOCHEMISTRY

ME- ICP06 and OA- GRA05

ANALYSIS OF MAJOR OXIDES BY ICP- AES

ME- ICP06

SAMPLE DECOMPOSITION

Lithium Metaborate/Lithium Tetraborate (LiBO₂ /Li₂ B₄ O₇) Fusion[®] (FUS-LI01)

ANALYTICAL METHOD

Inductively Coupled Plasma - Atomic Emission Spectroscopy (ICP-AES)

A prepared sample (0.200 g) is added to lithium metaborate/lithium tetraborate flux (0.90 g), mixed well and fused in a furnace at 1000°C. The resulting melt is then cooled and dissolved in 100 mL of 4% nitric acid/2% hydrochloric acid. This solution is then analyzed by ICP-AES and the results are corrected for spectral inter-element interferences. Oxide concentration is calculated from the determined elemental concentration and the result is reported in that format.

ELEMENT	SYMBOL	UNITS	LOWER LIMIT	UPPER LIMIT
Aluminum	Al ₂ O ₃	%	0.01	100
Barium	BaO	%	0.01	100
Calcium	CaO	%	0.01	100
Chromium	Cr ₂ O ₃	%	0.01	100
Iron	Fe ₂ O ₃	%	0.01	100
Magnesium	MgO	%	0.01	100
Manganese	MnO	%	0.01	100
Phosphorus	P ₂ O ₅	%	0.01	100
Potassium	K ₂ O	%	0.01	100
Silicon	SiO	%	0.01	100
Sodium	Na ₂ O	%	0.01	100
Strontium	SrO	%	0.01	100
Titanium	TiO ₂	%	0.01	100

*NOTE: For samples that are high in sulphides, we may substitute a peroxide fusion in order to obtain better results.



GEOCHEMICAL PROCEDURE

ME- MS81

ULTRA- TRACE LEVEL METHODS

SAMPLE DECOMPOSITION

Lithium Metaborate Fusion (FUS-LI01)

ANALYTICAL METHOD

Inductively Coupled Plasma - Mass Spectroscopy (ICP - MS)

A prepared sample (0.200 g) is added to lithium metaborate flux (0.90 g), mixed well and fused in a furnace at 1000°C. The resulting melt is then cooled and dissolved in 100 mL of 4% HNO₃ / 2% HCl₁ solution. This solution is then analyzed by inductively coupled plasma - mass spectrometry.

ELEMENT	SYMBOL	UNITS	LOWER LIMIT	UPPER LIMIT
Silver*	Ag	ppm	1	1000
Barium	Ba	ppm	0.5	10000
Cerium	Ce	ppm	0.5	10000
Cobalt*	Co	ppm	0.5	10000
Chromium	Cr	ppm	10	10000
Cesium	Cs	ppm	0.01	10000
Copper*	Cu	ppm	5	10000
Dysprosium	Dy	ppm	0.05	1000
Erbium	Er	ppm	0.03	1000
Europium	Eu	ppm	0.03	1000
Gallium	Ga	ppm	0.1	1000
Gadolinium	Gd	ppm	0.05	1000
Hafnium	Hf	ppm	0.2	10000
Holmium	Ho	ppm	0.01	1000
Lanthanum	La	ppm	0.5	10000
Lutetium	Lu	ppm	0.01	1000
Molybdenum*	Mo	ppm	2	10000

ME- MS81

ELEMENT	SYMBOL	UNITS	LOWER LIMIT	UPPER LIMIT
Niobium	Nb	ppm	0.2	10000
Neodymium	Nd	ppm	0.1	10000
Nickel*	Ni	ppm	5	10000
Lead*	Pb	ppm	5	10000
Praseodymium	Pr	ppm	0.03	1000
Rubidium	Rb	ppm	0.2	10000
Samarium	Sm	ppm	0.03	1000
Tin	Sn	ppm	1	10000
Strontium	Sr	ppm	0.1	10000
Tantalum	Ta	ppm	0.1	10000
Terbium	Tb	ppm	0.01	1000
Thorium	Th	ppm	0.05	1000
Thallium	Tl	ppm	0.5	1000
Thulium	Tm	ppm	0.01	1000
Uranium	U	ppm	0.05	1000
Vanadium	V	ppm	5	10000
Tungsten	W	ppm	1	10000
Yttrium	Y	ppm	0.5	10000
Ytterbium	Yb	ppm	0.03	1000
Zinc*	Zn	ppm	5	10000
Zirconium	Zr	ppm	2	10000

*NOTE: Some base metal oxides and sulfides may not be completely decomposed by the lithium borate fusion. Results for Ag, Co, Cu, Mo, Ni, Pb, and Zn will not likely be quantitative by this method.